

Travail de Fin d'Etudes : Contribution to the implementation of robustness in European design recommendations for steel and composite structures

Auteur : Gemoets, Killian

Promoteur(s) : Demonceau, Jean-Francois

Faculté : Faculté des Sciences appliquées

Diplôme : Master en ingénieur civil des constructions, à finalité spécialisée en "civil engineering"

Année académique : 2019-2020

URI/URL : <http://hdl.handle.net/2268.2/9020>

Avertissement à l'attention des usagers :

Tous les documents placés en accès ouvert sur le site le site MatheO sont protégés par le droit d'auteur. Conformément aux principes énoncés par la "Budapest Open Access Initiative"(BOAI, 2002), l'utilisateur du site peut lire, télécharger, copier, transmettre, imprimer, chercher ou faire un lien vers le texte intégral de ces documents, les disséquer pour les indexer, s'en servir de données pour un logiciel, ou s'en servir à toute autre fin légale (ou prévue par la réglementation relative au droit d'auteur). Toute utilisation du document à des fins commerciales est strictement interdite.

Par ailleurs, l'utilisateur s'engage à respecter les droits moraux de l'auteur, principalement le droit à l'intégrité de l'oeuvre et le droit de paternité et ce dans toute utilisation que l'utilisateur entreprend. Ainsi, à titre d'exemple, lorsqu'il reproduira un document par extrait ou dans son intégralité, l'utilisateur citera de manière complète les sources telles que mentionnées ci-dessus. Toute utilisation non explicitement autorisée ci-avant (telle que par exemple, la modification du document ou son résumé) nécessite l'autorisation préalable et expresse des auteurs ou de leurs ayants droit.



Liège University
Faculty of Applied sciences
Academic year 2019-2020

Contribution to the implementation of robustness in European design recommendations for steel and composite structures

Dissertation submitted as part requirement for the degree of
Master in Civil Engineering

by Killian Gemoets

Jury members:

Jean-François Demonceau (promoter)

Jean-Pierre Jaspart (co-promoter)

Jean-Marc Franssen

Sébastien Seret

Je tiens tout d'abord à remercier profondément mon promoteur, Jean-François Demonceau, et mon co-promoteur, Jean-Pierre Japsart, pour leur disponibilité malgré les conditions particulières et pour m'avoir guidé tout au long de la réalisation de ce travail. Je remercie également Jean-Marc Franssen et Sébastien Seret, membres du jury, pour l'attention portée à ce travail.

Ensuite, le travail de fin d'études marquant l'achèvement d'un cycle, je tiens à remercier les personnes qui ont été présentes tout au long de ce parcours académique. Je remercie mon professeur de math de 5e et 6e secondaires, José Wuïdar, qui m'a motivé à réaliser des études d'ingénieur civil et m'a préparé à l'examen d'entrée. Je remercie également tous les professeurs qui m'ont donné cours durant ces 5 années passées au sein de l'Université de Liège, et qui ont su me transmettre leur savoir et leur expérience avec passion. Finalement, je remercie mes proches, ma famille, et plus particulièrement mes parents qui m'ont soutenu tout au long de mes études et qui ont toujours veillé à ce que je sois dans des conditions de travail optimales.

Killian Gemoets

Statement

Titre du travail: Version anglaise: Contribution to the implementation of robustness in European design recommendations for steel and composite structures

Version française: Contribution à l'implémentation de règles de robustesse dans les normes européennes de dimensionnement pour les structures métalliques et mixtes

A l'heure actuelle, les Eurocodes intègrent la notion de robustesse structurale. Mais le contenu se limite aujourd'hui au seul énoncé de principes généraux.

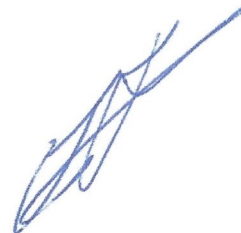
C'est pourquoi de nombreuses recherches ont été réalisées ces dernières années dans le monde dans le but de développer des stratégies et des outils de calcul et de conception à la robustesse. Chacune de ses recherches a apporté son lot de connaissances nouvelles, mais l'absence actuelle de philosophie globale, communément acceptée et reconnue au niveau international, tend à limiter la portée de ces travaux individuels aux cadres précis sélectionnés pour les études et dès lors à en rendre la généralisation à des problèmes similaires connexes fort compliquée.

Le présent travail vise donc, dans un premier temps, à prendre connaissance des travaux déjà réalisés, à les analyser et à les comparer afin de développer une approche globale de traitement de la problématique de la robustesse intégrant ces développements récents, formant ainsi un ensemble cohérent de recommandations et d'outils de calcul et de conception.

Dans un second temps, ce travail s'intéressera plus particulièrement à la méthode prescriptive dite « des tirants ». En effet, l'Eurocode présente de nombreuses incohérences à cet égard. Des propositions d'amélioration du document normatif ont été récemment formulées par quelques chercheurs, mais celles-ci nécessitent d'être validées sur base d'une approche scientifique solide, ce qui sera envisagé dans le cadre du présent mémoire pour les bâtiments en acier.

Promoteurs : Jean-François DEMONCEAU

Jean-Pierre JASPART



Etudiant : Killian GEMOETS



Résumé

A l'heure actuelle, l'Eurocode 1 Partie 1-7 présente différentes stratégies dans le but de traiter la problématique de la robustesse. Cependant, pour chacune de ces stratégies, le contenu se limite à l'énoncé de principes généraux. Dès lors, ces dernières années, de nombreuses recherches ont été réalisées afin de développer des outils de calcul et de conception à la robustesse. Grâce à ces recherches, un grand nombre de nouveaux outils et travaux sont à la disposition des praticiens, mais l'absence d'approches globales limite la portée et l'utilisation de ceux-ci.

Dans ce travail, des approches de traitement de la problématique de robustesse dans les structures métalliques et mixtes sont développées pour les stratégies présentées dans l'Eurocode, et sur base des outils actuellement disponibles. Pour chacune des approches développées, les outils qu'elle nécessite d'utiliser, les limitations qu'elle présente et les étapes d'analyse et de vérification à suivre sont présentés en détail. De plus, toutes ces informations sont résumées au sein d'un organigramme global proposé pour traiter la problématique de robustesse.

Cette première tâche met en évidence un grand nombre d'incohérences concernant la méthode prescriptive des tirants actuellement proposée par l'Eurocode. Des propositions d'améliorations ont d'ailleurs été formulées récemment.

Dès lors, dans un second temps, cette thèse s'intéresse plus particulièrement à cette méthode des tirants. Afin d'évaluer la pertinence des règles proposées actuellement par l'Eurocode à propos de la méthode des tirants, ainsi que le degré de robustesse que ces règles permettent d'atteindre, une étude d'une structure contreventée subissant la perte d'une colonne est réalisée. Dans le cadre de cette étude, les assemblages poutre-colonne de la structure possèdent d'abord la résistance spécifiée par la méthode des tirants, et ensuite différentes configurations d'assemblages sont étudiées. En comparant les résultats obtenus, plusieurs conclusions sont faites à propos de la méthode des tirants. De plus, cette étude montre que les assemblages articulés tels que les *header plate connections* possèdent un degré de robustesse trop faible, et qu'il est plus intéressant d'utiliser des assemblages semi-rigides/rigides tels que les *flush end-plate connections*.

Summary

At present, Eurocode 1 Part 1-7 presents different strategies to deal with the problem of robustness. However, for each of these strategies, the content is limited to the statement of general principles. Consequently, in recent years, several researches have been carried out to develop calculation and design tools for robustness. Thanks to these researches, many new tools and works are available to practitioners, but the lack of comprehensive approaches limits their scope and use.

In this work, approaches for handling the robustness problem in steel and composite structures are developed for the strategies presented in the Eurocode, and based on the tools currently available. For each of the approaches developed, the tools it requires to use, the limitations it presents and the analysis and verification steps to be followed are presented in detail. In addition, all this information is summarized in a global flowchart proposed to deal with the robustness problem.

This first task highlights several inconsistencies concerning the prescriptive tying method currently proposed by the Eurocode. Proposals for improvements have actually already been made recently.

Therefore, in a second step, this thesis focuses more specifically on this tying method. To assess the relevance of the rules currently proposed by the Eurocode regarding the tying method and the degree of robustness which these rules allow to reach, a study of a braced structure undergoing the loss of a column is carried out. In the context of this study, the beam-column joints of the structure first have the resistance specified by the tying method. Subsequently, different joint configurations are studied. By comparing the results obtained, several conclusions are drawn about the tying method. Also, this study shows that simple joints such as header plate connections have a too low degree of robustness, and that it is more advantageous to use semi-rigid/rigid joints such as flush end-plate connections.

Contents

| | | |
|----------|--|-----------|
| 1 | General introduction | 1 |
| 1 | General context | 1 |
| 1.1 | Introduction to robustness of structures | 1 |
| 1.2 | Eurocode background | 2 |
| 1.2.1 | Definitions | 3 |
| 1.2.2 | Additional verification | 3 |
| 2 | Work organisation and thesis objectives | 4 |
| 2 | Design strategies | 5 |
| 1 | Introduction | 5 |
| 2 | Strategies based on identified exceptional actions | 6 |
| 3 | Strategies based on limiting the extent of localised failure | 6 |
| 3.1 | Indirect methods | 6 |
| 3.2 | Direct methods | 7 |
| 4 | Conclusion | 8 |
| 3 | Design approaches | 9 |
| 1 | Introduction | 9 |
| 2 | Limiting the extent of localised failure | 9 |
| 2.1 | Alternative load paths method | 10 |
| 2.1.1 | Prescriptive approach | 10 |
| 2.1.2 | Analytical approach | 12 |
| 2.1.3 | Numerical approach | 24 |
| 2.1.4 | Case of 3D structures | 26 |
| 2.2 | Key element method | 27 |
| 2.2.1 | Primary structure approach | 27 |
| 2.2.2 | Fuse approach | 27 |
| 2.2.3 | Summary of the key element method | 27 |
| 3 | Identified exceptional actions | 28 |
| 3.1 | Design under impact loading | 28 |
| 3.1.1 | Equivalent static force | 28 |
| 3.1.2 | Dynamic force | 29 |
| 3.2 | Design under blast loading | 39 |
| 3.2.1 | Equivalent static force | 39 |
| 3.2.2 | Dynamic force | 40 |
| 4 | Conclusion | 47 |
| 4 | Study of a structure subject to a loss of column | 48 |
| 1 | Objectives of this study | 48 |
| 2 | Description of the structure | 49 |
| 3 | Load combinations | 49 |
| 3.1 | Loads | 49 |
| 3.2 | Load combinations | 50 |

| | | |
|----------|--|-----------|
| 4 | Structure design | 51 |
| 4.1 | Linear calculation | 51 |
| 4.1.1 | Under ULS Loads | 51 |
| 4.1.2 | Under SLS Loads | 53 |
| 4.2 | Non-linear calculation | 53 |
| 4.2.1 | Structure loading method | 53 |
| 4.2.2 | Stop criteria | 54 |
| 4.2.3 | Initial imperfections | 54 |
| 4.2.4 | Results | 55 |
| 5 | Damaged structure | 57 |
| 5.1 | Without taking into account the resistance of the joints | 57 |
| 5.1.1 | Column loss simulation method | 57 |
| 5.1.2 | Steel behavior law | 58 |
| 5.1.3 | Results | 58 |
| 5.1.4 | Results analysis | 59 |
| 5.1.5 | Assumptions about joints | 61 |
| 5.2 | With joints having the resistance specified by the tying method proposed by the Eurocode | 62 |
| 5.2.1 | Calculation of tying force | 62 |
| 5.2.2 | Joint design | 63 |
| 5.2.3 | Joint modeling | 63 |
| 5.2.4 | Results | 64 |
| 5.2.5 | Results interpretation | 66 |
| 5.3 | With header plate connections sized to ULS | 67 |
| 5.3.1 | Joint design | 67 |
| 5.3.2 | Joint modeling | 69 |
| 5.3.3 | Results | 72 |
| 5.3.4 | Conclusion about header plate connections sized at ULS | 75 |
| 5.4 | With header plate connections with the best possible properties | 75 |
| 5.4.1 | Joint design | 75 |
| 5.4.2 | Joint modeling | 77 |
| 5.4.3 | Results | 77 |
| 5.4.4 | Conclusion about header plate connections | 79 |
| 5.5 | With flush end-plate connections with the best possible properties | 80 |
| 5.5.1 | Joint design | 80 |
| 5.5.2 | Joint modeling | 82 |
| 5.5.3 | Results | 83 |
| 5.5.4 | Second approach | 84 |
| 5.5.5 | Conclusion about flush end-plate connections | 87 |
| 6 | Parametric study | 88 |
| 6.1 | Variation of the number of spans | 89 |
| 6.2 | Variation of the number of storeys | 90 |
| 7 | Conclusion of the study | 91 |
| 5 | General conclusion | 92 |
| 1 | Conclusion | 92 |
| 2 | Perspectives | 94 |
| | Annexes | 99 |
| A | Sizing of header plate connections at ULS | 99 |
| A.1 | Main joint data | 99 |
| A.2 | Detailed characteristics | 99 |
| A.3 | Applied forces | 100 |
| A.4 | Ductility and rotation requirements | 100 |

| | | |
|-----|--|------------|
| A.5 | Calculation of the shear resistance | 101 |
| A.6 | Calculation of ultimate tensile strength | 102 |
| A.7 | Calculation of design tensile strength | 103 |
| A.8 | Calculation of the tensile rigidity and the elongation capacity of the joint | 104 |
| B | Sizing of header plate connections with the best possible properties | 104 |
| B.1 | Main joint data | 104 |
| B.2 | Detailed characteristics | 104 |
| B.3 | Ductility and rotation requirements | 106 |
| B.4 | Calculation of the joint shear resistance | 106 |
| B.5 | Calculation of ultimate tensile strength | 108 |
| B.6 | Calculation of design tensile strength | 108 |
| B.7 | Calculation of the tensile rigidity and the elongation capacity of the joint | 109 |
| C | Sizing of end-plate connections flush with the best possible properties | 110 |
| C.1 | Main joint data | 110 |
| C.2 | Detailed characteristics | 110 |
| C.3 | Ductility requirements | 112 |
| C.4 | Moment resistance and rotational stiffness | 112 |
| C.5 | Shear resistance | 112 |
| C.6 | Design tensile strength | 112 |
| C.7 | Ultimate tensile strength | 112 |
| C.8 | Calculation of the tensile rigidity and the elongation capacity of the joint | 113 |
| D | Structures studied during the parametric study | 113 |
| | Bibliography | 117 |

Chapter 1

General introduction

1 General context

1.1 Introduction to robustness of structures

The robustness field has only started to develop relatively recently. Indeed, designing structures to withstand exceptional events such as earthquakes, major fires, hurricanes or even explosions did not seem realistic a few decades ago. However, several catastrophic events have raised awareness of the need to ensure the integrity of buildings in the face of exceptional events, i.e., events that have a very low probability of occurrence but which can cause very significant damage.

The first catastrophic event that sparked reactions was the accident at Ronan Point (England) in 1968. The structure of the 22-storey tower block was made up of precast concrete elements, and no particular attention had been paid to the connections between the elements. A gas explosion occurred on the 18th floor, and the structure then collapsed like a house of cards, the floors falling on top of each other (see Figure 1.1). This is called a progressive collapse, i.e. a disproportionate ruin compared to the cause which gave birth to it.

After this disaster, the English were the first to introduce recommendations in the *British Standards* to ensure structural integrity and avoid a progressive collapse. The other codes will be primarily inspired by *British Standards*.



Figure 1.1: Ronan Point, 1968 (researchgate.net)

Another catastrophic event that caused a progressive collapse concerns the Murrah building, located in Oklahoma City. In 1995, it was severely damaged after the explosion of a truck filled with explosives located at the front of the building (see Figure 1.2).



Figure 1.2: Oklahoma City, 1995 (ici.radio-canada.ca)

Finally, a last well-known example concerns the September 11, 2001, terrorist attack on the towers of the World Trade Center (see Figure 1.3). The towers already had a certain degree of robustness since they were designed to remain stable against the impact of a Boeing. However, the planes were full of fuel and fuel spilled over several floors, causing a fire in several compartments. The compartmentalisation no longer worked and the towers gradually collapsed.



Figure 1.3: World Trade Center, 2001 (ibtimes.sg)

All three of these disasters have resulted in harmful material and human losses. They occurred because the exceptional loads which these buildings underwent had not been taken into account in the dimensioning. Indeed, their probability of occurrence had been considered too low. Consequently, the occurrence of these exceptional charges caused a progressive collapse. The buildings first suffered the loss of some structural elements, which then caused the progressive collapse of a significant part of the structure, see the entire structure.

Today, robustness is, therefore, of great interest to civil engineers, and a lot of research and development has been carried out in the field in recent years to avoid a gradual collapse in future constructions. The main objectives are to save lives, reduce the risks for emergency services, and limit collateral damage.

1.2 Eurocode background

As mentioned earlier, codes and standards have emerged to include recommendations to limit the risk associated with an exceptional event.

In Europe, these standards are currently listed in Eurocode 1 Part 1-7 [1]. They mainly provide definitions and guidelines for good practice.

1.2.1 Definitions

At first, it seems relevant to explain certain concepts related to the robustness domain which are defined in Eurocode.

In Eurocode 1-7 [1], the robustness of a structure is defined as follows : *the ability of a structure to withstand events like fire, explosions, impact or the consequences of human error, without being damaged to an extent disproportionate to the original cause.*

This definition is very subjective. Indeed, the concept "without being damaged to an extent disproportionate to the original cause" is very subjective. Acceptable risk and loss should be discussed with the client and the appropriate authorities.

More precisely, it can be said that robustness is a structural ability which provides sufficient resistance against failures for exceptional events which were not taken into account in the initial design. It aims to ensure structural integrity and avoid a progressive collapse.

Where,

- *An exceptional event* is an event that has a probability of occurrence that is too low to be taken into account directly in the design. However, it is an event that can cause very significant damage if it occurs. An exceptional event can be of natural cause (storm, tsunami, earthquake, exceptional snow, ...) or human cause (impact, explosion, ...). It can be static (snow accumulating on the roof) or dynamic (storm).
- *Ensuring structural integrity* means that the structure must remain globally stable. The structure can have local ruptures and undergo significant displacements and deformations as long as it reaches a new equilibrium configuration for which it remains globally stable.
- *A progressive collapse* is a disproportionate ruin compared to the cause which gave birth to it.

1.2.2 Additional verification

An exceptional event has a probability of occurrence that is too low to be taken into account directly in the design. Indeed, this would lead to the design of too expensive indestructible structures. As a result, an additional verification must be performed in addition to the traditional verifications. A structure must, therefore, be subject to verifications under three load combinations:

- Under the combination of design loads, at ultimate limit state (ULS): the stability and resistance of the structure are checked.
- Under the combination of service loads, at service limit state (SLS): the displacements of the structure are checked.
- Under the combination of exceptional loads: structural integrity is checked. Displacements are not checked. On the contrary, the massive displacements and the second-order effects will make it possible to reach a new equilibrium configuration. In this case, the ultimate resistance of the elements f_u is used. The exceptional loads or the exceptional scenarios under which the structure must be verified are defined in agreement with the client and the competent authorities, depending on the acceptable risk. The Eurocode then proposes several design strategies that can be envisaged. These will be presented in the next chapter.

2 Work organisation and thesis objectives

As explained, at present, the concept of robustness is integrated to Eurocode 1 Part 1-7. In this part, different strategies to deal with the problem of robustness are proposed. The second chapter of this thesis will present these strategies.

However, as will be explained, the content of these strategies is limited to the statement of general principles and some guidelines of good practice. No clear and detailed calculation procedure is presented for each of these strategies. Consequently, in recent years, a lot of research and development has been carried out to develop calculation tools and to bring new knowledge concerning design to robustness.

Today, thanks to this research, a large number of new tools and works are available to the practitioner. Yet, the lack of comprehensive approaches limits the scope and use of these works. The first objective of this thesis will, therefore, be to develop global procedures for dealing with the problem of robustness in steel and composite structures, based on the tools available for each of the strategies presented in the second chapter. These approaches and the tools they require will be presented in detail in the third chapter.

Then, the last chapter will focus on the prescriptive method called *Tying method*. In annex A of Eurocode 1 Part 1-7 (therefore for information), design rules are proposed for this method but they present a large number of inconsistencies, and proposals for improvement have been made very recently. These proposals are still being researched. However, to develop new rules, it seems interesting to know the limits and the relevance of the rules currently proposed by the Eurocode. This will constitute the second objective of this thesis. With this purpose in mind, a structure subjected to the loss of a column will be analysed in detail, giving different properties to the joints. This study will also explain the degree of robustness for various commonly used joint configurations.

Chapter 2

Design strategies

1 Introduction

In the Eurocode, the strategies to be followed to reduce the risk of damage due to an exceptional situation are divided into two main categories. Each category has several strategies, as shown in Figure 2.1.

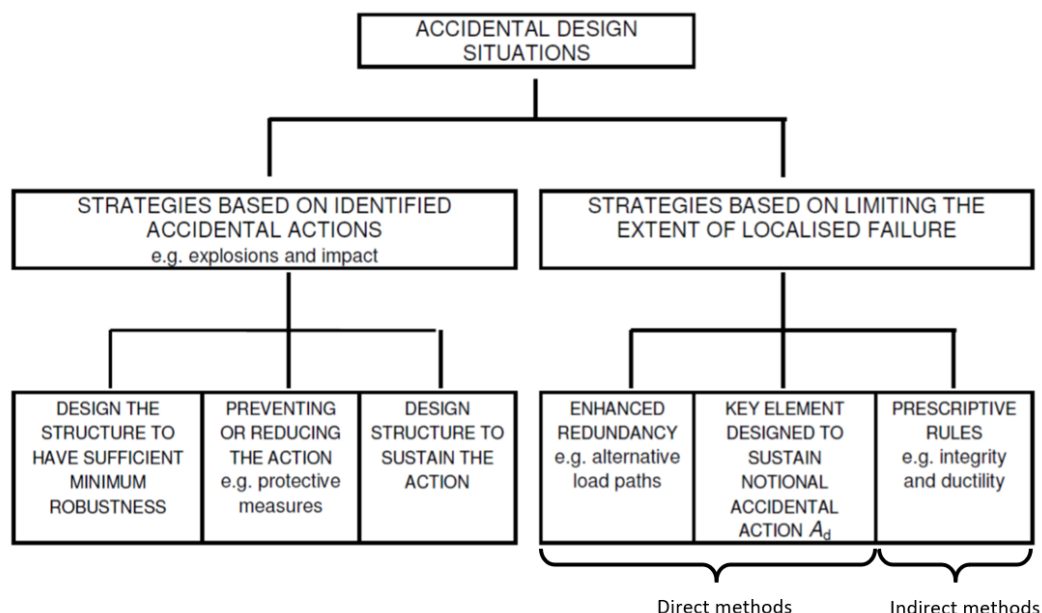


Figure 2.1: Strategies for exceptional situations

Note that the Eurocode speaks of accidental actions and not of exceptional actions because it does not dissociate the notions of exceptional event and accidental event. Still, an accidental action has a higher probability of occurrence than an exceptional action and is subject to traditional design (at ULS and SLS using f_y).

The strategy chosen will depend on the risk that is acceptable and the level of robustness desired. This can be discussed with the client and the competent authorities. Also, Eurocode 1 Part 1-7 offers a system for classifying structures into different consequence classes. Structures can be classified into different classes according to the potential consequences due to an exceptional event. These consequence classes are as follows :

- CC1: Low consequences of failure (for example a single-family house)
- CC2: Medium consequences of failure (for example an apartment building with a maximum of 4 floors)

- CC3: High consequences of failure (for example a hospital with more than 3 floors or a stadium with more than 5,000 people)

Depending on the consequence class of a structure, a more or less complicated and precise analysis will be carried out. Eurocode 1 Part 1-7 makes the following recommendations :

- CC1: No specific consideration is necessary for exceptional actions. The consequences are negligible and total ruin is accepted.
- CC2: A simplified analysis by equivalent static load may be adopted, or prescriptive rules may be applied.
- CC3: A more sophisticated structural analysis must be carried out, and risk analysis will have to be carried out to assess the risk linked to the exceptional event or the exceptional scenario considered.

2 Strategies based on identified exceptional actions

As shown in Figure 2.1, on the one hand, there are strategies based on identified exceptional actions. Among these are three strategies.

The first strategy is to design the structure to have sufficient minimum robustness. This strategy consists in ensuring a adequate level of robustness without specifically considering the exceptional action identified. This strategy, therefore, refers to the strategy of the right category which will be presented later.

The second possible strategy is to take protective measures. By definition, the risk of damage linked to an event is equal to the probability of occurrence of the event multiplied by its consequences. Taking protective measures consists in reducing the risk related to an exceptional event by reducing its probability of occurrence. For example, it is possible to reduce the probability that a vehicle impacts a column on a parking lot by placing protective barriers around the columns, it is possible to reduce the risk of flooding by placing a dam, or even the risk of terrorist attack in a building can be reduced by placing security gates at the entrances to the building.

Finally, the last possible strategy is to take structural measures. This strategy consists of reducing the risk linked to an exceptional event by reducing its consequences. Taking structural measures consists in giving the structure sufficient properties and in designing it so that it can withstand the exceptional action identified. In this case, large displacements and large deformations are acceptable, and the ultimate resistance of the elements f_u can be used. The structure may suffer local damage, but it must remain globally stable, and the structural integrity must be ensured.

3 Strategies based on limiting the extent of localised failure

As shown in Figure 2.1, the second category of strategies concerns strategies based on limiting the extent of localised failure. These strategies can be divided into two main families: direct methods and indirect methods.

3.1 Indirect methods

First, indirect methods provide prescriptive rules. By using these methods, a particular damage scenario is not considered, but good properties are given to the structure. As an indirect method, the Eurocode proposes the tying method.

The tying method consists of installing vertical and horizontal ties with sufficient tensile strength. This makes it possible to ensure continuity between the elements and to have a redistribution of forces between the storeys of the structure in the event of loss of an element. Eurocode 1 Part 1-7 [1] gives indications concerning the positions in which the ties must respect and proposes formulas to calculate the tensile strength which they must have. This strategy is generally considered for a CC2 consequence class structure.

3.2 Direct methods

Then, direct methods require the specific resistance of certain elements for particular scenarios. Among these methods are the key element method and the alternative load paths method.

First, **the key element method** focuses on the design of a key element that ensure the structural integrity of the structure. There are two versions of this method :

- Certain elements are designed to support the structure against an exceptional event. These elements must, therefore, be sized and protected to remain intact against an exceptional event. This is the case, for example, of the mega beam and the mega columns of the system illustrated in Figure 2.2. Thanks to this system, if an element is lost in the middle of the building, it does not affect the rest of the structure, which is suspended from the mega beam.

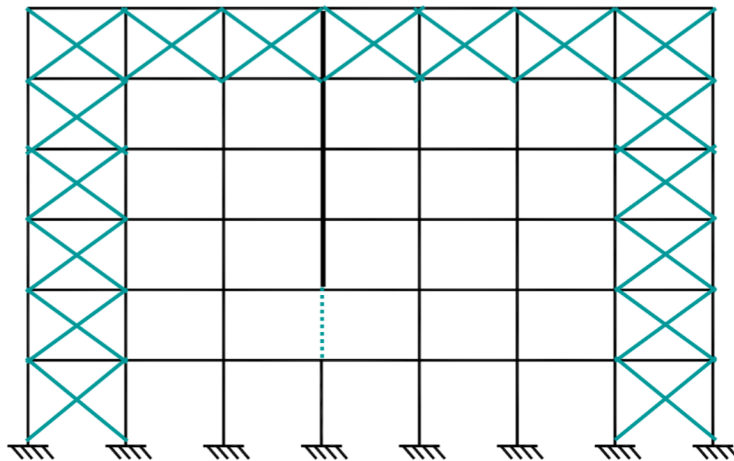


Figure 2.2: Key element version 1 [2]

- Conversely, certain key elements are designed to break quickly to avoid the propagation of the damages to the rest of the structure. These elements must, therefore, have a rather weak resistance and a fragile ruin so that they yield before transmitting high efforts to their neighbors and thus avoid propagating the ruin.

This method is illustrated in Figure 2.3. It shows a structure losing a column. The beam-column joints are not very resistant to axial forces and are very little ductile (fragile ruin) so that the part of the structure above the lost column will collapse quickly. This makes it possible to avoid transmitting excessive forces to the rest of the structure and to preserve the integrity of the rest of the structure. This method is not used for any type of structure, but it is, for example, used for storage racks.

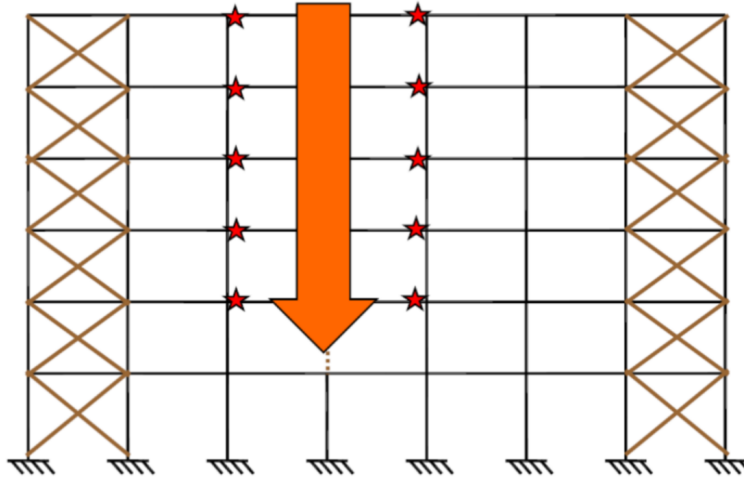


Figure 2.3: Key element version 2 [2]

A last method is **the alternative load paths method**. It consists of first identifying, in a structure, the local damage associated with a predefined scenario. Then, the alternative load path is identified in the partially damaged structure. Finally, structural integrity is checked. Structural integrity is ensured if the structure can redistribute the load which was carried by the lost element and if it is sufficiently ductile to find a new equilibrium configuration.

This method requires to enter the field of large displacements and large deformations, while taking into account what happens at the ends of the beams. Also, the operation must be repeated for each predefined scenario. This method therefore takes time and requires performing a non-linear calculation. However, it is an economical method because it allows the engineer to identify the elements to be reinforced precisely.

4 Conclusion

The Eurocode proposes a series of strategies that can be envisaged to reduce the risk of damage due to an exceptional situation. Also, using the consequence class system, it gives recommendations on the considerations to be made.

However, for each of these strategies, the Eurocode only sets out general principles. It mainly gives definitions and guidelines of good practice but does not describe any calculation procedure and any transparent approach. Once the strategy is chosen, the practitioner has no indications of the procedure to follow in order to implement it.

Chapter 3

Design approaches

1 Introduction

As described in the previous chapter, Eurocode offers several strategies for dimensioning a structure in the face of an exceptional event and ensuring its robustness. However, for each of these strategies, no clear and detailed calculation procedure is presented. This is why a lot of research has been carried out in recent years to develop procedures and calculation tools for the design of robust steel (and composite) structures.

An essential part of this Master thesis was devoted to investigating the work already done on robustness design, analysing it, and identifying its usefulness. The works studied concern the development of different calculation tools and different analytical approaches, which may prove useful depending on the strategy chosen.

After learning about the tools available, it was possible to develop detailed approaches for dealing with the problem of robustness in steel and composite structures, depending on the strategy chosen. This chapter will present these approaches, their limits, and the tools they need to have available. Thus, for a chosen strategy, the engineer will be able to choose the approach that best suits him based on the tools he has and the scenarios/loadings he wishes to study.

Note that approaches will be presented for all the strategies presented in the previous chapter except the first two. Indeed, the strategy consisting of designing the structure to have sufficient minimum robustness refers to the category of strategy based on limiting the extent of localised failure. No approach should, therefore, be developed for this strategy. Second, the strategy of preventing or reducing the action simply requires taking protective measures. No calculation procedure is necessary when choosing this strategy.

2 Limiting the extent of localised failure

As explained in the previous chapter, three different strategies can be envisaged to limit the extent of localised failure : the prescriptive tying method, the alternative load paths method, and the key element method.

The prescriptive tying method can, however, be seen as a possible approach when the strategy of the alternative load paths is considered rather than as a strategy in its own right. Indeed, this method is a quick way to ensure continuity between the elements and to ensure an alternative load path if an element is lost.

Therefore, the flowchart presented in Figure 3.1 can be established.

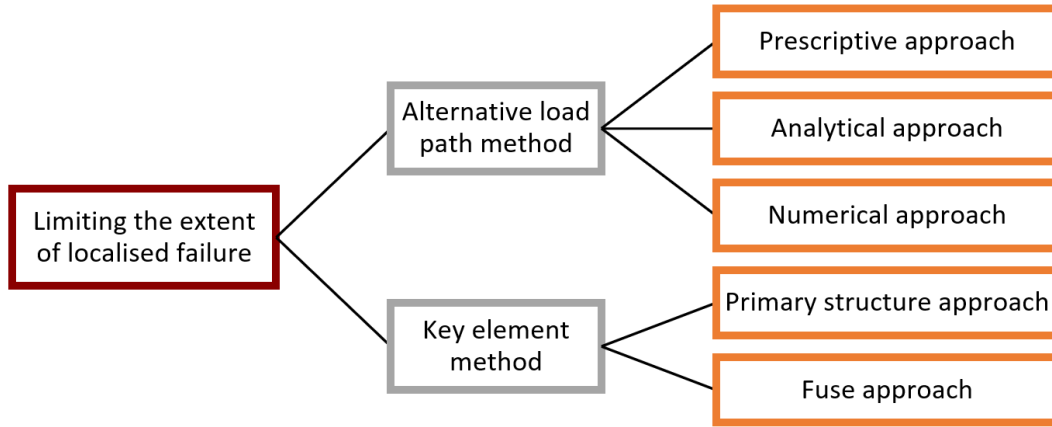


Figure 3.1: Flowchart for strategies based on limiting the extent of localised failure

2.1 Alternative load paths method

As presented in Figure 3.1, three different approaches are possible if the strategy of alternative load paths is considered. The calculation procedure to be followed and the tools to be used for each of these approaches will now be detailed.

2.1.1 Prescriptive approach

The prescriptive approach is to use the tying method. This approach is a simplified approach. It does not require to calculate the behaviour of the structure, but it is based on the principle that if sufficient links exist between the elements, the structure should behave well. Therefore, it will generally be used for consequence class structures CC2.

For this approach, a procedure is currently proposed in annex A of Eurocode 1 Part 1-7 (so as informative). However, there are some inconsistencies and a more realistic treatment is under development. The procedure proposed by Eurocode and the inconsistencies it contains will first be explained before presenting the new treatment.

2.1.1.1 Approach currently proposed by Eurocode

Analysis

Annex A to Eurocode 1 Part 1-7 gives information on the positions to be taken by horizontal and vertical ties in the case of framed structures or in the case of wall structures.

Then, different formulas are proposed to calculate the tensile strength that horizontal and vertical ties must have in the design of framed structures and wall structures to ensure certain robustness.

For example, for framed structure, the Eurocode indicates that each continuous horizontal tie, including its end connections, should be capable of sustaining the following design tensile load:

$$\text{For internal ties: } T_i = 0,8 \cdot (g_k + \psi \cdot q_k) \cdot s \cdot L \text{ or } 75kN \quad (3.1)$$

$$\text{For perimeter ties: } T_p = 0,4 \cdot (g_k + \psi \cdot q_k) \cdot s \cdot L \text{ or } 75kN \quad (3.2)$$

Where,

- s is the (average) spacing of ties
- L is the span of considered tie
- Ψ is the factor according to the accidental load combination

- g_k is the permanent characteristic load applied on the considered floor
- q_k is the variable characteristic load applied on the considered floor

Verification

It must then be verified that each tie, including its end connections, is capable of sustaining the design tensile load obtained.

Limitations

This approach presents several limitations and inconsistencies.

Firstly, the positions that the ties must respect are not clearly indicated.

Secondly, the proposed formulas do not take into account the dynamic effects and the ductility of the elements and joints. If the ruin is fragile, membrane efforts will not have time to develop before the ruin of the structure. Robustness will then not be ensured even if the criteria of positions and resistances are met.

Finally, the Eurocode does not indicate the degree of robustness that this method achieves.

2.1.1.2 More realistic treatment

Because of the limitations and inconsistencies of the procedure described in Eurocode, a more realistic treatment is being developed within CEN (European Committee for Standardization), [3] and [4].

Analysis

The position of the horizontal and vertical ties will be indicated by new, more precise and clearer criteria.

Subsequently, new formulas will make it possible to determine the design tensile forces which the ties must sustain, taking into account the ductility and the dynamic effects.

For horizontal ties in the case of framed structures, the following formula is proposed:

$$f = \eta \cdot \rho \left(\frac{i_f}{\alpha_{0.2}} \right) \cdot \omega \cdot L \quad (3.3)$$

Where,

- η : dynamic amplification factor
- ρ : reduction factor to account for additional contributions
- $\alpha_{0.2}$: normalized rotational ductility ($\alpha/0.2$)
- i_f : base intensity factor at $\alpha = 0.2$ rad

Verification

As before, it will be necessary to verify that each tie, including its end connections, is capable of sustaining the design tensile force.

In addition, it will be necessary to verify that these ties and their end connections have a ductility at least equal to the ductility associated with the design tensile force obtained.

Limitations

The proposed formula (Equation 3.3) can be used provided that the rotational ductility α is more significant than a minimum threshold. Below this limit, another approach should be considered.

Also, the new treatment has yet to be verified and validated by comparing the results to experimental tests and numerical tests, and the factors have yet to be calibrated. It is therefore still too early to be able to apply it, but it will constitute a new, more realistic procedure of the prescriptive tying method.

2.1.1.3 Summary of the approach

Figure 3.2 summarizes the main points of the procedure currently proposed by Eurocode and of the procedure under development.

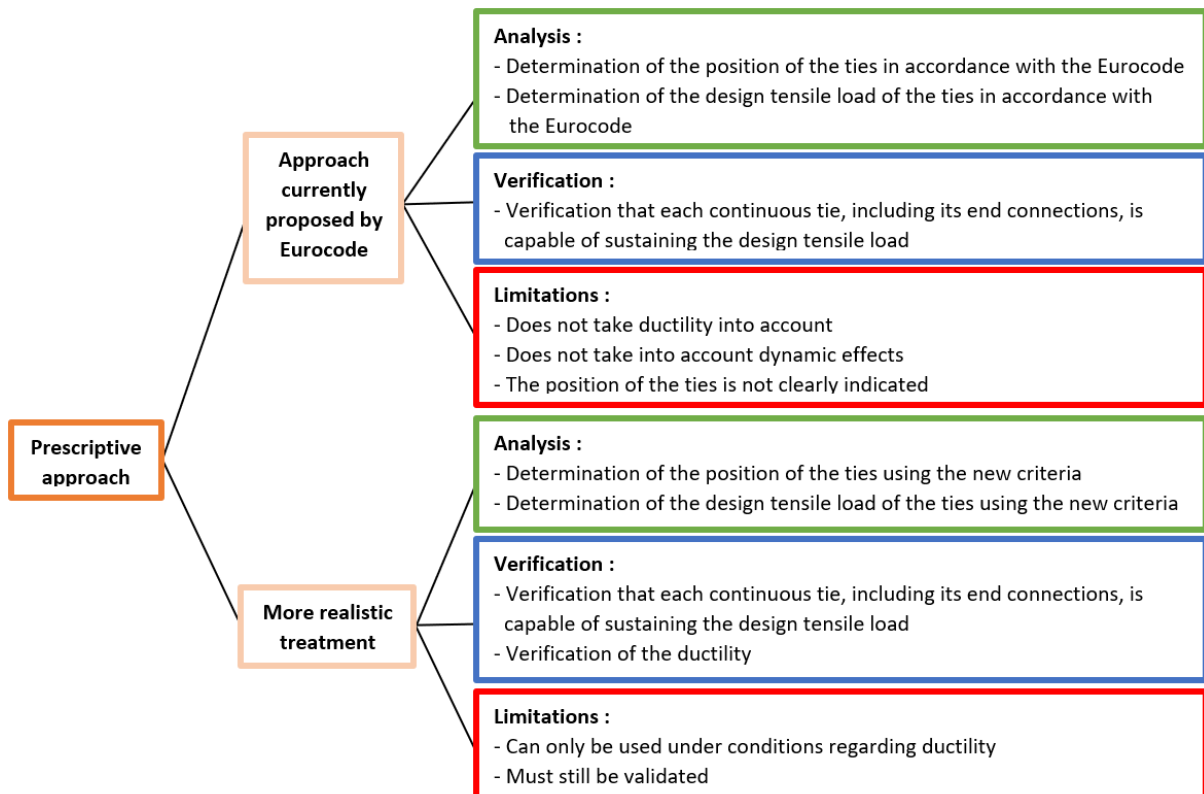


Figure 3.2: Procedure by opting for the prescriptive approach

2.1.2 Analytical approach

As shown in Figure 3.1, another possible approach to the alternative load paths method is an analytical approach. This will generally be used for consequence class structures CC3. It is based on an analytical model developed within the University of Liège (Belgium), allowing to describe the response of a 2D steel frame subjected to column loss, which will be presented below.

2.1.2.1 Description of the analytical model developed

Consider the scenario of the loss of the column in red in Figure 3.3.

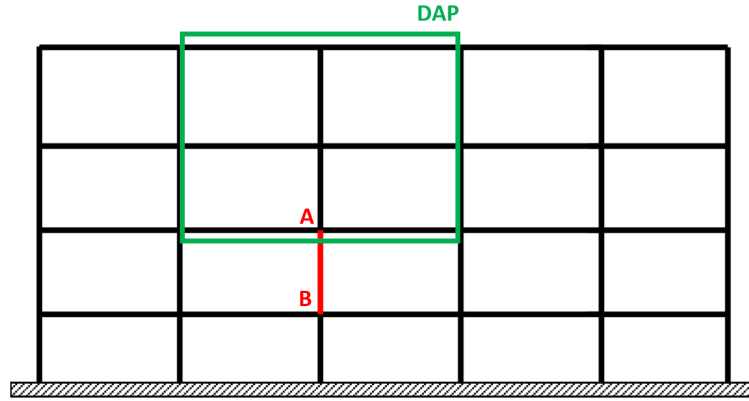


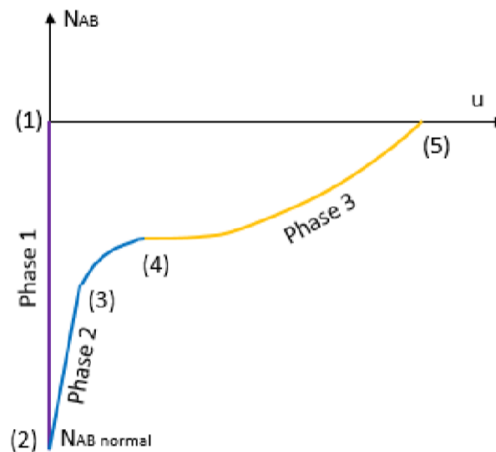
Figure 3.3: Column loss scenario

When a frame is subject to column loss, two parts can be identified in the structure :

- The directly affected part (DAP): contains all the beams, columns, and beam-column joints located just above the lost column (part framed in green in Figure 3.3).
- The indirectly affected part (IAP): contains the rest of the structure (i.e., the lateral parts and the storeys under the lost column).

The structure is then supposed to collapse following the formation of a plastic mechanism in the DAP.

The loss of the column can be represented using the relation $N_{AB} - u$, where N_{AB} is the axial load in the lost column, and u is the vertical displacement at the top of this column. This relation is represented in Figure 3.4. In this figure, three phases can then be distinguished.


 Figure 3.4: $N_{AB} - u$ relationship [2]

Phase 1: This phase is the loading of the structure in its normal situation. During this phase, the axial force in the beam evolves in compression and the vertical displacement u is zero (the column shortens a little, but this is assumed to be negligible). An effort $N_{AB,design}$ is then reached under the design loads.

Phase 2: During this phase, the column begins to be lost. First, the response of the structure is in the elastic domain up to point 3 (see Figure 3.4). In point 3, a loss of rigidity appears. This is due to the appearance of a plastic hinge in the DAP (see Figure 3.5). Plastic hinges then continue to appear in the DAP until the appearance of a plastic mechanism in point 4.

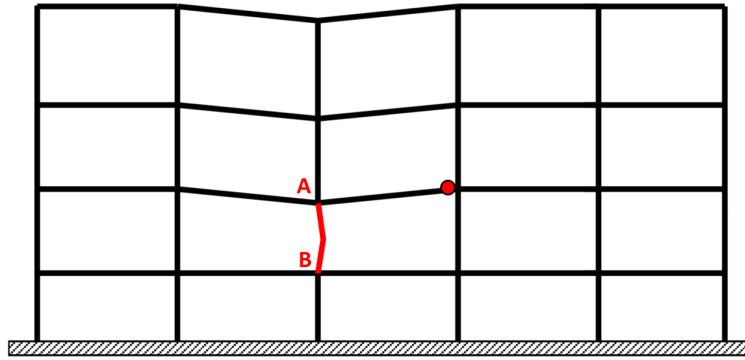


Figure 3.5: Appearance of a first plastic hinge

Phase 3: This phase begins when a plastic mechanism has formed in the DAP (see Figure 3.6). Significant deformations and displacements will then appear in the DAP. As a result, membrane forces will develop. In beams linked to the lost column, there will be a significant tensile force. This effort will be less in the upper beams. Also, if the structure is high enough, compression forces can develop in the beams of the top storey due to arc effect.

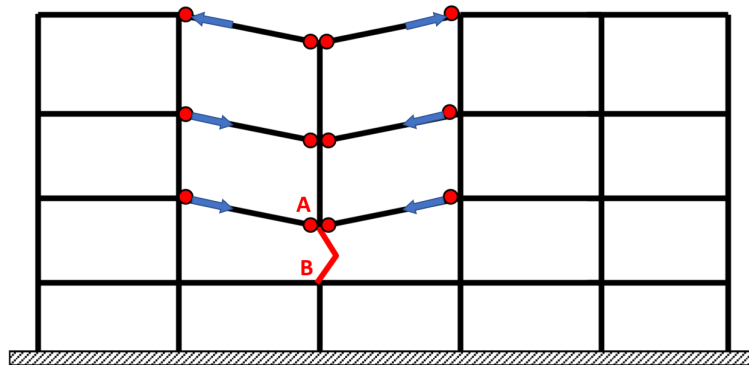


Figure 3.6: Formation of a plastic mechanism

The first two phases can be obtained quite easily. On the other hand, phase 3 is more complex to predict. This is why, in recent years, the University of Liège has developed an analytical model capable of reproducing this third phase of the response of a structure undergoing a column loss. This model was developed and perfected through various theses, including Demonceau's Ph.D. thesis in 2008 [5], Hai's Ph.D. thesis in 2008 [6], Huvelle's Master thesis [7] in 2011 and his research conducted in Liège [8], and Mathilde's Master thesis in 2019 [9].

The model is developed from a substructure. It is based on a second-order elastic-perfectly plastic analysis of this substructure. Indeed, significant displacements occur during phase 3, and a second-order analysis is necessary. The model takes into account the lateral restraint of the IAP, the M-N interaction in the plastic hinges and the elongation of the plastic hinges, following the development of catenary actions.

Analytical model assumptions

The analytical model is, however, based on several hypotheses listed below:

- It is assumed that the IAP remains in the elastic domain. That is to say that a plastic hinge will not form in the IAP before the complete formation of the plastic mechanism in the DAP.
- The elements making up the DAP follow an elastic-perfectly plastic law and are supposed to be infinitely ductile.

- The dynamic effects associated with the loss of the column are neglected. The loss of the column is assumed to be quasi-static.
- All plastic hinges are assumed to form at the same time, and no plastic hinge forms in the columns.
- The model only applies to the loss of an internal column in the structure so that the structure collapses following the development of a complete plastic mechanism in the DAP.
- The structural effect of the slabs is neglected. The analytical model applies to steel structures for which the structural elements are beams and columns only.
- Only the elastic axial extension of the beams is taken into account. Beams are assumed to have infinite flexural stiffness. This hypothesis can be made because phase 3 is governed by the development of membrane forces.

Definition of the substructure

The substructure from which the analytical model is developed is shown in Figure 3.7.

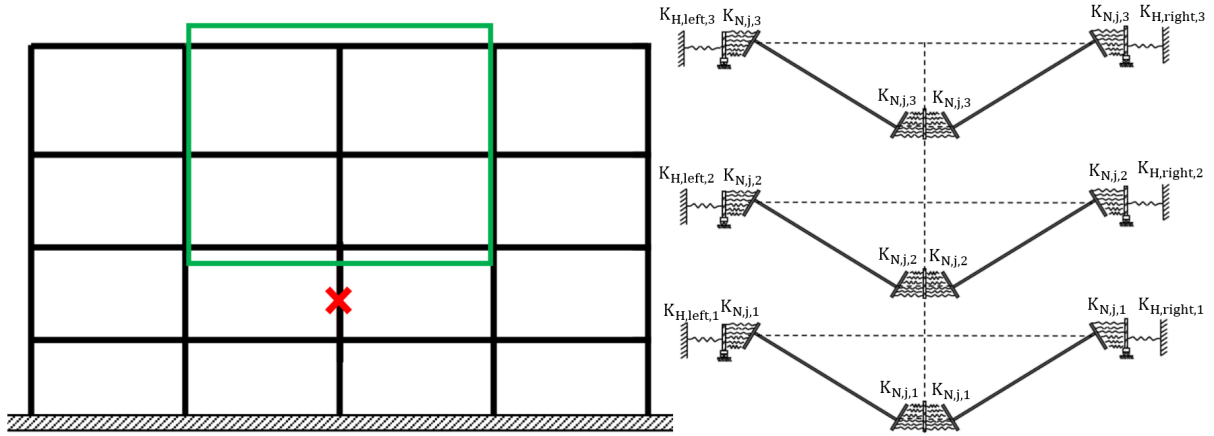


Figure 3.7: Substructure

This substructure is made up of all the storeys of the directly affected part (DAP) to take into account the effects of coupling between them. The coupling effects between the indirectly affected part (IAP) and the directly affected part (DAP) are also taken into account using horizontal stiffness springs $K_{H,left,i}$ and $K_{H,right,i}$.

Then, each set of parallel springs of stiffness $K_{N,j,i}$ represents a plastic hinge. The analytical model allows plastic hinges to form either at the ends of the beams (in the case of full strength joints) or in the joints (in the case of partial strength joints).

Note that the columns are not modeled because their elongation is neglected and the assumption has been made that no plastic hinges forms in the columns. Also, the substructure does not take into account the distributed loads because Demonceau has demonstrated in his Ph.D. thesis [5] that they do not influence the third phase of the response of the structure.

Parameters $K_{H,left,i}$ and $K_{H,right,i}$

As mentioned, these parameters take into account the coupling effects between the IAP and the DAP. The unique horizontal left (or right) spring of the i^{th} storey of stiffness $K_{H,left,i}$ (or $K_{H,right,i}$) is, in fact, a series of N springs of flexibility $S_{left,ij}$ (or $S_{right,ij}$), where N is the number of storeys

of the DAP and $i, j = 1, 2, \dots, N$.

$S_{left,ij}$ (or $S_{right,ij}$) characterizes the displacement to the left (or to the right) on storey i of the DAP when a unitary horizontal force acts on the IAP on the left (or right) of storey j of the DAP. The interactions between the movements occurring on one side of the substructure and the forces acting on the other are neglected.

Therefore,

- S_{left} is the flexibility matrix (of size $N \times N$) characterizing the displacements on the left side of the DAP, with $K_{H,left} = 1/S_{left}$.
- S_{right} is the flexibility matrix (of size $N \times N$) characterizing the displacements on the right side of the DAP, with $K_{H,right} = 1/S_{right}$.

These matrices can be determined by a first-order analysis of the IAP. As shown in Figure 3.8, by applying a unit force to a storey of the IAP, it is possible to obtain the displacements of each storey corresponding.

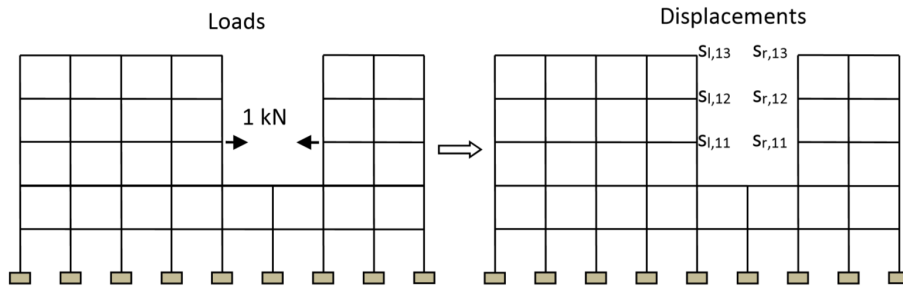


Figure 3.8: Determination of flexibility matrices [8]

Also, since the IAP remains in the elastic domain (see hypotheses), the springs simulating the IAP remain in the elastic domain.

Parameters $K_{N,j,i}$

As explained above, $K_{N,j,i}$ are parameters that represent the formation of plastic hinges either in the beam or in the joints.

a) Plastic hinges in the beam:

If the joints are at full strength, the plastic hinges will form in the beam.

In this case, a series of hypotheses is hidden behind the analytical model to represent the plastic hinges. The assumptions are as follows:

- Spring represents a part of the plastic hinge's section.
- The springs follow a symmetrical elastic-perfectly plastic law.
- The yielded zone is assumed to be finite and constant during phase 3.
- The sections at the extremities of the spring remain straight.

Then, a plastic hinge is represented by a set of 6 parallel springs (see Figure 3.9). Indeed, the section of the plastic hinge can be divided into six parts. Therefore, two springs represent the flanges (of resistance $F_{Rd,1}$ and stiffness K_1) and four springs represent the web (of resistance $F_{Rd,2}$ and stiffness K_2). Therefore, $K_{N,j,i} = K_1$ for $j = 1$ or 6 , and $K_{N,j,i} = K_2$ for $j = 2, 3, 4, 5$.

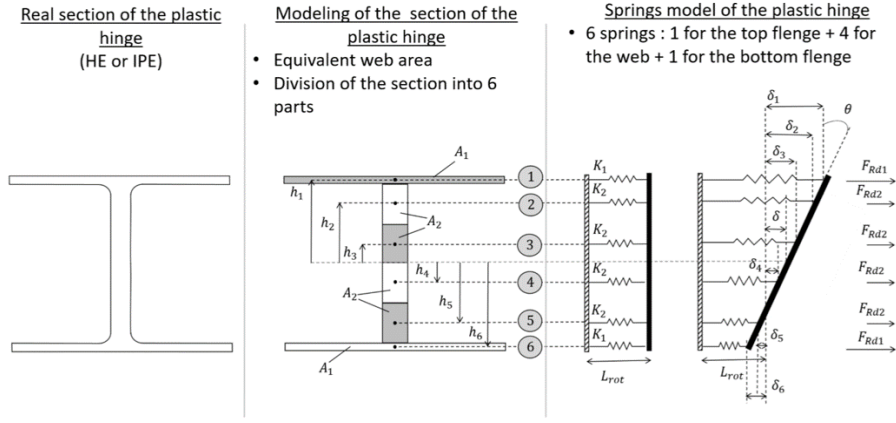


Figure 3.9: Modeling of plastic hinges in the beam [9]

Plastic hinges can, therefore, be characterized by:

1. The length of the plastic hinge L_{rot} :

$$L_{rot} = \frac{L}{2} \cdot \left(1 - \frac{M_{el}}{M_{pl}}\right) \quad (3.4)$$

Where L is the length of the beam in which the hinge is formed, and M_{el} and M_{pl} are the elastic and plastic bending moments of the beam, respectively.

2. The axial resistance of the springs:

$$\begin{cases} N_{pl,Rd} = 4 \cdot F_{Rd,2} + 2 \cdot F_{Rd,1} \\ M_{pl,Rd} = 2 \cdot F_{Rd,1} \cdot h_1 + 2 \cdot F_{Rd,2} \cdot (h_2 + h_3) \end{cases} \quad (3.5)$$

$$\begin{cases} F_{Rd,1} = \frac{2 \cdot M_{pl,Rd} - 0.25 \cdot (h_2 + h_3) \cdot N_{pl,Rd}}{h_1 - 0.5 \cdot (h_2 + h_3)} \\ F_{Rd,2} = 0.25 \cdot (N_{pl,Rd} - 2 \cdot F_{Rd,1}) \end{cases} \quad (3.6)$$

3. The stiffness of the springs:

$$\begin{cases} K_1 = \frac{E \cdot A_1}{L_{rot}} \\ K_2 = \frac{E \cdot A_2}{L_{rot}} \end{cases} \quad (3.7)$$

Where A_1 and A_2 are the areas of portions illustrated in Figure 3.9.

b) Plastic hinges in joints:

The plastic hinges will form in the joints when they are partially resistant.

In this case, the assumptions made by the analytical model are as follows:

- Spring represents a component of the joint (or a part of the slab which is part of the joint).
- The springs follow a non-symmetric elastic-perfectly plastic law.
- The components are assumed to have infinite ductility.
- The bolts have no compressive strength.

- Concrete is assumed to have no tensile strength.
- The length of a plastic hinge is assumed to be zero.
- The characteristics (resistance and stiffness) of the springs representing a component of the joint are determined by the component method (Eurocode 3 and Eurocode 4).
- The characteristics of the springs representing a part of the slab are determined by the method developed by Démonceau [5].

Also, if the plastic hinges form in the joints, the elongation will be made at the joints, and the beams will not elongate.

System of equations to solve

a) Plastic hinges in the beam:

Knowing the characteristics of the plastic hinges described above as well as the flexibility matrices, it is, therefore, possible to solve the system of $21N + 1$ equations and $21N + 1$ unknowns (with N representing the number of storeys of the DAP) presented in Table 3.1. The resolution of this system enables to obtain the value of N_{lost} (force applied to the structure due to the removal of the column) associated with the value of u (vertical displacement at the top of the lost column) introduced into the system. Therefore, by solving the system for all value of u , it is possible to draw the phase 3 of the relation $N_{lost} - u$. It is also possible to draw phase 3 of the relation $N_{AB} - u$ represented in Figure 3.4 knowing that the effort N_{AB} in the lost column is worth $N_{AB} = N_{AB,design} - N_{lost}$.

Note that the equation system assumes that the lost column is located in the center of the structure. If the lost column is not a column located in the center of the structure, the IAP is not symmetrical. Consequently, the flexibility matrices S_{left} and S_{right} defined previously are not identical, and a horizontal shift appears towards the most rigid side of the IAP (see Figure 3.10). To solve the system of equations, this horizontal shift is neglected, and equivalent flexibility matrices are considered.

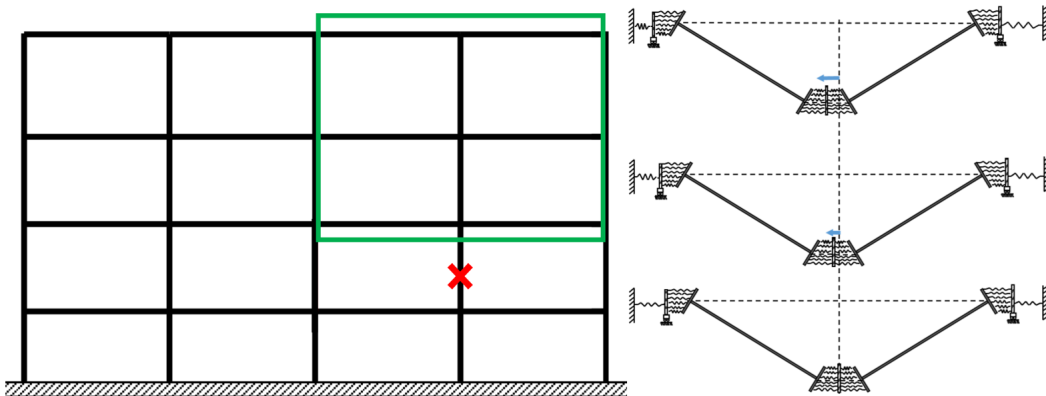


Figure 3.10: Horizontal shift of the substructure

| Unknown | Descriptions | Equations | Number of unknowns |
|--------------------|---|---|--------------------|
| θ_i | Angle of rotation of the beams' extremities of storey i | $\sin(\theta_i) = \frac{u}{L_0 - 2L_{rot,i+i}}$ | N |
| δ_i | Horizontal displacement at the middle of the beams' extremities of the storey i | $\cos(\theta_i) = \frac{L_0 - 2L_{rot,i} - \lambda_{H,i} - 2\lambda_i}{L_0 - 2L_{rot,i+i}}$ | N |
| Δ_{Li} | Elastic elongation of the beams of storey i between the yielded zones | $\Delta_{L,i} = F_{H,i} \cdot \frac{L_0 - 2L_{rot,i}}{EA_i}$ | N |
| δ_{ji} | Horizontal displacement of the spring j (j=1,...,6) of the storey i | $\delta_{ij} = \delta_i + h_{ji} \cdot \theta_i \text{ with } j = 1, \dots, 6$ | 6N |
| F_{ji} | Horizontal force on spring j of storey i | $\left. \begin{array}{l} -F_{Rd1,i} \\ \min(F_{Rd1,i}; F_{pre,ji} + K_{1,i}\delta_{pre,ji}) \end{array} \right\} \text{if } j=1,6$ $\left. \begin{array}{l} -F_{Rd2,i} \\ \min(F_{Rd2,i}; F_{pre,ji} + K_{2,i}\delta_{pre,ji}) \end{array} \right\} \text{if } j=2,3,4,5$ | 6N |
| F_{Hi} | Internal horizontal force at the ends of the beams of storey i | $F_{H,i} = \sum_{j=1}^6 F_{ji}$ | N |
| M_i | Internal bending moment at the ends of the beams of storey i | $M_i = \sum_{j=1}^6 F_{ji} \cdot h_{ji}$ | N |
| P_i | External vertical force applied above the lost column | $-0.5 \cdot P_i \cdot (L_0 - \delta_{H,i}) + F_{H,i}u + 2 \cdot M_i = 0$ | N |
| $\delta_{left,i}$ | Horizontal displacement of the IAP to the left of storey i | $\delta_{left,i} = \sum_{j=1}^N S_{left,ij} \cdot F_{H,j}$ | N |
| $\delta_{right,i}$ | Horizontal displacement of the IAP to the right of storey i | $\delta_{right,i} = \sum_{j=1}^N S_{right,ij} \cdot F_{H,j}$ | N |
| δ_{Hi} | Equivalent horizontal displacement of storey i | $\delta_{H,i} = 0.5 \cdot (\delta_{left,i} + \delta_{right,i})$ | N |
| N_{lost} | Vertical force applied to the structure due to the removal of the column | $N_{lost} = \sum_{i=1}^N P_i$ | 1 |

Table 3.1: System of equations to solve if the plastic hinges are located in the beam

 b) Plastic hinges in joints:

The system to solve presents this time $(9 + 4 \cdot n_s) \cdot N + 1$ equations and $(9 + 4 \cdot n_s) \cdot N + 1$ unknowns, where n_s is the number of parallel springs. This system is detailed in Table 3.2.

| Unknown | Descriptions | Equations | Number of unknowns |
|--------------------|--|--|--------------------|
| θ_i | Angle of rotation of the beams' extremities of storey i | $\sin(\theta_i) = \frac{u}{L_0}$ | N |
| $\delta_{SAG,i}$ | Horizontal displacement at the end of the sagging moment side | $L_0 \cdot (\cos(\theta_i) - 1) + \delta_{Hi} + \delta_{SAG,i} + \delta_{HOG,i}$ | N |
| $\delta_{HOG,i}$ | Horizontal displacement at the end of the hogging moment side | $F_{Hi} = \sum_{j=1}^n {}_sF_{SAG,ji}$ | N |
| F_{Hi} | Internal horizontal force at the ends of the beams of storey i | $F_{H,i} = \sum_{j=1}^6 F_{ji}$ | N |
| $\delta_{left,i}$ | Horizontal displacement of the IAP to the left of storey i | $\delta_{left,i} = \sum_{j=1}^N S_{left,ij} \cdot F_{H,j}$ | N |
| $\delta_{right,i}$ | Horizontal displacement of the IAP to the right of storey i | $\delta_{right,i} = \sum_{j=1}^N S_{right,ij} \cdot F_{H,j}$ | N |
| δ_{Hi} | Equivalent horizontal displacement of storey i | $\delta_{H,i} = 0.5(\delta_{left,i} + \delta_{right,i})$ | N |
| $M_{SAG,i}$ | Sagging moment at storey i | $M_{SAG,i} = \sum_{j=1}^n {}_sF_{SAG,ji} \cdot h_{ji}$ | N |
| $M_{HOG,i}$ | Hogging moment at storey i | $M_{HOG,i} = \sum_{j=1}^n {}_sF_{HOG,ji} \cdot h_{ji}$ | N |
| $F_{SAG,ji}$ | Horizontal force applied to the spring j of the storey i on the side of the sagging moment | $F_{SAG,ji} = f(\delta_{SAG,ji})$ | $n_s N$ |
| $F_{HOG,ji}$ | Horizontal force applied to the spring j of the storey i on the side of the hogging moment | $F_{HOG,ji} = f(\delta_{HOG,ji})$ | $n_s N$ |
| $\delta_{SAG,ji}$ | Horizontal displacement of the spring j of the storey i on the side of the sagging moment | $\delta_{SAG,ji} = \delta_{SAG,i} + h_{ji} \cdot \theta_i$ | $n_s N$ |
| $\delta_{HOG,ji}$ | Horizontal displacement of the spring j of the storey i on the side of the hogging moment | $\delta_{HOG,ji} = \delta_{HOG,i} + h_{ji} \cdot \theta_i$ | $n_s N$ |
| N_{lost} | Vertical force applied to the structure due to the removal of the column | $N_{lost}(L_0 \cos(\theta_i)(F_{Hi}u + M_{HOG,i} - M_{SAG,i}) = 0$ | 1 |

Table 3.2: System of equations to solve if the plastic hinges are located in the joints

2.1.2.2 Analysis

Using the analytical approach, the analysis of the structure is then done in several stages using the analytical model which has just been presented.

Firstly, it is necessary to identify the damaged column in the structure for the exceptional scenario considered.

Secondly, by carrying out a first-order analysis of the undamaged structure under the combination of accidental loads, it is possible to obtain the initial compression force N_0 in the column which will be lost.

Thirdly, the flexibility matrices taking into account the coupling effects between the IAP and the DAP can be obtained from a first-order analysis of the IAP, by applying a unit force to a storey as explained above (see Figure 3.8).

Finally, it is possible to solve the appropriate system of equations depending on the position of the plastic hinges (in the beam or the joints). As a reminder, the system of equations is based on a second-order elastic-perfectly plastic analysis of the substructure considered. Solving this system by increasing the value of u (vertical displacement at the top of the lost column) leads to gradually draw phase 3 of the graph $u - N_{lost}$.

2.1.2.3 Verification

The verifications will concern the structural elements (beams and columns) and also the joints.

a) Verification of structural elements:

First, when the joints are at full strength, it is necessary to check the ductility of the beams of the DAP when $N_{lost} = N_0$ (i.e., when the column is completely lost) because these beams were supposed to be infinitely ductile and can, therefore, be extended indefinitely. When the plastic hinges form in the beams, they lengthen. The resolution of the system of equations provides the elongations in the beams at each storey. It is then possible to check if the beams are sufficiently ductile to undergo these elongations.

Then, it is necessary to check the top beam of the DAP under M-N interaction. Indeed, if the structure is high enough and the IAP is not too rigid, compression forces will appear in this beam. This beam may then yield by lateral buckling under M-N interaction (if the lateral buckling is not prevented). However, ruin by lateral buckling is not covered by the analytical model developed and must, therefore, be verified.

Finally, the equation system is based on the assumption that the IAP remains in the elastic domain (because the flexibility matrices are constant). However, it turns out that this hypothesis is not always respected. In some cases, plastic hinges can form in the IAP before the column is completely lost. It is, therefore, important to check the resistance of the IAP. However, note that in his Master thesis [9], Mathilde Jacques introduced the yielding of the IAP in the analytical model. This implementation has a fairly limited scope (applicable only in the event of the loss of a column on the ground floor), and the precision and limits of the models still need to be studied, but this constitutes a first interesting improvement. In the future, the yielding of the IAP could probably be introduced into the analytical model, and the IAP should no longer be subject to verification.

b) Verification of joints:

When the joints are partially resistant, the plastic hinges are formed in the joints. In this case,

the resistance and the stiffness of the components of the joints were introduced into the model, but their ductility was supposed to be infinite. It is therefore necessary to check the ductility of these components.

On the other hand, when the joints have been assumed to be fully resistant, it must be verified that this is the case. The system of equations provides the moment M_i and the horizontal force $F_{H,i}$ at the ends of the beams of storey i . It is, therefore, necessary to verify that these efforts respect the M-N interaction criterion. There are two M-N interaction criteria that can be used. First, an M-N interaction criterion is proposed in Part 1-8 of Eurocode 3, but this criterion presents some inconsistencies. Then, a more coherent M-N interaction criterion can also be obtained by using an improved analytical assembly procedure developed within the University of Liège [10]. These interaction criteria will be presented below.

2.1.2.4 Criterion of the resistance of joints under M-N interaction

The design of structural steel joints is covered by Eurocode 3. In this Eurocode, the behaviour of joints is studied by the component method. This method provides the main mechanical properties of a joint (its rigidity, its resistance and the associated failure mode).

This method is divided into three steps:

1. The identification of the active components of the joint: a joint is made up of different components and it is necessary to identify those which are stressed by the efforts.
2. Characterisation of the mechanical properties of these components: for each component, it is necessary to calculate its mechanical properties such as its resistance and its stiffness.
3. The assembly of the components to obtain the mechanical properties of the joint: the resistance of the joint will be equal to the smallest resistance of its components.

However, in the case of a structure undergoing the loss of a column, the joints (as long as they have a certain rigidity) are subjected to an M-N interaction, and the efforts vary following the development of membrane forces. Therefore, the activated components within the joint vary according to the values of the bending moments and the applied axial forces, and an appropriate assembly procedure is necessary.

Part 1-8 of Eurocode 3

Part 1-8 of Eurocode 3 proposes an approach in which the influence of the interaction M-N is ignored as long as $N_{Ed} < 5\% \cdot N_{pl,Rd}$, where N_{Ed} is the axial force applied to the joint and $N_{pl,Rd}$ is the axial design plastic resistance of the connected beam cross-section. On the other hand, when $N_{Ed} > 5\% \cdot N_{pl,Rd}$, the interaction between M and N is linear.

The resistance criterion of a joint would, therefore, have the appearance hereafter (Figure 3.11).

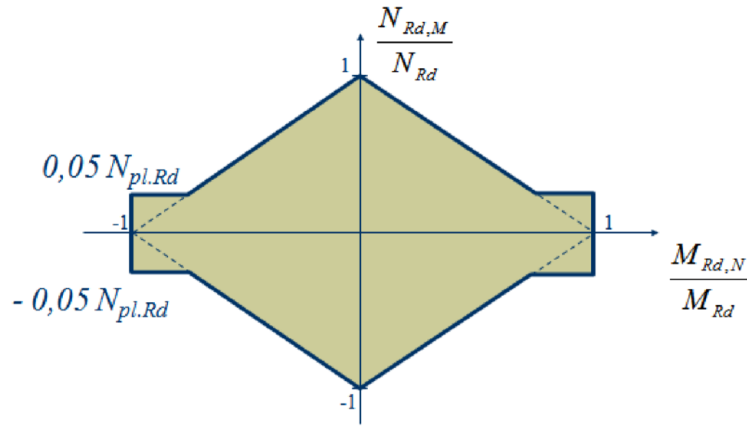


Figure 3.11: Criterion of the resistance of a joint under M-N proposed by Eurocode 3 Part 1-8 [2]

This criterion assumes that axial forces less than $5\% \cdot N_{pl,Rd}$ do not significantly influence the response in the rotation of the joints. However, it turned out that the choice of 5% is completely arbitrary and is not always satisfactory.

Also, in Cerfontaine’s Ph.D. thesis [11], it has been shown that the linear interaction criterion M-N in Figure 3.11 is often too safe. Still, on the other hand, the criterion of 5% overestimates the resistance.

Improved analytical assembly procedure

In view of the problems concerning the criterion proposed in Part 1-8 of Eurocode 3, an improved analytical assembly procedure has been developed at the University of Liège. It was developed and validated for steel joints, and then it was extended to composite steel-concrete joints. This procedure is presented in [10] by focusing only on the calculation of the resistance, but the rigidity under M-N interaction is treated in [11].

For example, in the context of a single-sided joint consisting of bolts and a column web panel in shear, each component of the joint can be represented by a spring, and each spring has a non-linear force-displacement relationship (see Figure 3.12). The analytical method developed will then enable, after calculating the properties of each component, to assemble the components, and to calculate the resistance under M-N interaction of the joint.

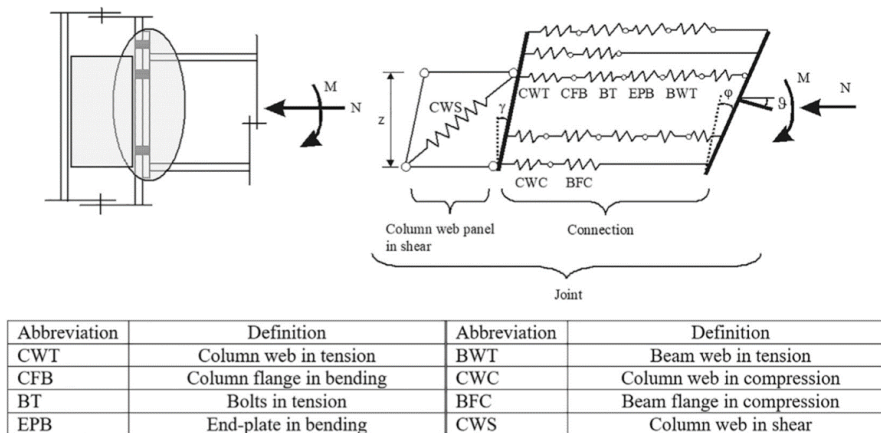


Figure 3.12: Modeling of a single-sided joint [10]

The interaction criterion developed meets the requirements in terms of group effects and interaction between components. Indeed, group effects can appear when certain bolts are close to each

other because a common failure mechanism will then develop around these bolts. These group effects are taken into account when calculating the resistance of the rows. Then, interactions between components can appear in the components extracted from the column. These are taken into account by criteria provided in Eurocode 3 Part 1-8.

Finally, it is interesting to note that the analytical assembly procedure developed is different if the connection is ductile or fragile. In the case of a ductile connection, the model is based on the assumption that the behavior of each component of the connection has infinite ductility. From then on, there will be a plastic redistribution of internal forces within the connection. On the other hand, when the connection is fragile, i.e., when the ductility of certain components (tension bolts, welds, etc.) is not sufficient to allow a total plastic redistribution of internal forces, there will be a fragile rupture of the whole connection. The presence of fragile components, therefore, reduces the resistance capacity of the connection. Consequently, in the case of a fragile connection, an adaptation of the resistance curve to the M-N interaction is carried out (see [10]).

2.1.2.5 Limitations

The analytical approach has some limitations. First, it is only applicable to the loss of one column per scenario. Also, this column must be internal. Finally, this approach does not take into account the structural effect of the slabs.

2.1.2.6 Summary of the approach

Figure 3.13 summarizes the procedure to be followed by choosing the analytical approach and the limitations of this approach.

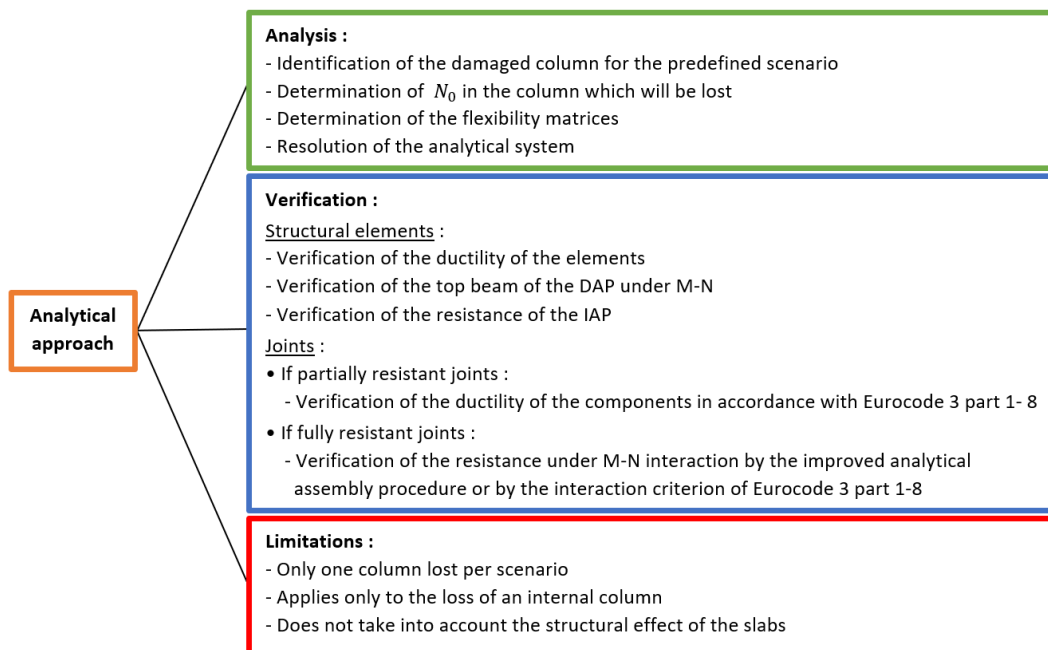


Figure 3.13: Procedure by opting for the analytical approach

2.1.3 Numerical approach

As presented in Figure 3.1, a third possible approach for the strategy of the alternative load paths is a numerical approach using non-linear calculation software.

2.1.3.1 Analysis

As with the analytical approach, the first thing to do is to identify the damage for the predefined scenario. The difference is that, using the numerical approach, it is possible to consider that several elements (internal or external) are damaged for the same scenario.

Then, using a non-linear calculation software (such as the finite element calculation software *FINELG*), it is possible to perform a second-order non-linear analysis of the damaged structure under the combination of accidental loads. The loss of a column can, for example, be simulated as follows.

The first step consists of applying, on the damaged structure, the combination of accidental loads as well as the forces V_0 , M_0 and N_0 (which are the efforts that the column initially took up before being lost) of the lost column, as shown in Figure 3.14.

Then, the second step consists of gradually applying forces λV_0 , λN_0 and λM_0 which are respectively opposite to the forces V_0 , M_0 and N_0 (see Figure 3.15). The load factor λ will gradually vary between 0 (the situation where the column is not damaged) and 1 (the situation where the column is completely lost). Reaching a factor $\lambda = 1$, therefore, means that the structure has been able to find a new configuration of equilibrium after the total loss of the column considered. Note that this procedure can also be used for scenarios for which several elements are damaged.

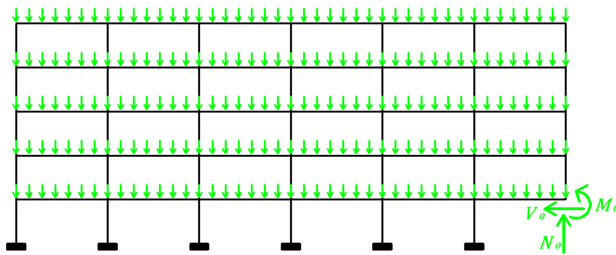


Figure 3.14: Simulation of the loss of column - Step 1 [2]

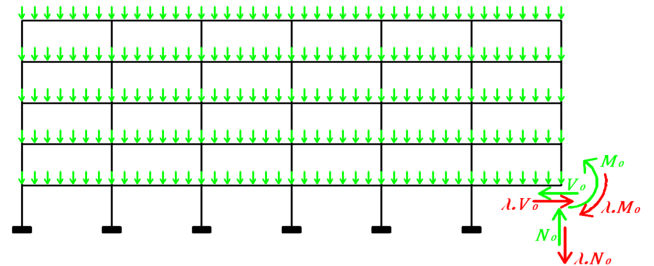


Figure 3.15: Simulation of the loss of column - Step 2 [2]

It is also important to note that the numerical model can take different things into account, and the more complete the model, the faster the verification phase.

First, if the structure studied is a braced structure with pinned joints (i.e., joints which are not at all moment resistant and allow for free rotation between the connected structural members), the properties of the joints (i.e., the elongation capacity and the resistance) can be introduced into the numerical model. Therefore, the joint should not be subject to subsequent verification.

On the other hand, if the structure studied is a structure with semi-rigid or rigid joints, it is currently not yet possible to introduce the properties of the joints in the numerical model. Indeed, in this case, an M-N interaction will develop in the joints and there are not yet finite elements capable of correctly taking into account the M-N interaction developing in joints. This is the subject of a Master thesis currently carried out.

Then, in the case of large structures, it is possible to model only a substructure defined beforehand. The rest of the structure must then be subject to verification.

2.1.3.2 Verification

a) Verification of structural elements:

It must be checked that the load factor λ reaches a value at least equal to 1, signifying that the structure has been able to find a new configuration of equilibrium having suffered the total loss of the damaged elements for the scenario considered.

Then, it is necessary to verify what was not taken into account in the model. If only a sub-structure was the subject of the non-linear analysis of the second-order, it is necessary to verify the resistance of the remainder of the structure.

b) Verification of joints:

In the case of pinned joints, if their properties (resistance and ductility) were not taken into account in the analysis, the resistance must be checked in accordance with Eurocode 3 Part 1-8.

Then, in the case of semi-rigid or rigid joints, there are two methods to verify the resistance of the joints, which are subjected to M-N interaction. As for the analytical approach, the verification of the resistance can be done with the improved analytical assembly procedure developed within the University of Liège [10] or possibly with the criterion proposed in Part 1-8 of the Eurocode 3.

2.1.3.3 Limitations

There are no particular limitations with the numerical approach. It applies to the loss of several elements by scenarios, and these elements can be both internal and external elements.

2.1.3.4 Summary of the approach

Figure 3.16 summarizes the procedure to be followed by choosing the numerical approach.

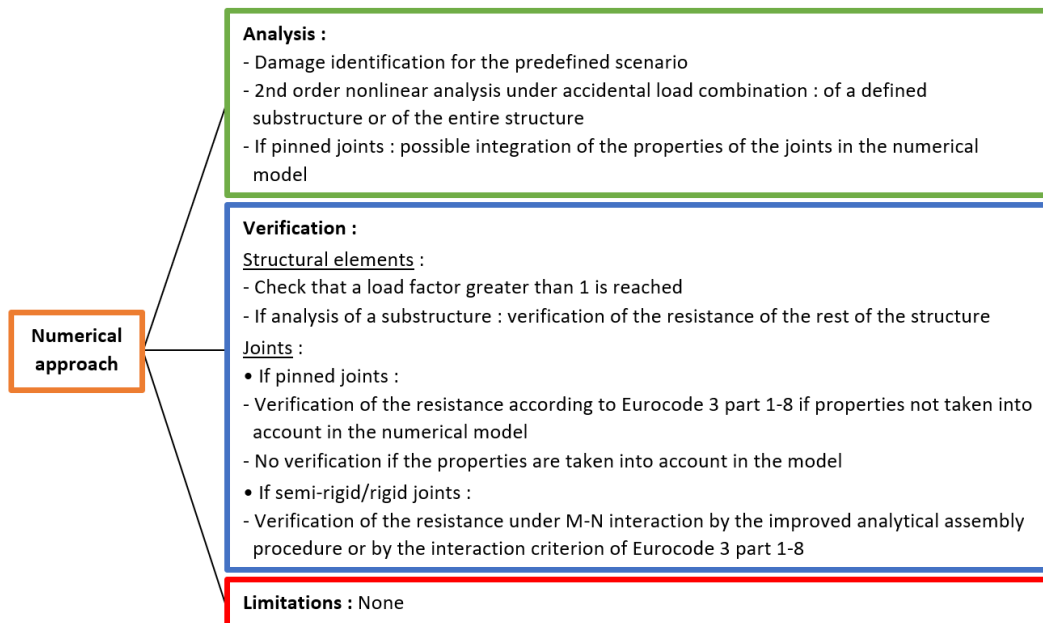


Figure 3.16: Procedure by opting for the numerical approach

2.1.4 Case of 3D structures

A 3D structure losing an internal column can be treated using the analytical approach or the numerical approach. Indeed, in their Master theses, Florence Lemaire [12] and Sergii Kulik [13]

studied the behavior of a 3D structure. They demonstrated that the response of a 3D structure losing one of its columns could be obtained quickly. It suffices to calculate the response of each of the 2D frames concerned by the loss of the column (a primary frame and a secondary frame) and to add the two responses.

However, if the 3D structure is subjected to the damage of several elements for the same scenario, it must be treated by a numerical approach in realising a three-dimensional model.

2.2 Key element method

As explained in the second chapter, and as shown in Figure 3.1, the key element method presents two approaches. On the one hand, certain elements are designed to support the structure against an exceptional event. These elements must, therefore, be sized and/or protected to remain intact against an exceptional event and will be sized by following the primary structure approach. On the other hand, certain key elements are designed to break quickly to avoid the propagation of the damages to the rest of the structure. These elements must, therefore, have fairly low resistance and a fragile failure mode so that they break quickly before transmitting excessive forces to their neighbors. They will be sized following the fuse approach.

2.2.1 Primary structure approach

2.2.1.1 Analysis

In the case of the primary approach, the first thing to do is to define the primary structure (i.e., the key structure), which supports the rest of the structure if an exceptional event occurs and which must be sized accordingly.

Then, it is necessary to determine the internal forces which this structure must be able to resist, according to the scenario of damage envisaged.

2.2.1.2 Verification

It is then necessary to verify that the primary structure (elements and joints) is capable of withstanding the forces determined.

2.2.2 Fuse approach

2.2.2.1 Analysis

In the case of the fuse approach, it is necessary to define the fuse elements which will have to yield before transmitting too great efforts.

It is also necessary to determine under which load they have to yield, i.e., which load is too important and can cause the progressive collapse of the structure if the fuse elements do not yield before.

2.2.2.2 Verification

It is necessary to check that the fuse elements yield for the load considered and that they break fast enough (that the ductility of the ruin is low enough) to avoid a progressive collapse of the structure. It is therefore also necessary to check the resistance of the rest of the structure.

2.2.3 Summary of the key element method

Figure 3.17 summarizes the possible approaches by choosing the method of the key element.

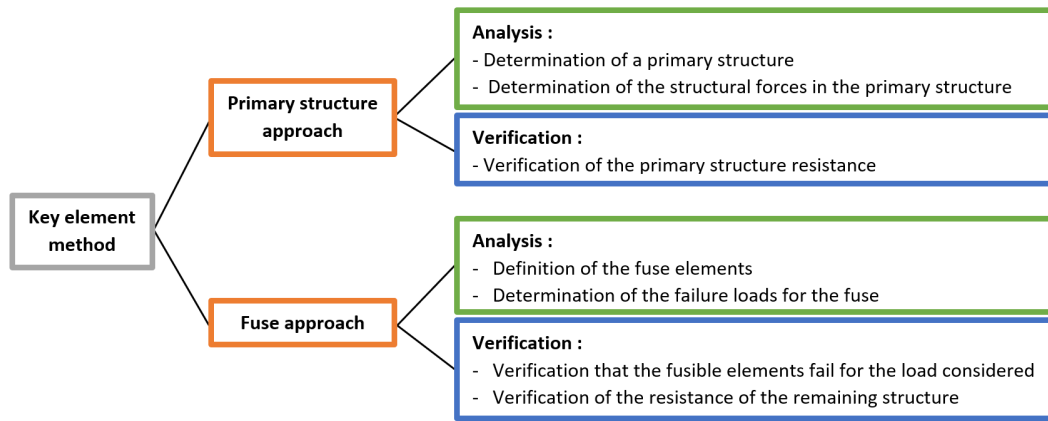


Figure 3.17: Possible approaches by opting for the key element strategy

3 Identified exceptional actions

As explained, three strategies can be envisaged to design a structure under an identified exceptional action. However, approaches will only be developed for the strategy involving the design of the structure to sustain the action. These approaches will concern two types of loading: impacts and blast loadings.

3.1 Design under impact loading

Under the impact load, the approaches presented in Figure 3.18 can be considered.

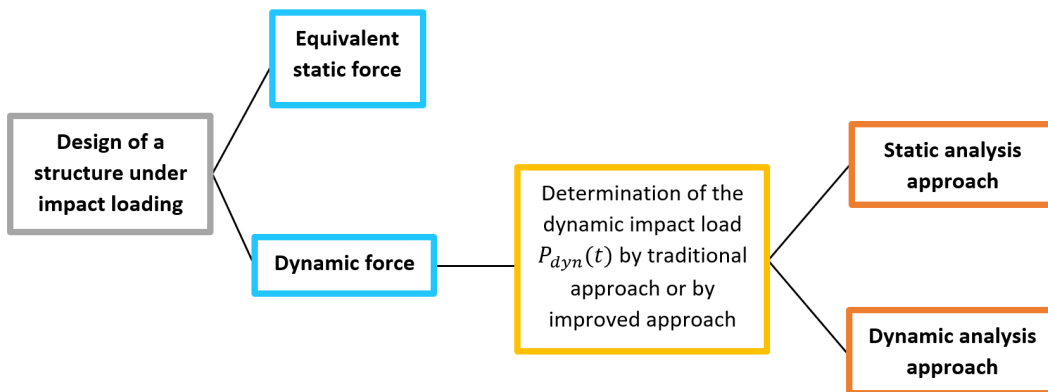


Figure 3.18: Possible approaches to design under impact loading

3.1.1 Equivalent static force

If the consequence class is sufficiently low (consequence class CC2), an equivalent static force approach can be performed.

3.1.1.1 Analysis

The first thing to do is then to determine the equivalent static force. Eurocode offers tables with equivalent static forces to be applied to a column impacted by a vehicle, for example.

Then, the structure must be analysed under the combination of accidental loads and by applying the equivalent static force representing the impact. To do this, a first-order linear analysis can be performed.

3.1.1.2 Verification

a) Verification of structural elements:

It is necessary to carry out a plastic verification of the resistance (in section and instabilities) of the elements of beams and columns.

b) Verification of joints:

The resistance of the joints must also be checked in accordance with Eurocode 3.

3.1.1.3 Summary of the approach

Figure 3.19 summarizes the procedure to be followed by choosing the equivalent static force approach.

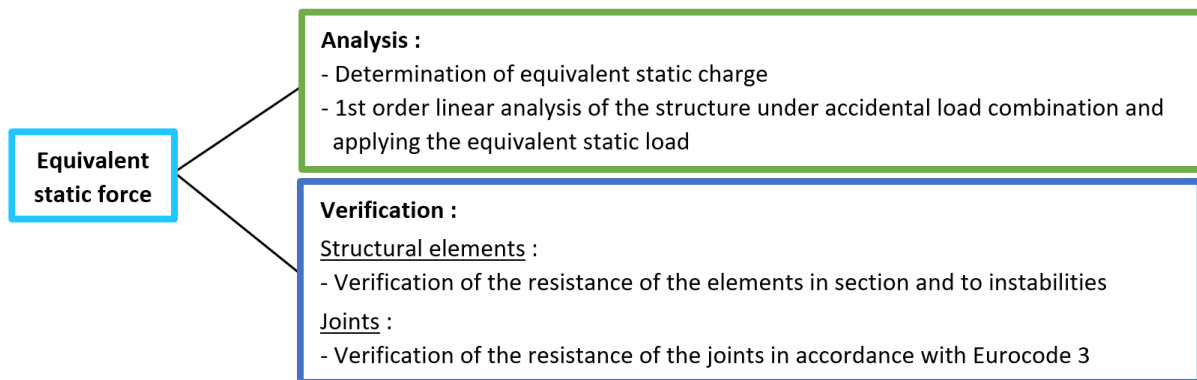


Figure 3.19: Procedure by opting for the equivalent static force approach

3.1.2 Dynamic force

When the consequence class of the structure is CC3, it will be necessary to consider a dynamic load. The first thing to do is to determine the dynamic impact load $P_{dyn}(t)$ (as shown in Figure 3.18). Then, two main approaches can be envisaged, the static analysis approach and the dynamic analysis approach.

3.1.2.1 Determination of the dynamic load $P_{dyn}(t)$

To represent an impact on a column, different scenarios can be considered, and therefore different possibilities for the charge $P_{dyn}(t)$. The dynamic load $P_{dyn}(t)$, which characterises how the bearing capacity of a column decreases when it is subjected to an impact, can be determined in two ways. There is a traditional method, and then, in his work, C. Colomer established an improved procedure [14].

First, it is possible to use a traditional analysis. In this case, the first thing to do is to calculate the maximum lateral deformation of the damaged column w_{max} based on the energy conservation principle, as described in [14]. To do this, it is necessary to know the kinetic energy of the impact. For a vehicle impact, for example, it is therefore necessary to determine the mass and the speed of the vehicles which would risk impacting the column. Then, there are two possibilities to determine the dynamic impact load $P_{dyn}(t)$. Either the lateral deformation w_{max} is sufficiently weak and it is supposed that there is no damage, or this deformation w_{max} is too important and it is supposed that the column is completely lost. This loss will then be linear, or eventually instantaneous (see Figure 3.20).

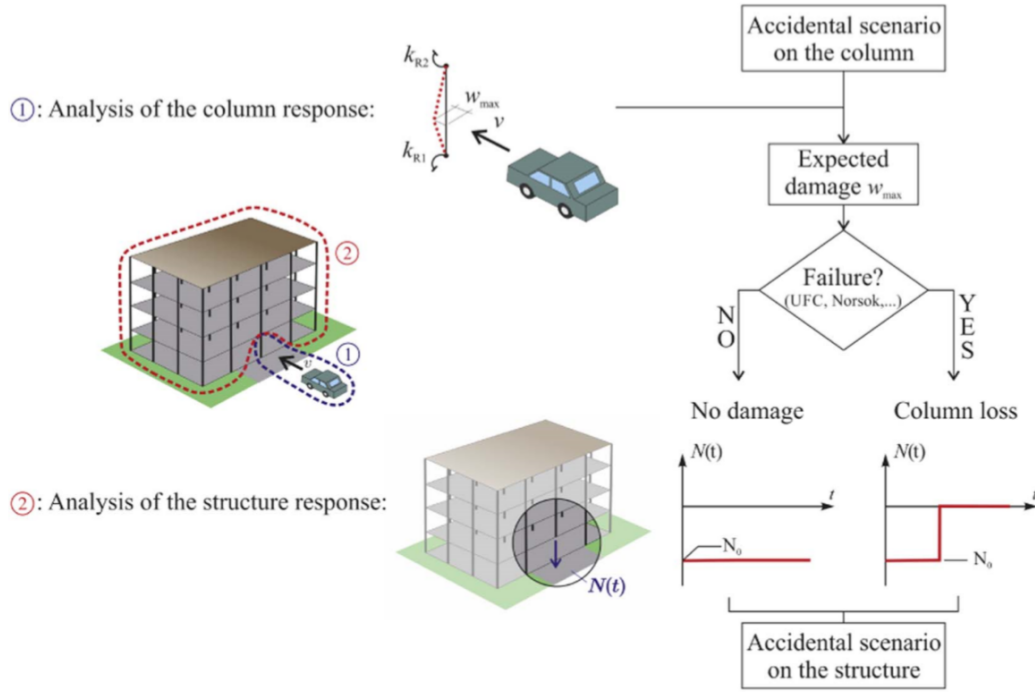


Figure 3.20: Traditional approach [14]

However, this simplified analysis presents a problem. It does not take into account mechanical coupling that exists between the column and the structure. This is why Colomer proposed an improved approach to take into account the link between the local response of the column subjected to an impact load and the overall response of the structure.

According to the approach he proposed, depending on the deformation of the column and its interaction with the rest of the structure, the column will be considered more or less damaged, and the function $P_{dyn}(t)$ will be different (see Figure 3.21). The following scenarios can be distinguished: no damage, moderate damage, critical damage, column tearing and column loss. Note that the *Critical damage* and *Column tearing* scenarios present loading functions which could be more unfavorable than the *Column loss* scenario. This method, therefore, requires taking into account the properties of the structure from which the column is derived and, more particularly, the connections between this column and the rest of the structure. The methodology to be followed is presented in [14].

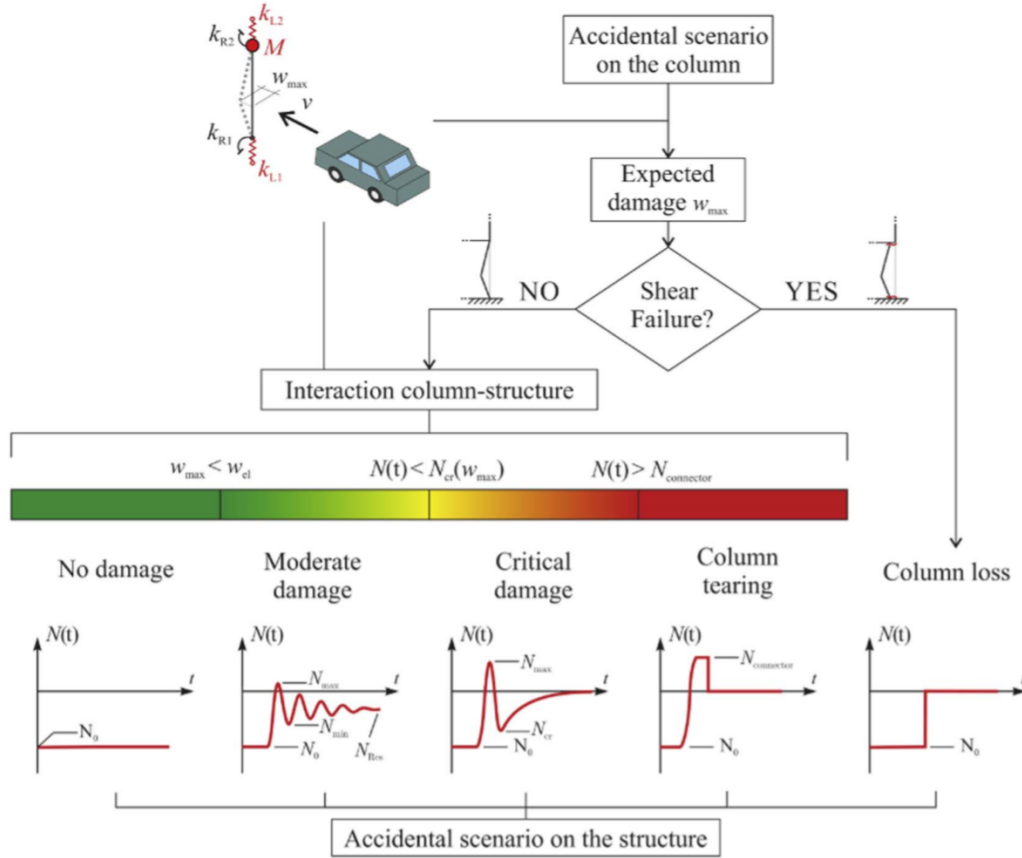


Figure 3.21: Improved approach [14]

3.1.2.2 Static analysis approach

If the approach by static analysis is chosen, it is necessary to calculate the maximum displacement at the top of the damaged column which will appear under the determined dynamic load. Then it will be possible to perform a static analysis of the structure. The verifications to be performed and the limitations will also be presented.

Calculation of the maximum displacement at the top of the damaged column

To calculate the maximum displacement at the top of the lost column, it is possible to use a simplified method allowing to predict the response of a structure subjected to a dynamic impact load. This method was developed by L. Comelieu and is described in [15]. It will be presented below.

Dynamic behavior of structures:

Before explaining the analytical procedure developed, it is essential to distinguish the two types of dynamic responses that can appear when a structure is subjected to the loss of a column.

Let N_0 be the charge in a column before it is damaged. A load $P_{dyn}(t)$ (determined as it has just been presented) will be applied downwards to simulate the loss of the column (see Figure 3.22).

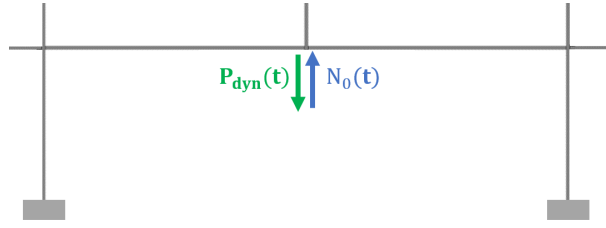


Figure 3.22: Load simulating the loss of a column

Two types of response can be observed depending on the maximum value reached by $P_{dyn}(t)$ and the duration of the loss of the column (both calculated according to the traditional approach or according to the improved approach as explained). These two types of behavior can be explained by comparing the dynamic curve $u_d(t)$, expressing the temporal evolution of the displacement induced by the application of $P_{dyn}(t)$, and the static curve $u_s(t)$, providing at all times t^* the static displacement $u_s(t^*)$ associated with the value of the force $P^* = P_{dyn}(t)$.

For a response of type 1 (see Figure 3.23), the displacement increases until a displacement called $u_{plateau}$ and then the dynamic curve stabilises. The maximum displacement reached is then much higher than the maximum displacement reached by the static curve. On the other hand, for a response of type 2 (see Figure 3.24), the displacement increases until a displacement named $u_{plateau}$ lower than the maximum displacement reached by the static curve. Then, the dynamic curve joins the static curve to oscillate around it.

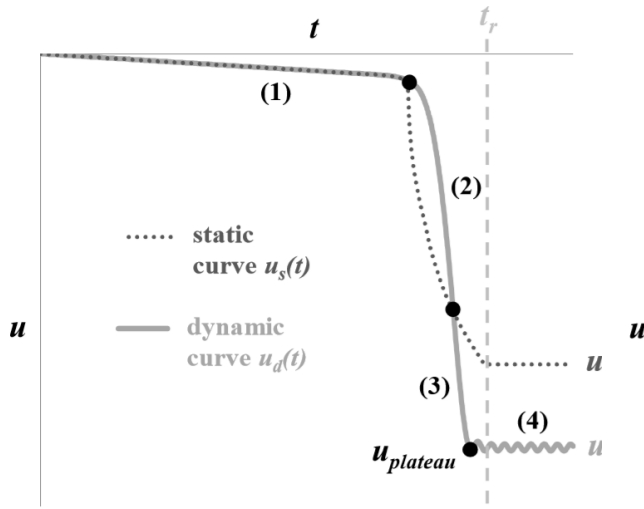


Figure 3.23: Type 1 response [15]

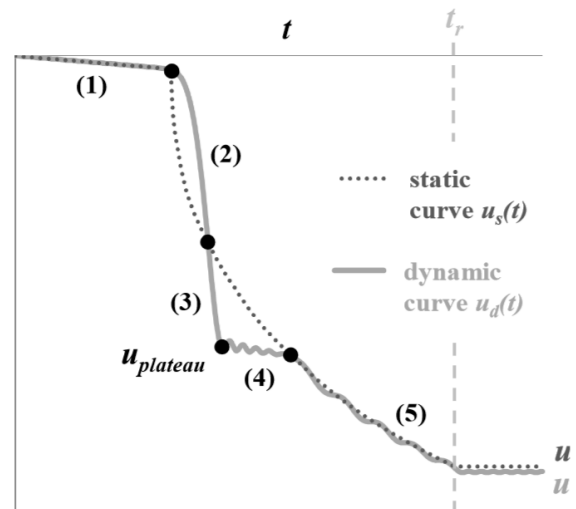


Figure 3.24: Type 2 response [15]

The analytical procedure developed will, therefore, be able to plot the dynamic response of the appropriate structure according to the type of response observed.

Hypotheses:

To do this, the procedure was developed by making several assumptions. The assumptions are as follows:

- Not taking into account the effects of the strain rate. Indeed, the strain rate is supposed to be sufficiently low so that the behavior law of materials remains the same under dynamic load as under static load.
- No damping is introduced into the system. This is a conservative approach.

- The deformation mode of the structure is supposed to be the same under static and dynamic elimination of the column. Also, the deformation energy corresponding to a given displacement is equal in both cases. This hypothesis was validated by the FEM analysis.

Model equation:

The model is then based on the energy conservation equation below, which can be developed based on the hypotheses which have just been made:

$$E_{kinetic} + E_{defo} = W_e \quad (3.8)$$

Kinetic energy is given by:

$$E_{kinetic} = \frac{1}{2} \cdot M_g \cdot \dot{u}^2 \quad (3.9)$$

Where M_g is the generalised mass of the system, whose calculation will be presented later.

Then, in view of the last hypothesis, the strain energy can be calculated by considering the static response. Therefore,

$$E_{defo} = E_{defo,stat} = W_{e,stat} = \left[\int P(u) \cdot du + \int N_0(u) \cdot du + \int p(u) \cdot du \right]_{stat} \quad (3.10)$$

Where,

- p represents the vertical loads applied to the structure in the initial situation,
- N_0 is the load in the column which will be lost, before the damage
- P is the load simulating the loss of column (varying from 0 to N_0).

Finally, the work done by the external loads is worth:

$$W_e = \left[\int P(u) \cdot du + \int N_0(u) \cdot du + \int p(u) \cdot du \right]_{dyn} \quad (3.11)$$

The equation (3.8) can, therefore, be written:

$$\frac{1}{2} \cdot M_g \cdot \dot{u}^2 + \left[\int P(u) \cdot du + \int N_0(u) \cdot du + \int p(u) \cdot du \right]_{stat} = \left[\int P(u) \cdot du + \int N_0(u) \cdot du + \int p(u) \cdot du \right]_{dyn} \quad (3.12)$$

However, the charges N_0 and p are constant. Therefore, the work carried out by these forces for a given displacement is the same no matter if this displacement is reached statically or dynamically. The equation can, therefore, be simplified.

Then, by deriving by time and dividing by \dot{u} , the equation finally becomes:

$$\frac{1}{2} \cdot M_g \cdot \ddot{u}^2 + P_{stat}(u(t)) = P_{dyn}(t) \quad (3.13)$$

This equation nevertheless has a domain of validity. It is valid:

- In the elastic range.
- Until the first maximum of the obtained curve $u(t)$ after yielding has occurred.

Calculation of the generalised mass:

Then, the generalised mass, introduced into the term of kinetic energy and necessary for the resolution of the energy conservation equation, is calculated according to the equation (3.14):

$$M_g = \int m(x) \cdot \phi(x)^2 \cdot dx \quad (3.14)$$

Where,

- $m(x)$ is the distributed mass,
- $\phi(x)$ is the vertical displacement corresponding to the deformation mode due to the formation of the global plastic mechanism of the beam in the directly affected part of the structure, with $\phi_{max} = 1$.

The deformation mode may not be exactly the same if the response of the structure is static or dynamic. The plastic hinges will not necessarily form at the same horizontal distance a from the lost column (see Figure 3.25) because this distance depends on the speed to remove the column. The generalised mass M_g is therefore calculated based on the static deformation mode.

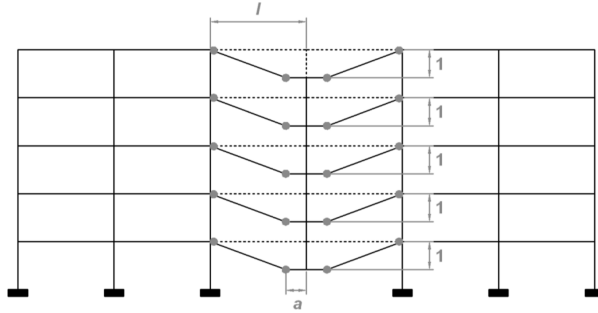


Figure 3.25: Calculation of the generalised mass [15]

Resolution procedure:

Finally, to solve the equation (3.13), boundary conditions must be provided.

To determine the first part of the dynamic curve, the boundary conditions are as follows:

- The displacement of the system is that corresponding to the initial position of the structure (before the column is removed): $u(t = 0) = u_0$
- The velocity of the displacement of the system is zero: $\dot{u} = 0$.

However, as explained above, when a plastic hinge has developed in the structure, this curve is only valid until its first maximum. This first maximum is the $u_{plateau}$ presented previously (Figures 3.23 and 3.24).

As explained above, two different types of responses can be observed depending on the value of $u_{plateau}$. The resolution procedure then differs for these two types of responses.

The response will be of type 1 if the first maximum $u_{plateau}$ is greater than the plateau of the static response u_{stat} . In this case, the part of the curve after the maximum can be simply represented by an infinite horizontal plateau, and the maximum dynamic displacement $u_{d,max}$ is equal to $u_{plateau}$. An example of type 1 response obtained by the analytical procedure is presented in Figure 3.26. It can be seen that the results correspond well to the results obtained by numerical

method (with the finite element calculation software FINELG).

Then, the response will be of type 2 if the first maximum $u_{plateau}$ is lower than the plateau of the static response u_{stat} . After solving the equation (3.13) a first time up to the first local maximum $u_{plateau}$, a horizontal plateau is then drawn up to the static curve. Then, the equation (3.13) is solved a second time, with new boundary conditions (a displacement equal to $u_{plateau}$ and a zero speed), up to a second local maximum. This procedure is repeated until the maximum obtained is greater than u_{stat} . This maximum is then the global maximum of the curve, called $u_{d,max}$, and the end of the dynamic curve is approximated by an infinite horizontal plateau. An example of type 2 response obtained by the analytical model is shown below (Figure 3.27).

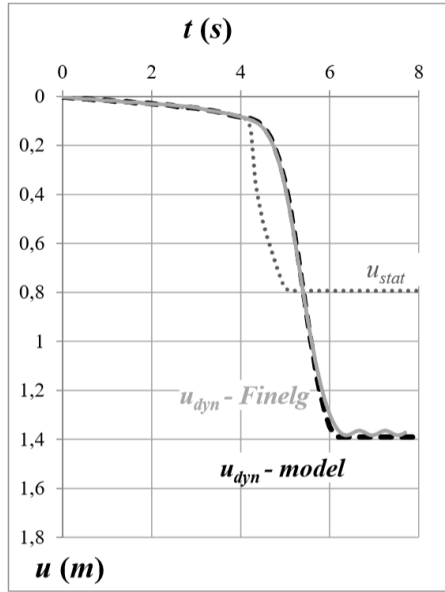


Figure 3.26: Example of type 1 response [15]

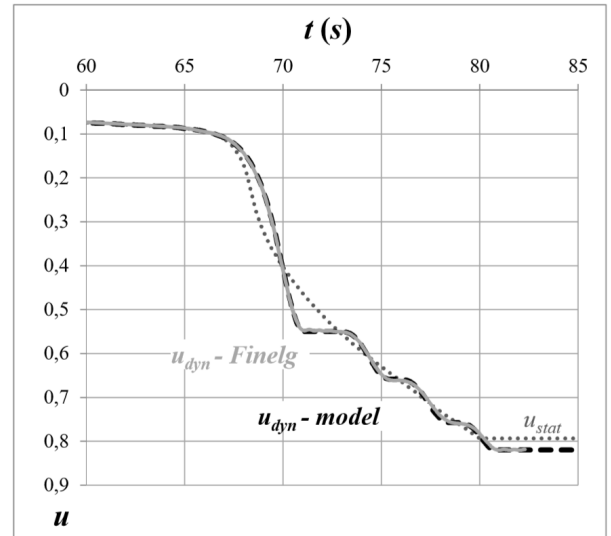


Figure 3.27: Example of type 2 response [15]

Required input data:

As presented, several data are therefore necessary to use the analytical procedure described. These required input data are grouped below:

- The static response of the frame $u_s(t)$ providing at all times t^* the static displacement $u_s(t^*)$ associated with the value of the force $P^* = P_{dyn}(t)$. This answer can be obtained using the analytical method developed within the University of Liège, which has already been presented for the analytical approach of the alternative load paths method or using software of non-linear calculation.
- The location of the plastic hinges involved in the plastic mechanism of the directly affected part (to calculate M_g). As a reminder, the static deformation mode is considered.
- The $P_{dyn}(t)$, function which describes how the critical bearing capacity of the column decreases. How to obtain this function has been explained previously.

Analysis

Knowing the maximum vertical displacement at the top of the damaged column $u_{d,max}$, it is then possible to use static analysis. Indeed, for a given value of the vertical displacement at the top of the damaged column, the distribution of the internal forces in the structure is the same regardless of whether this displacement is achieved statically or dynamically (provided that it is reached for the first time). This has been demonstrated by finite element analyses. Therefore, if the structure

is able to statically reach $u_{d,max}$, the robustness under dynamic load is ensured.

Static (non-linear second-order) analysis can be done in two different ways.

Either, it can be done using the analytical method developed within the University of Liège. In this case, it is first necessary to determine the flexibility matrices taking into account the coupling effects between the IAP and the DAP as described above. Then, it is necessary to solve the adequate system of equations (according to the position of the plastic hinges) for a displacement $u = u_{d,max}$.

Or, this analysis can also be performed using non-linear calculation software (for example, the finite element calculation software *FINELG*). As presented for the alternative load paths method, the analytical model can take different things into account. If the joints are pinned joints, the properties of the joints (i.e., the elongation capacity and the resistance) can possibly be introduced into the numerical model. Then, if the structure studied is large, it is possible to model only a part of the structure defined beforehand.

Verification

a) Verification of structural elements:

If the analysis was carried out using the analytical method and the joints are at full strength, it is necessary to check the ductility of the elements of the DAP because these were supposed to be infinitely ductile. Also, as already explained, it is necessary to check the lateral buckling resistance of the top beam of the DAP under M-N. Finally, the system of equations is based on the assumption that the IAP remains in the elastic domain. It is, therefore, necessary to check the resistance of the IAP.

Then, if the numerical method was used and only a part of the structure was modeled, it is necessary to check the resistance of the rest of the structure.

b) Verification of joints:

If the analysis was carried out using the analytical method, the verification procedure is almost the same as that presented for the analytical approach of the alternative load paths method. If the joints are partially resistant, the resistance and stiffness of the components must already have been introduced into the system of equations during the analysis. However, it is necessary to check the ductility of these components, which have been assumed to be infinitely ductile. On the other hand, if the joints were supposed to be fully resistant, their resistance must be checked using the criterion given by the improved analytical procedure or the criterion presented in Eurocode 3 Part 1-8.

Then, when the analysis has been carried out using the numerical method, the verification procedure is also almost identical to that presented in the numerical approach of the alternative load paths method. If the joints are semi-rigid or rigid, their resistance under M-N interaction will be checked with one of the two criteria presented. And if the joints are pinned joints and their properties have not been introduced in the analysed model, their resistance under axial force will be checked in accordance with Eurocode 3 Part 1-8.

However, the difference is that in the present case, there are dynamic effects which it may be interesting to take into account because it has been demonstrated experimentally that dynamic effects increase the resistance of the joints.

Indeed, a campaign of experimental tests was carried out in Liège, [16] and [17]. The objective of this one was to study the behavior of the joints and their components under impact load

(dynamic load), and more particularly to highlight the influence of the strain rate effects on the response of the joints studied and their components.

A study of the response of the different components under impact load was therefore carried out, for different energy levels (low, medium, high level). In parallel, quasi-static tests were carried out. The responses obtained under impact load were thus compared with the responses of the quasi-static tests to highlight the dynamic effects, and it turned out that the impact resistance is greater than the corresponding resistance obtained by the static tests :

$$R_{dyn} > R_{stat} \quad (3.15)$$

This result is due to the strain rate effects in some joint components. Indeed, the plasticity of certain materials depends on the strain rate (with some exceptions: certain very rigid components, such as a beam flange in compression). This phenomenon is called strain-rate-sensitivity, or viscoplasticity.

It is, therefore, interesting to identify this influence and take it into account correctly in the design of joints. But this experimental campaign is only a first step, and there is not yet a precise method allowing to take into account the dynamic effects in the calculation of the resistance.

A doctoral thesis currently being drafted by M. D'Antimo [18] nevertheless suggests using a coefficient called DIF (Dynamic increase factor), determined on an experimental basis, which will give an overall estimate of the dynamic effect:

$$DIF = \frac{R_{dyn}}{R_{stat}} \quad (3.16)$$

Limitations

If the analysis is performed by the analytical method, only one lost column can be considered per scenario, and this column must be internal.

Summary of the approach

Figure 3.28 summarizes the procedure to be followed by choosing the dynamic force approach but static analysis.

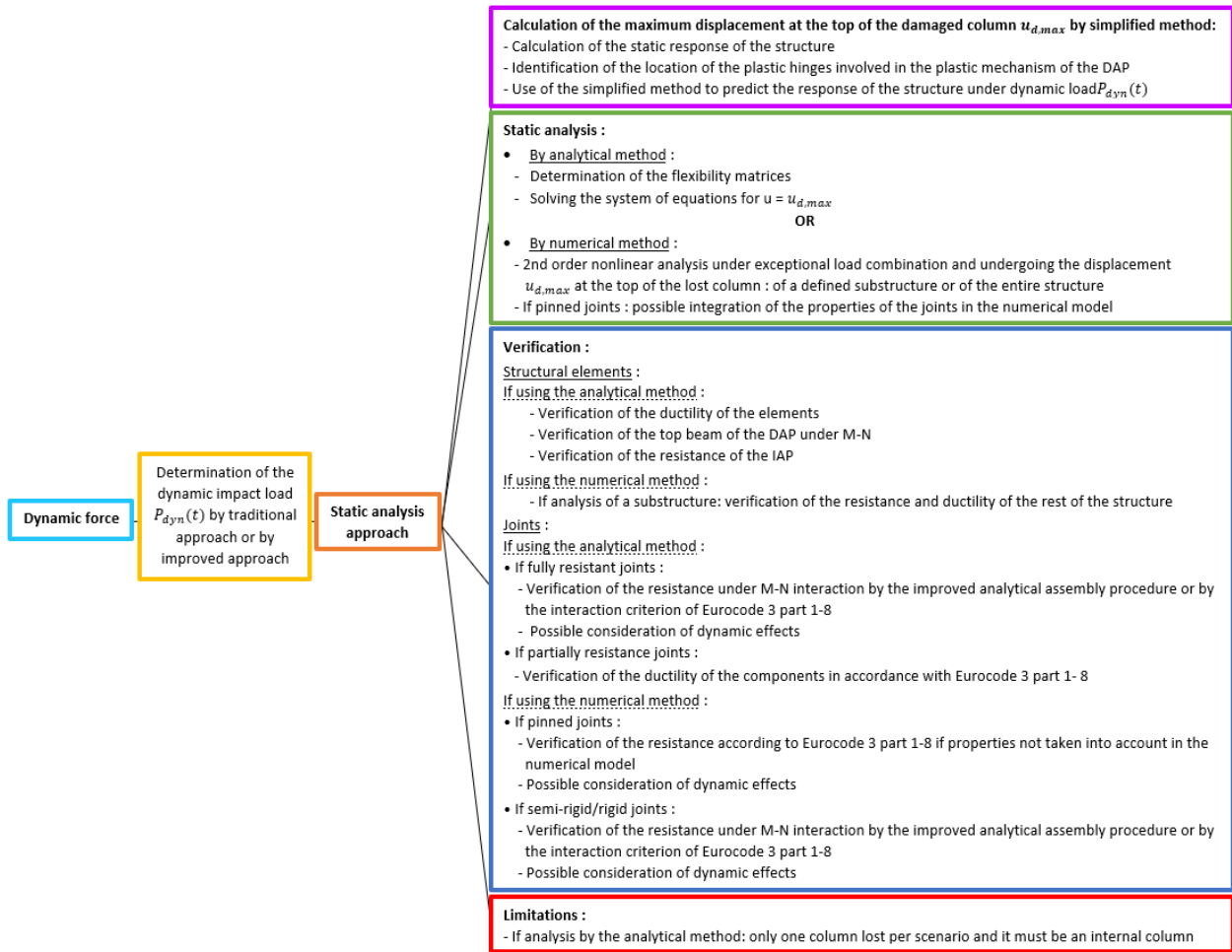


Figure 3.28: Procedure by opting for the dynamic force and static analysis approach

3.1.2.3 Dynamic analysis approach

Dynamic analysis

Using a non-linear calculation software, it is also possible to perform an analysis under dynamic load. More precisely, a second-order non-linear analysis of the structure will be carried out under accidental load combination and dynamic impact load.

As before, if the structure is too large, only one substructure can be modeled. Also, if the joints are pinned joints, their properties can be integrated into the numerical model.

Verification

a) Verification of structural elements :

The only verifications required concern the elements that were not the subject of the second-order non-linear analysis. Therefore, if only a substructure has been modeled, the rest of the structure must be checked.

b) Verification of joints :

As before, it is necessary to check the resistance of the joints under M-N interaction if they have a certain rigidity and under N only if they are pinned joints. Also, it is interesting to take into account the dynamic effects but there is not yet a precise procedure to take it into account.

On the other hand, if the joints are pinned joints and their properties have been introduced into the model (with possible consideration of the dynamic effects on the resistance), they should not be subject to verification.

Limitations

There are no particular limitations to this approach.

Summary of the approach

Figure 3.29 summarizes the procedure to be followed by choosing the approach by dynamic force and dynamic analysis.

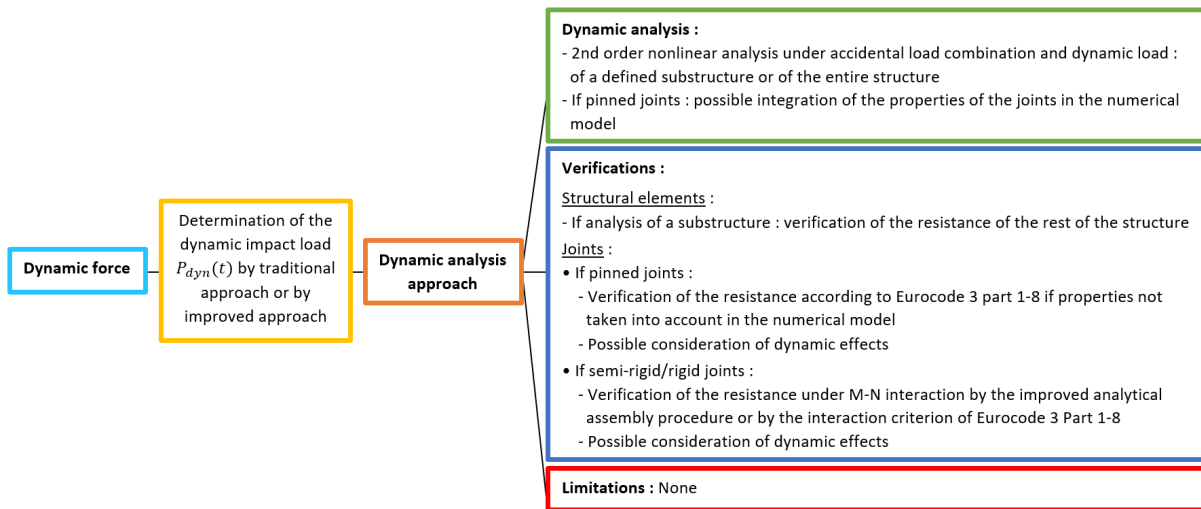


Figure 3.29: Procedure by opting for the dynamic force approach and dynamic analysis

3.2 Design under blast loading

Under blast loading, the approaches presented in Figure 3.30 can be considered.

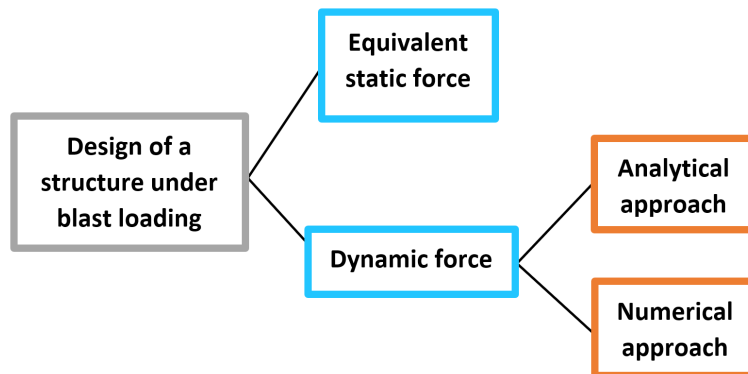


Figure 3.30: Possible approaches to design under blast loading

3.2.1 Equivalent static force

As under impact load, when the consequence class of the studied structure is sufficiently low (CC2 and some structures of CC3), an equivalent static force approach is considered sufficient.

3.2.1.1 Analysis

As under impact load, after determining the equivalent static load, the structure must be analysed under the combination of accidental loads and the equivalent static load. A first-order linear analysis can be performed.

3.2.1.2 Verification

a) Verification of structural elements:

It is necessary to carry out a plastic verification of the elements of beams and columns in section and instabilities.

b) Verification of joints:

The resistance of the joints must also be checked in accordance with Eurocode 3.

3.2.1.3 Summary of the approach

Figure 3.31 summarizes the procedure to be followed by choosing the equivalent static force approach. This flowchart is identical to the flowchart of the equivalent static force approach under impact loading.

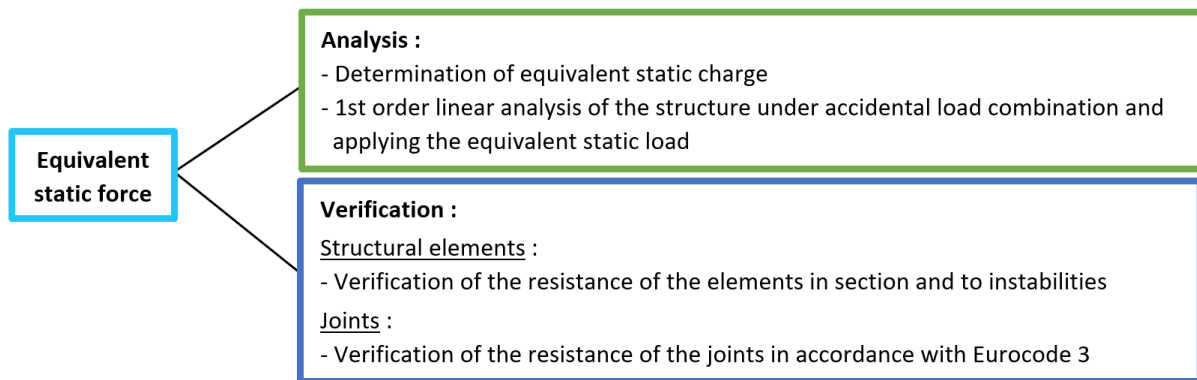


Figure 3.31: Procedure by opting for the equivalent static force approach

3.2.2 Dynamic force

For several structures of class CC3, it is necessary to carry out an analysis under dynamic load. It is therefore possible to choose an analytical or numerical approach.

3.2.2.1 Analytical approach

For beam elements, it is possible to use an analytical approach involving a simplified method for the derivation of the p-I diagram. This method will first be presented below, and then its usefulness for the analysis will be explained. Finally, the verifications to be carried out and the limitations of this approach will also be presented.

Simplified method for the derivation of the p-I diagram

In her work, L. Hamra developed a simplified method for the derivation of the p-I (pressure-impulse) diagram for a frame beam subjected to a uniformly distributed blast load [19]. The method takes into account the development of membrane forces, the M-N interaction in the plastic hinges, and the interaction with the IAP of the structure.

The p-I diagram is useful to design a structure against a blast because it can be used to assess the damage caused by the explosion. In the case of a beam subjected to bending for example, it is possible to obtain the required ductility, which is a good index of damage.

Formulation of the problem:

The analytical method is developed from the substructure shown in Figure 3.32 (a).

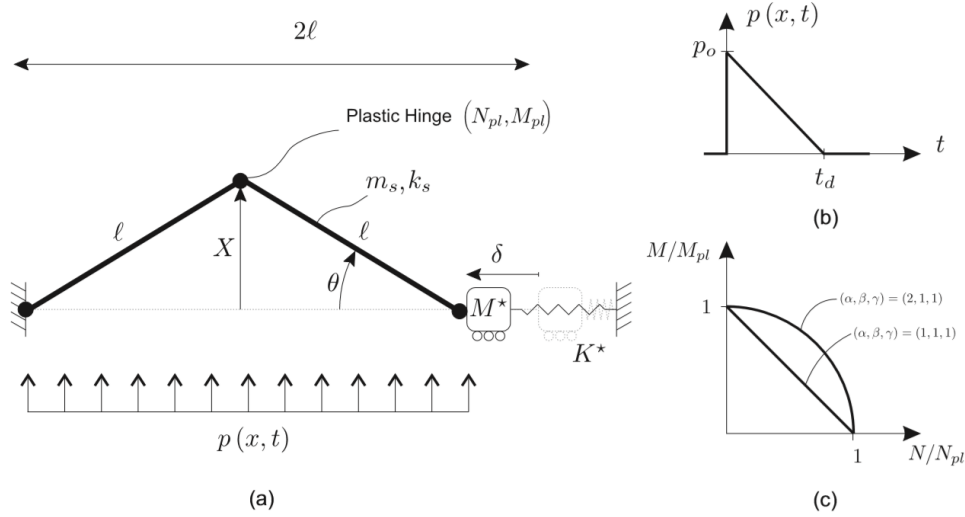


Figure 1: (a) Sketch of the considered problem, (b) Idealized blast loading, (c) Axial force-bending moment interaction law

Figure 3.32: Description of the problem [19]

As can be seen, the beam studied has a length 2ℓ , a linear mass m_s and an equivalent elastic bending stiffness k_s known. Also, when the beam is deformed, three plastic hinges develop.

The interaction of the beam with the IAP is modeled by a mass M^* and a spring with a stiffness K^* . These parameters can be obtained from the equation of the movement of the structure, as described in [19].

The only degree of freedom of the system is X . The kinematics is thus entirely described by X (or by the rotation $\theta = X/\ell$).

The blast loading is supposed uniformly distributed and is idealised by a triangular impulse (see Figure 3.32 (b)). In reality, a depression phase appears after a certain time t_d , as shown in Figure 3.33. However, this phase of depression can be overlooked.

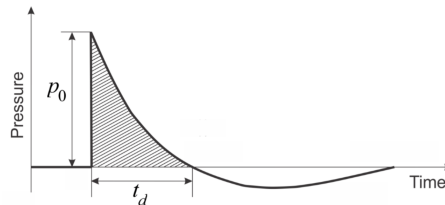


Figure 3.33: Evolution of pressure over time during for a blast [2]

Therefore,

$$p(x; t) = p_0 \left(1 - \frac{t}{t_d}\right) \quad (3.17)$$

Where t represents the time variable, p_0 is the maximum pressure, and t_d is the duration of the

phase during which the pressure is positive. The explosion charge is therefore set by p_0 and t_d .

The associated momentum I is:

$$I = \frac{p_0 \cdot t_d}{2} \cdot l \quad (3.18)$$

Finally, membrane forces $K \cdot \delta$ will develop in the spring. Therefore, the model takes into account the M-N interaction:

$$\left(\frac{M}{M_{pl}}\right)^\beta + \gamma \cdot \left(\frac{N}{N_{pl}}\right)^\alpha = 1 \quad (3.19)$$

Where α , β and γ must be chosen according to the appropriate interaction law (Figure 3.32 (c)), and N_{pl} and M_{pl} are respectively the resistance to the normal forces and the resistance to bending of the beam.

This interaction law, therefore, assumes that the joints are fully resistant, but it could be reduced to take account of certain partially resistant connections.

Hypotheses:

The main assumptions of the model are as follows:

- The IPA remains in the elastic domain. Indeed, the lateral restriction K^* remains in the elastic domain.
- The beam-to-column joints are assumed to be perfectly rigid.
- The axial elongation of the plastic hinges and the elastic elongation of the beam are neglected.
- The law of materials is elastic-perfectly plastic.
- The effect of the strain rate on the resistance is not taken into account, so the properties are assumed to be constant over time.
- The position of the plastic hinges is fixed.
- Shear failure is not taken into account.

Energy conservation equation:

Then the analytical method is based on energy conservation which is written as follows:

$$K + U = W \Leftrightarrow K + U_1 + U_2 + U_3 = W \quad (3.20)$$

Where,

K is the kinetic energy:

$$K = \frac{1}{2}M_s\dot{X}^2 + \frac{1}{2}(M_s + 4M^*\frac{X^2}{l^2})\dot{X}^2 \quad (3.21)$$

W is the external work carried out by the explosion charge:

$$W = 2 \int_0^l \int_0^X p(1 - \frac{X}{l})dXdx = 2 \int_0^l pX(1 - \frac{x}{l})dx = p \cdot l \cdot X \quad (3.22)$$

$U = U_1 + U_2 + U_3$ is the elastic-plastic strain energy with:

U_1 is the energy stored in the beam (i.e., the energy of elastic deformation):

$$U_1 = \begin{cases} \frac{1}{2}k_s X^2 & \text{for } X \leq X_y \\ \frac{1}{2}k_s X_y^2 & \text{for } X > X_y \end{cases} \quad (3.23)$$

Where $\theta_y = X_y/l$ is the yield rotation, for which plastic hinges develop.

It is assumed that all plastic hinges form at the same time when the mid-span displacement reaches X_y (i.e., when the rotation at the ends of the beam reaches θ_y) for a pressure $p_s = 4M_p/l^2$ corresponding to the pressure required to form the third plastic hinge.

- U_2 is the energy dissipated in the plastic hinges after they have formed (i.e., the yielding has occurred):

$$U_2 = 4 \int_{X_y/2}^{X/l} M[N(\theta, \dot{\theta}, \ddot{\theta})]d\theta = \frac{4}{l} \int_{X_y}^X M[N(\frac{X}{l}, \frac{\dot{X}}{l}, \frac{\ddot{X}}{l})]dX \text{ for } X > X_y \text{ and } \dot{X} \geq 0 \quad (3.24)$$

This energy decreases when X increases. Indeed, when X increases, membrane forces develop and the resistant moment decrease due to the M-N interaction.

- U_3 is the energy stored in the lateral spring:

$$U_3 = \int_0^\lambda K^* \Delta d\Delta = \int_0^X K^* \frac{X^2}{l} \frac{2X}{l} dX = \frac{1}{2} K^* X^2 \frac{X^2}{l^2} \quad (3.25)$$

The evolution of U_1 , U_2 and U_3 as a function of X is shown in Figure 3.34 below.

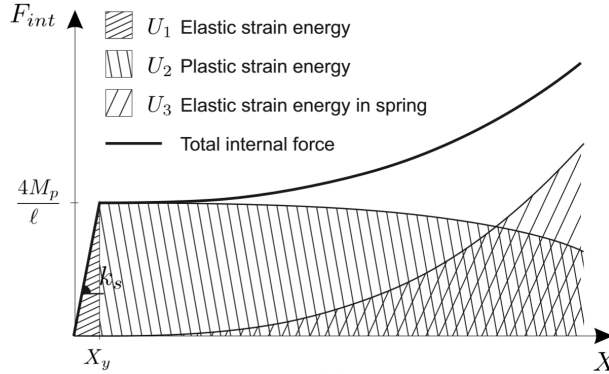


Figure 3.34: Evolution of the terms of the energy of deformation [19]

Finally, energy conservation is therefore written:

$$\frac{1}{2}(M_s + 4M^* \frac{X^2}{l^2})\dot{X}^2 + U_{int,b} + \frac{1}{2}K^* X^2 \frac{X^2}{l^2} = p \cdot l \cdot X \quad (3.26)$$

With,

$$U_{int,b} = \begin{cases} \frac{1}{2}k_s X^2 & \text{for } X \leq X_y \\ \frac{1}{2}k_s X_y^2 + \frac{4}{l} \int_{X_y}^X M[N(X, \dot{X}, \ddot{X})]dX & \text{for } X > X_y \text{ and } \dot{X} \geq 0 \end{cases}$$

By differentiating the equation (3.26) as a function of time, then dividing this conservation of power by the speed \dot{X} , it is possible to obtain the equation of motion. Then, by introducing dimensionless quantities, it is possible to get a dimensionless formulation of the equation of motion, as described in [19]. It is this dimensionless formulation that must be solved using a non-linear solver, to obtain the evolution of the displacement $X(t)$ for the blast load considered.

The maximum displacement then characterises the ductility demand of the beam to face the blast load considered:

$$\mu = \max_{t \in R^+} \bar{X}(t) \quad (3.27)$$

This ductility demand depends on:

- The behavior of the IAP characterised by K^* and M^* , and characteristics m_s and k_s of the beam
- Axial and flexural strength of the beam
- Kinematics of the problem, i.e., the yield rotation θ_y
- Parameters p and t_d related to the blast load

For a pressure-impulse relationship, therefore, corresponds a ductility value, as shown in dotted lines in Figure 3.35 below.

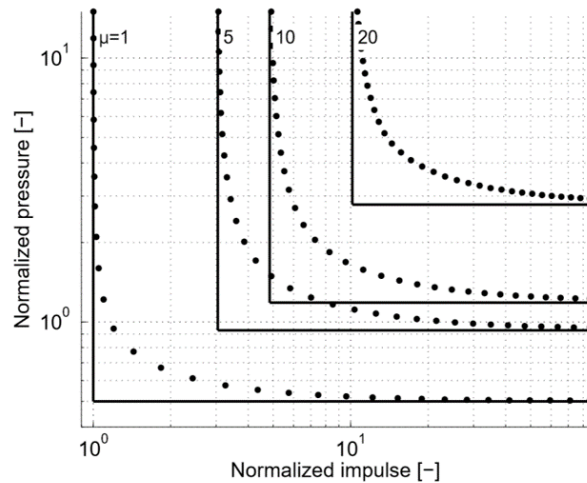


Figure 3.35: Asymptotes [19]

The asymptotes:

Three regimes can be observed depending on the parameter t_d , i.e., the speed at which the explosion develops.

For quasi-static regimes (t_d very large), the terms implying speed and acceleration are rejected from the energy conservation equation. The demand for ductility μ only depends on p_0 , not on the duration of the explosion t_d . It is then possible to obtain a relation which does not imply the impulse of the loading. Consequently, the representation of the ductility demand μ presents horizontal asymptotes in the p-I diagram (see Figure 3.35).

Then, for impulsive regimes (t_d close to zero), the ductility μ depends only on the impulse I . The representation of the ductility demand this time has vertical asymptotes in the p-I diagram (see Figure 3.35).

Finally, in the case of an intermediate dynamic regime, the dimensionless formulation of the equation of motion must be resolved.

Analysis

By opting for the analytical approach, the analysis is therefore carried out as follows. After having identified the beam to be studied, it is necessary to determine the blast loading which it must resist. This blast loading is set by p_0 (the maximum pressure reached) and t_d (the duration of the phase during which the pressure is positive).

Then, using the simplified method presented, it is possible to know the ductility demand of the beam (i.e., the maximum lateral displacement that the beam must undergo).

This method also gives the forces M and N appearing at the ends of the beam.

Verification

a) Verification of structural elements:

The first thing to check is the ductility of the modeled beam.

Then, the assumption was made that the IAP (i.e., the rest of the structure) remains in the elastic domain. The resistance of the rest of the structure must therefore be checked.

b) Verification of joints:

If the law of interaction M-N introduced supposes that the joints are fully resistant, it must be verified that this is indeed the case. Knowing the forces M and N appearing at the ends of the beam, it is possible to check the resistance of the joints either by the criterion of Eurocode 3 Part 1-8, or by the improved analytical assembly procedure. Also, as for the impact load, it can be interesting to take into account the dynamic effects.

Limitations

The analytical model is based on the assumption that the beam-column connections are perfectly rigid. It is therefore not applicable for joints of low rigidity or pinned joints.

Then, this model is applicable only for a beam.

Summary of the approach

Figure 3.31 summarizes the procedure to be followed by choosing the analytical approach with dynamic force.

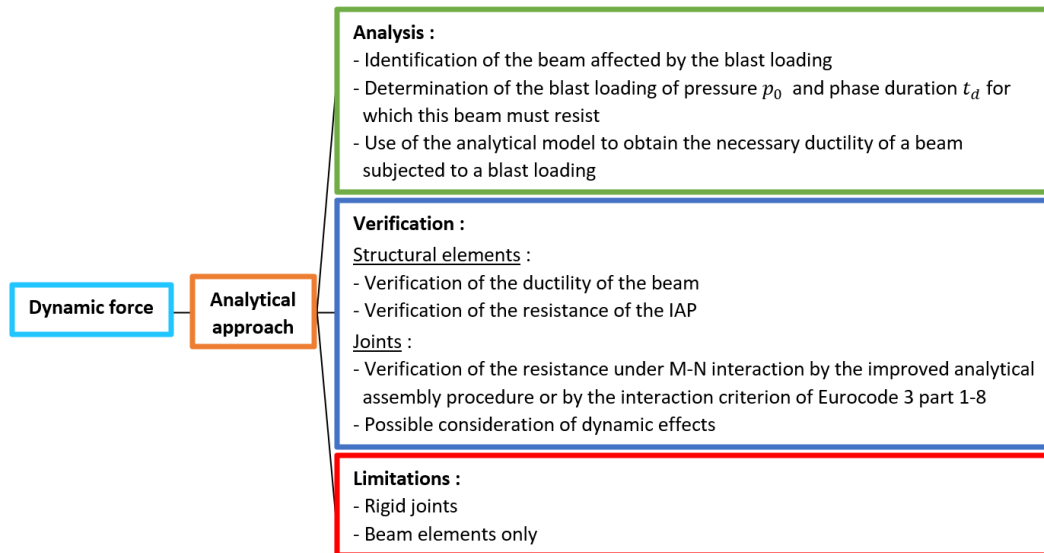


Figure 3.36: Procedure by opting for the analytical approach with dynamic force

3.2.2.2 Numerical approach

Analysis

When choosing the numerical approach, the first thing to do is to identify the elements affected by the blast considered and determine the blast load they must withstand.

Then, using a software, it is possible to perform a second-order non-linear analysis of the structure under accidental loads combination and stressed by the dynamic explosion charge. As for the previous strategies, a substructure can be modeled, and if the joints are pinned joints, it is possible to integrate the properties of the joints in the model.

Verification

a) Verification of structural elements :

If only a substructure was subjected to the non-linear analysis of the second-order, it is necessary to check the remainder of the structure.

b) Verification of joints :

If the joints are pinned joints, they must be checked following Eurocode 3, unless their properties have already been taken into account in the numerical model.

Then, if the joints are semi-rigid or rigid, they can be checked either with the criterion of Eurocode 3 Part 1-8, or with the improved analytical assembly procedure.

Also, the influence of dynamic effects on resistance can be taken into account.

Limitations

The numerical approach does not present any particular limitation.

Summary of the approach

Figure 3.37 summarizes the procedure to be followed by choosing the numerical approach with dynamic force.

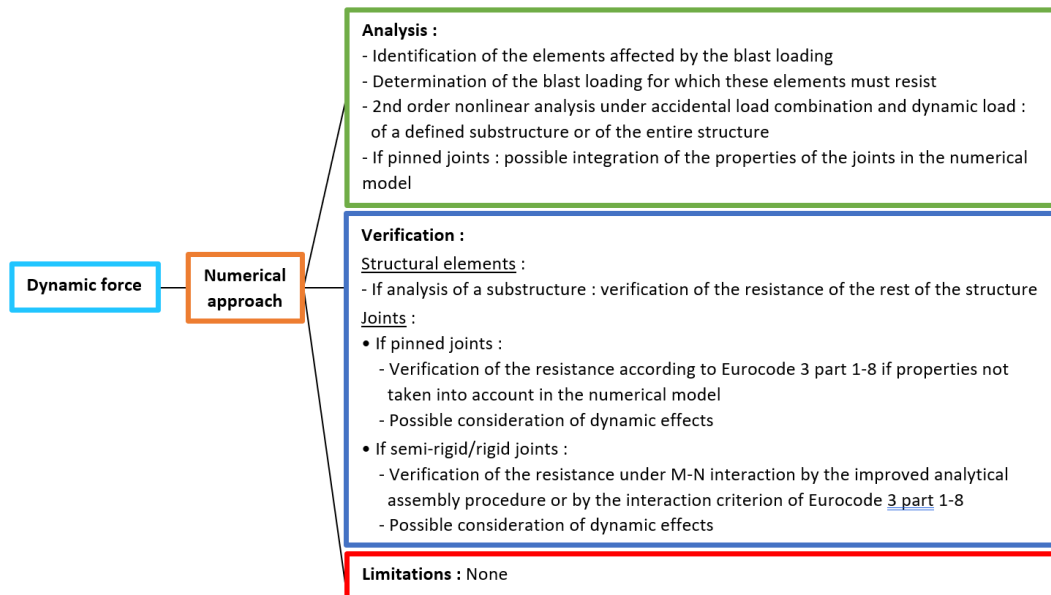


Figure 3.37: Procedure by opting for the numerical approach with dynamic force

4 Conclusion

In this chapter, different approaches to deal with the robustness problem in steel and composite structures, as well as the tools they involve, were presented for each of the strategies presented in the previous chapter and shown in Figure 2.1, except for the two first (*Design the structure to have sufficient minimum robustness* and *Preventing or reducing the action*) that do not require the development of specific approaches.

First, for the strategy of designing the structure to sustain the action, several developments and several tools have been developed in recent years about two particular actions, impacts and explosions, which are the two types of actions that it is generally desirable to guard against. Thanks to these developments and to existing numerical software, approaches that seem solid have been developed.

Then, for the key elements method, two main approaches were presented, the primary structure approach and the fuse approach. For these approaches no particular development has been carried out in recent years because it has not proven necessary.

Finally, for the strategy relating to the alternative load paths method, it is possible to have recourse to an analytical approach based on the analytical model developed within the University of Liège or a numerical approach requiring the use of non-linear calculation software. Also, as a reminder, the table of strategies in Figure 2.1 has been slightly revised since the prescriptive tying method has been considered as a third approach to the alternative load paths method. For this prescriptive tying method, it has been shown that the procedure which currently exists and which is presented in annex A of Eurocode 1 Part 1-7 has several limitations and inconsistencies. Therefore, more realistic treatment is being developed.

The approach using the tying method, therefore, seems to be, at the present, the least solid and least reliable approach to use because it presents several inconsistencies and the level of robustness achieved is not known. The next chapter of this thesis will, therefore, focus on this tying method and will aim to verify its relevance.

Chapter 4

Study of a structure subject to a loss of column

1 Objectives of this study

In this chapter, a braced structure subject to a loss of column will be analysed. First, it will be analysed without taking into account the properties of the joints, which will be assumed to be fully resistant and infinitely ductile. Then different properties will be given to the joints to observe their influence on the behavior of the structure.

The objective of this analysis is to verify the relevance of the tying method proposed in the Eurocode and to have an idea of the real robustness associated with compliance with the current rules on tying resistance. Indeed, as explained in the previous chapter, a more realistic treatment is being developed to improve/replace the current tying method. Before developing a new formula or improving the current one, it seems interesting to know the limits of the formula currently proposed by the Eurocode.

This study will also verify that the simple joints (i.e., joints which prevents from any rotational continuity between the connected members), generally used for braced structures, are able to take up the membrane forces that appear in the DAP beams when a column is lost. Indeed, following the loss of a column, the beam-column joints in the DAP will be subjected to significant axial forces for which they were not initially designed.

Note that a braced structure with simple joints was chosen because this type of structure develops greater membrane forces than a non-braced structure with rigid joints. In fact, in braced structures, the IAP is very rigid and not very deformable thanks to bracing, and greater forces can be transmitted there. Also, since the joints are simple joints, it is not necessary to develop plastic hinges to have a mechanism. Consequently, membrane forces will develop in the beams of the DAP as soon as the column is lost, and greater forces will be reached.

2 Description of the structure

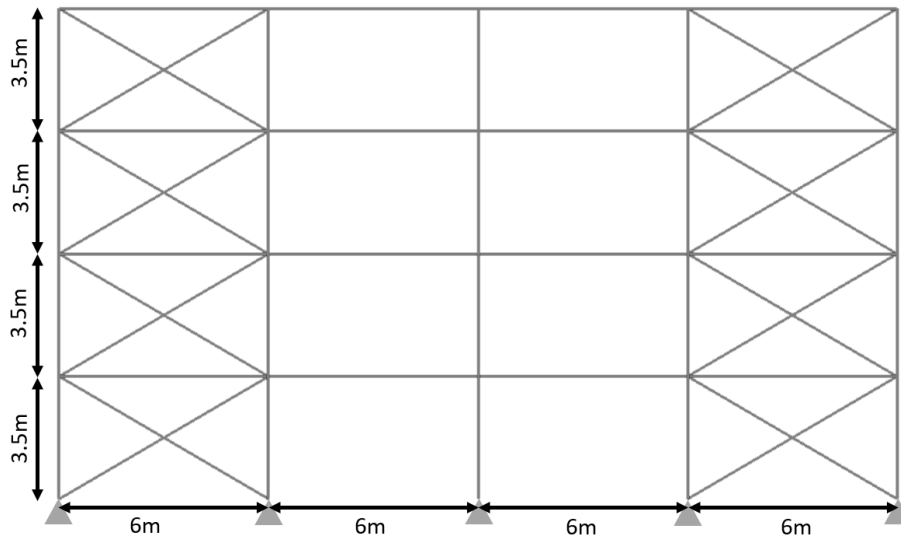


Figure 4.1: Structure studied

The structure studied has the geometry described in Figure 4.1.

The elements are in steel of grade S355, and all the elements work along their strong axis.

The structure is supposed to be built in Brussels (Belgium), so the land is category IV.

It is also important to say that out-of-plane instabilities are prevented. In addition, the bracing elements can work in compression and their buckling length is equivalent to their length.

Finally, as already mentioned, the joints are all simple joints so the rotation between the structural members is free.

It is important to note that this structure has already been studied by Farah Hjeir in his master's thesis [20]. As part of the latter, he had identified the structural requirements for a structure to remain in equilibrium in the face of the loss of one of its columns. He had carried out a parametric study by varying the number of levels and the number of spans of the structure. However, he did not take into account the strength and the ductility of the joints (which he assumed to be fully resistant), which will be the case in the present study. Also, in his study, he had assumed that the columns worked along their weak axis, whereas here, they will work along their strong axis so that the beam-column joints have better properties, as will be explained later.

3 Load combinations

Firstly, it is necessary to define the loads that will apply to the structure and the appropriate load combinations in accordance with Eurocode 0.

3.1 Loads

The surface loads below are transformed into linear loads by supposing that the studied frame is extracted from a 3D structure which has the same dimensions in the two directions.

Dead loads:

- Concrete: $\gamma = 25\text{kN/m}^3$ et $e = 20\text{cm} \Rightarrow 37.5\text{ kN/m}$
- Topping layer: $1.5\text{kN/m}^2 \Rightarrow 9\text{ kN/m}$
- Cladding: $16.5\text{kg/m}^2 \Rightarrow 0.972\text{ kN/m}$

$$\Rightarrow \text{Total: } G_k = 47.472 \text{ kN/m}$$

Live loads:

- Offices: $3 \text{ kN/m}^2 \Rightarrow LL_k = 18 \text{ kN/m}$
- Roof: $1 \text{ kN/m}^2 \Rightarrow R_k = 6 \text{ kN/m}$
- Snow: $0.4 \text{ kN/m}^2 \Rightarrow S_k = 2.4 \text{ kN/m}$
- Wind: according to Eurocode 1, PP_k (Pushing Pressure) = 2.94 kN/m and SP_k (Suction Pressure) = 1.84 kN/m

The loads are all shown in Figure 4.2 below.

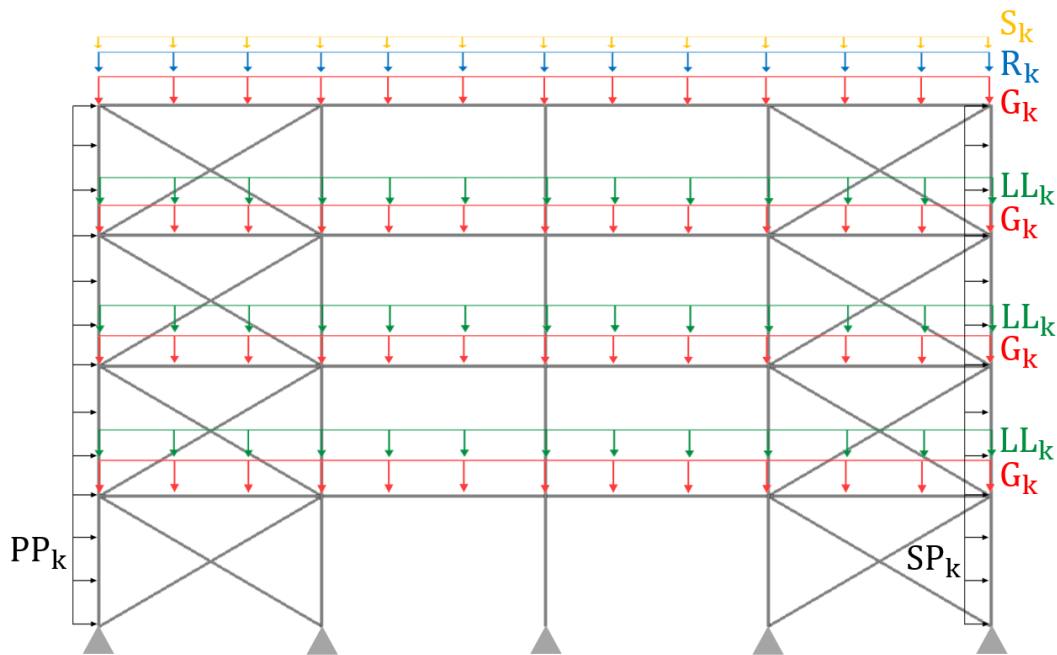


Figure 4.2: Loads

3.2 Load combinations

Three combinations must be made:

- A combination of loads at ultimate limit state (ULS) under which the strength and stability of the structure will be checked.
- A combination of loads at service limit state (SLS) under which the displacements of the structure will be checked.
- A combination of accidental loads under which the structure will have to find a new equilibrium configuration if a column is lost.

In accordance with Eurocode 0, the combinations are as follows:

$$\text{ULS: } E_d = \gamma_G G_k + \gamma_Q Q_{k,1} + \sum_i \gamma_Q \Psi_{0,i} Q_{k,i}$$

$$\Rightarrow E_d = 1.35 \cdot G_k + 1.5 \cdot LL_k + 1.5 \cdot [0 \cdot R_k + 0.5 \cdot S_k + 0.6 \cdot (PP_k + SP_k)]$$

Section resistance:

$$M_{pl,Rd} = \frac{W_{pl,y} \cdot f_y}{\gamma_{M_0}} = 778.9 \text{ kNm}$$

IPE100 members:

$$N_{Ed} = -66 \text{ kN}$$

Section resistance:

$$N_{pl,Rd} = \frac{A \cdot f_y}{\gamma_{M_0}} = 365.65 \text{ kN}$$

Strong axis buckling:

- $L_{fl} = L = 6.946 \text{ m}$

- $N_{cr,y} = \frac{\pi^2 \cdot E \cdot I_y}{L_{fl}^2} = 73.46 \text{ kN}$

- $\bar{\lambda}_y = \sqrt{\frac{N_{pl,Rd}}{N_{cr,y}}} = 2.23 > 0.2$

- $\Phi = 0.5 \cdot (1 + \alpha \cdot (\bar{\lambda} - 0.2) + \bar{\lambda}^2) = 3.20$ with $\alpha = 0.21$

- $\chi = \frac{1}{\Phi + [\Phi^2 - \lambda^2]^{0.5}} = 0.182$

$$\Rightarrow N_{b,Rd} = \chi \cdot N_{pl,Rd} = 66.6 \text{ kN}$$

HE200B columns:

$$N_{Ed} = -2073 \text{ kN}$$

Section resistance:

$$N_{pl,Rd} = \frac{A \cdot f_y}{\gamma_{M_0}} = 2\,772.55 \text{ kN}$$

Strong axis buckling:

- $L_{fl} = H = 3.5 \text{ m}$

- $N_{cr,y} = \frac{\pi^2 \cdot E \cdot I_y}{L_{fl}^2} = 9\,637.25 \text{ kN}$

- $\bar{\lambda}_y = \sqrt{\frac{N_{pl,Rd}}{N_{cr,y}}} = 0.536 > 0.2$

- $\Phi = 0.5 \cdot (1 + \alpha \cdot (\bar{\lambda} - 0.2) + \bar{\lambda}^2) = 0.701$ with $\alpha = 0.34$

- $\chi = \frac{1}{\Phi + [\Phi^2 - \lambda^2]^{0.5}} = 0.868$

$$\Rightarrow N_{b,Rd} = \chi \cdot N_{pl,Rd} = 2\,406.02 \text{ kN}$$

HE140B columns:

$$N_{Ed} = -1085 \text{ kN}$$

Section resistance:

$$N_{pl,Rd} = \frac{A \cdot f_y}{\gamma_{M_0}} = 1\,526.50 \text{ kN}$$

Strong axis buckling:

- $L_{fl} = H = 3.5 \text{ m}$

- $N_{cr,y} = \frac{\pi^2 \cdot E \cdot I_y}{L_{fl}^2} = 2\,553.13 \text{ kN}$

- $\bar{\lambda}_y = \sqrt{\frac{N_{pl,Rd}}{N_{cr,y}}} = 0.773 > 0.2$

- $\Phi = 0.5 \cdot (1 + \alpha \cdot (\bar{\lambda} - 0.2) + \bar{\lambda}^2) = 0.896$ with $\alpha = 0.34$

- $\chi = \frac{1}{\Phi + [\Phi^2 - \lambda^2]^{0.5}} = 0.741$

$$\Rightarrow N_{b,Rd} = \chi \cdot N_{pl,Rd} = 1\,131.13 \text{ kN}$$

4.1.2 Under SLS Loads

$$f_{allowable} = L/300 = 20 \text{ mm}$$

$$f_{max} = 16.7 \text{ mm}$$

$$\Rightarrow f_{max} < f_{allowable}, \text{ OK.}$$

Note : with IPE 450 beams $\rightarrow f_{max} = 21.5 \text{ mm}$, Not OK.

4.2 Non-linear calculation

The structure presented in Figure 4.3, obtained after the linear calculation, will now be the subject of a non-linear calculation using the software *FINELG*.

4.2.1 Structure loading method

The objective of the calculation is to check if the structure obtained by the linear calculation withstands the load combination at ULS and if it is not oversized. The structure of Figure 4.3 will, therefore, be loaded gradually by applying the load combination at ULS to it.

The loading was carried out using the method of the spherical step (automatic). This method was chosen for its effectiveness. Indeed, by using this method, the increment of force decreases automatically when approaching the maximum, as shown in the figure below 4.4.

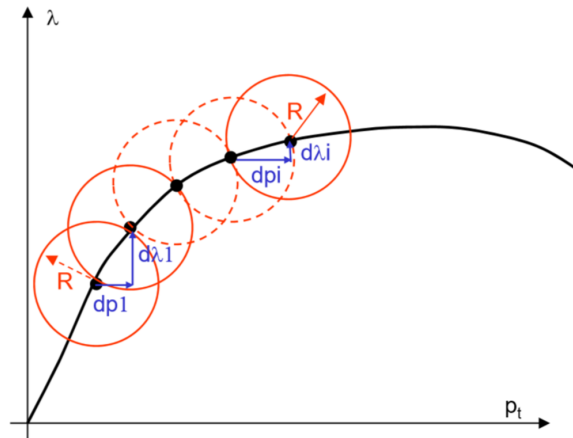


Figure 4.4: Spherical step method [21]

4.2.2 Stop criteria

The program must be given a stop criterion. This criterion will define the moment when the ruin is detected, and the calculation must stop.

The real behavior of a steel element is shown in Figure 4.5. It can be seen there the phenomenon of hardening which makes it possible to reach the ultimate limit of steel f_u when the strain reaches ϵ_u . Then there is a rupture of the steel element.

In *FINELG*, the behavior of steel elements is assumed to be elastic-perfectly plastic (see Figure 4.6). However, the elements can not deform indefinitely and a limit value of deformation must be defined. This limit of deformation is ϵ_u . It was chosen equal to 0.05, which corresponds to the default value entered in the program. Therefore, the program stops when ϵ_u reaches 0.05 in an element.

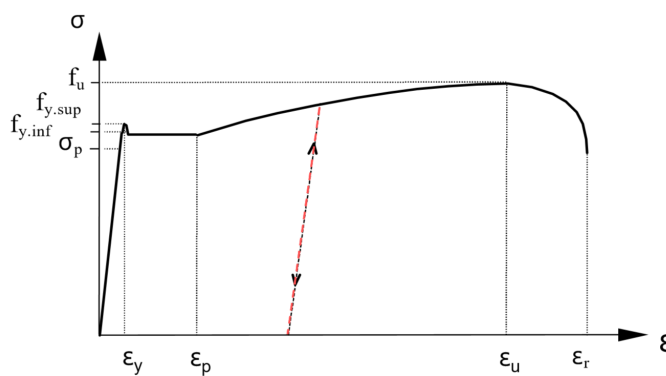


Figure 4.5: Real behavior law of steel

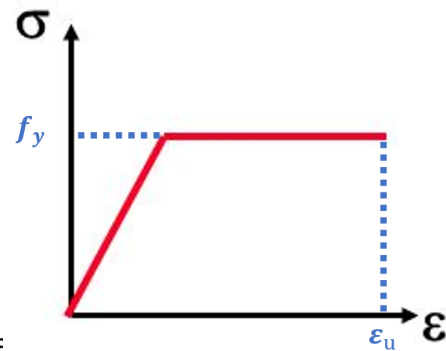


Figure 4.6: Elastic-perfectly plastic behavior law

4.2.3 Initial imperfections

It is important to introduce initial imperfections to the columns. Indeed, the latter work mainly in compression. Due to the initial imperfections, second-order moments will develop in the columns and they will break more quickly.

The initial imperfections of the columns were introduced into the model using equivalent forces, in accordance with Eurocode 3. Indeed, in Eurocode 3 Part 1-1, a procedure is described to replace the initial imperfection of a column by equivalent forces (see Figure 4.7).

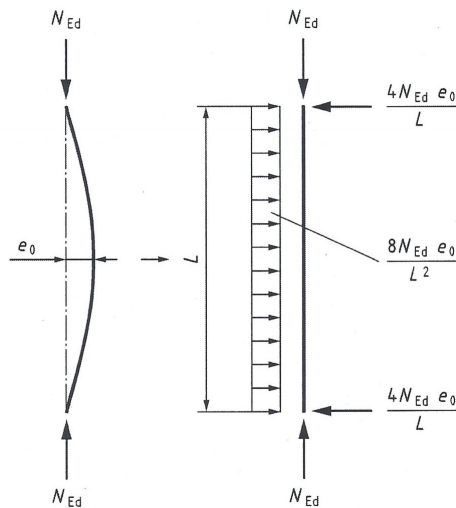


Figure 4.7: Equivalent forces to take into account the initial imperfection of a column

For the bracing elements, no initial imperfection was considered. Indeed, the latter will already be deformed under their self-weight. The elements will be put in place so that their initial imperfection is opposed to the deformation of the self-weight (concave function). Initial imperfections will, therefore, have a slightly beneficial effect and it is safe not to consider them.

4.2.4 Results

The results obtained are illustrated in Figure 4.8. In the upper left corner, there is the relationship between the load factor applied to the ULS combination (called M_{ulcc}) and the horizontal displacement of the point represented by a purple square on the structure.

The first thing to notice is that the load factor reaches the value of 1.12. This means that the structure resists under the ULS load combination and that the structure is not oversized since the load factor is close to 1.

Then, the maximum admissible deflection of $L/300 = 20\text{mm}$ is reached when the factor of the ULS load combination is 0.80. This corresponds to a factor of the SLS load combination of 1.18.

It can, therefore, be concluded that the structure is sized correctly.

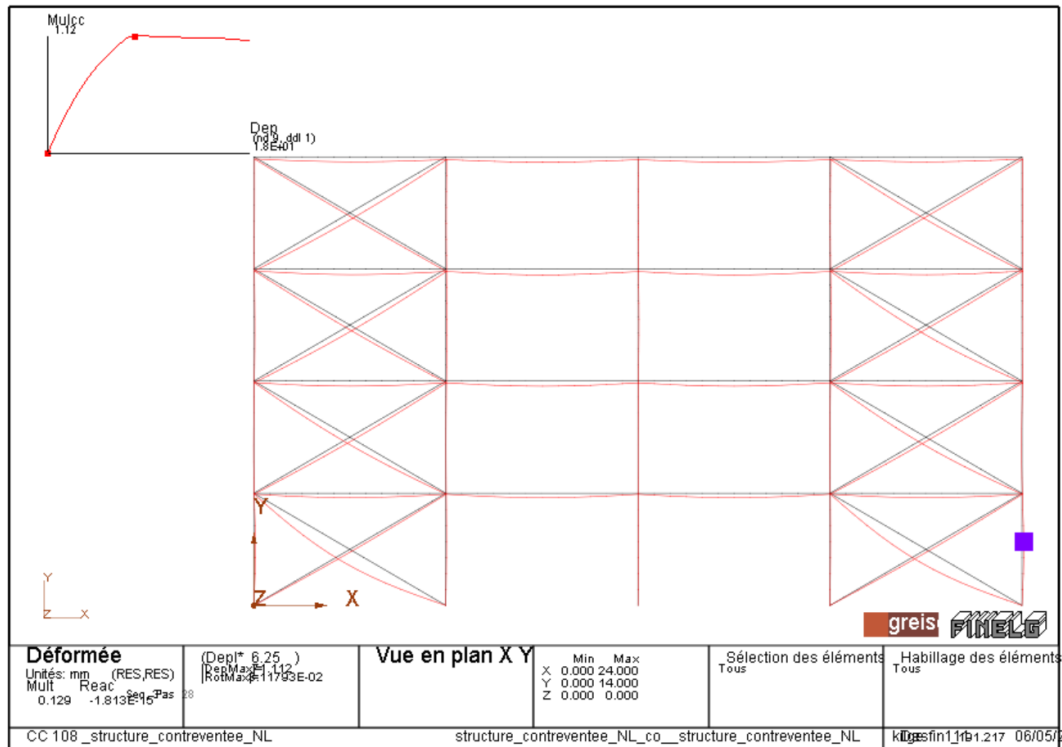


Figure 4.8: Results obtained

Another important information to note is the structural ruin criterion. The ruin appears in the column pointed by the purple square in Figure 4.8 due to the plastification of the column flange most stressed in compression following the M-N interaction. Indeed, the column is subjected to compression due to the loads transmitted by the upper storeys and to bending due to the wind forces (nevertheless very weak) and the effects of second-order. The program therefore stopped when ϵ_u reached 0.05 in this column.

The plastic zone when the load factor is 1.12 is shown in Figure 4.9 below.

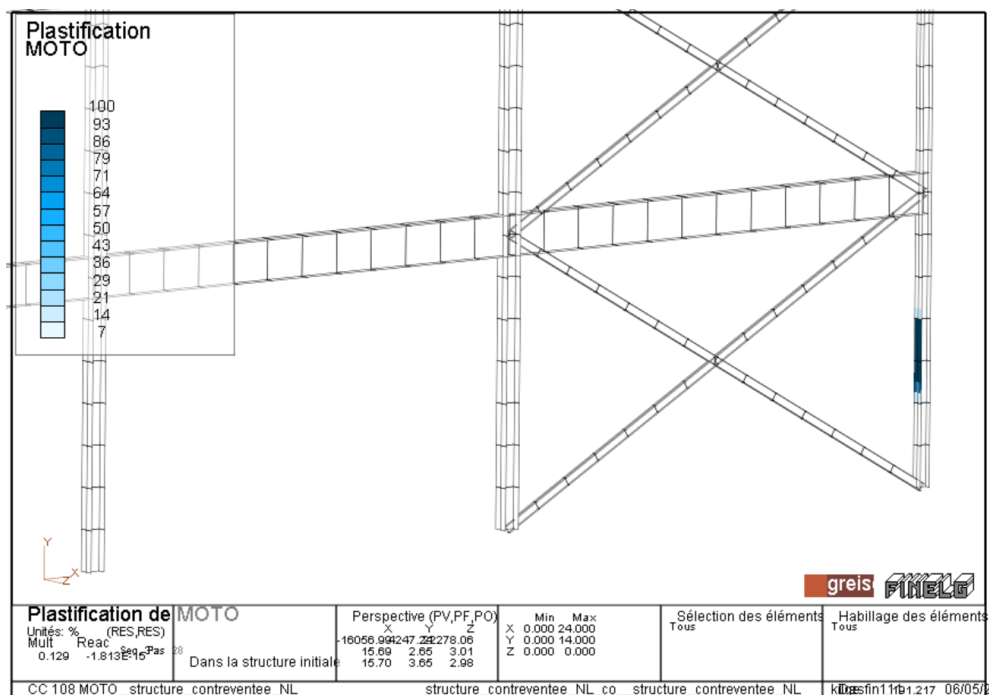


Figure 4.9: Plastic zone

5 Damaged structure

The loss of the column shown in red in Figure 4.10 below will now be simulated. A column on the ground floor was chosen because it is generally on the ground floor that the risk of losing a column is highest and it is the columns on the ground floor which take up the greatest efforts. In addition, the central column was chosen in order to develop a complete failure mechanism in the directly affected part (DAP).

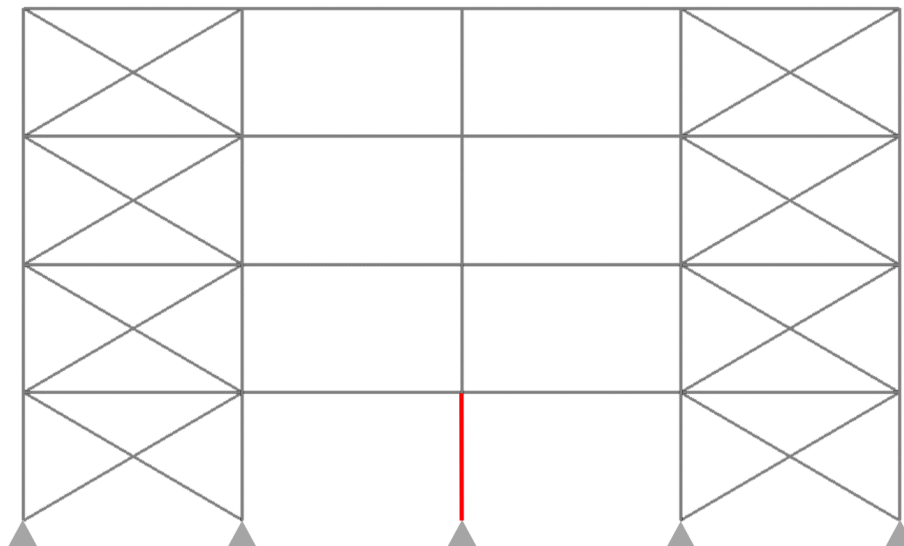


Figure 4.10: Lost column

5.1 Without taking into account the resistance of the joints

First, as explained in the introduction, the structure will be analysed by assuming fully resistant and infinitely ductile joints, as Farah Hjeir had supposed in his Master's thesis [20].

5.1.1 Column loss simulation method

First, the structure was fully loaded with the accidental load combination. To do this, the imposed loading method was used, making 10 steps of 0.1.

Then, to simulate the loss of the column, the method by imposed displacement was used. To do this, the column has been deleted and replaced by a support, as shown in Figure 4.11 below. Then a support settlement (downwards) was gradually applied to this support (purple arrow on Figure 4.11). The reaction of this support (exerted upwards) decreases as the support is lowered. This reaction corresponds to the compression force that there would actually be in the lost column. In addition, the support settlement is equal to the vertical displacement at the top of the lost column. It is, therefore, possible to trace the evolution of the relation "Vertical displacement at the top of the lost column - Axial load in the lost column".

So that the structure can find a new equilibrium configuration and remain stable despite the loss of the column, it is necessary to reach a compression force in the lost column of at least zero (i.e., a zero support reaction). Achieving a tensile force (i.e., a downward support reaction) would mean that the structure still has a certain reserve of robustness.

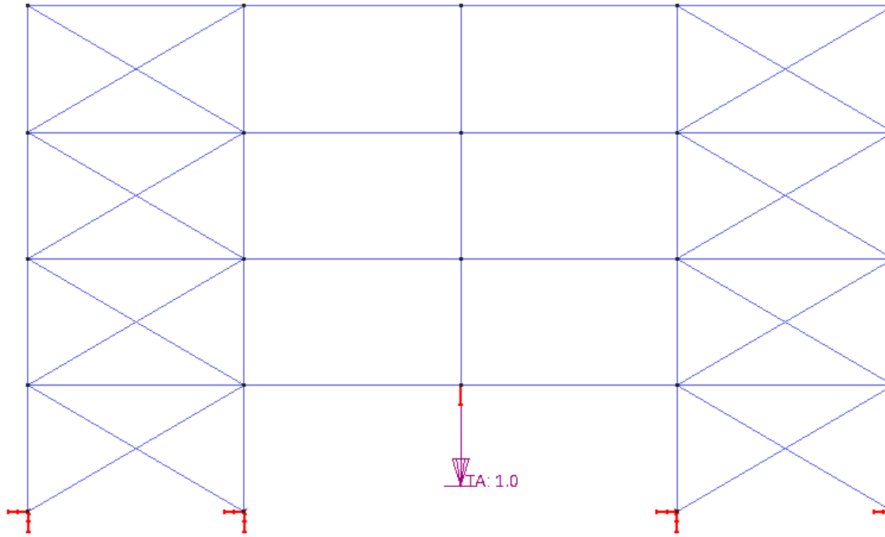


Figure 4.11: Column replacement by support and application of support settlement

5.1.2 Steel behavior law

Previously, the behavior of the elements was assumed to be elastic-perfectly plastic. However, when a plastic zone appears in the structure, this zone loses all rigidity and a very significant difference in rigidity appears between the different parts of the structure. In the present case, this difference in rigidity is not supported by the program which returns an error message.

To solve this problem, a slight rigidity is given to the steel elements after their plastification (i.e., after reaching f_y). This rigidity must remain very low because it will slightly overestimate the resistance of the elements. The constitutive law of the elements will thus be bi-linear, as presented in Figure 4.12.

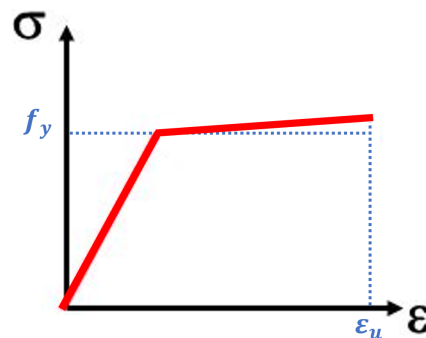


Figure 4.12: Bi-linear law

The criterion for stopping the program nonetheless remains the same as before. The ruin appears when $\epsilon_u = 0.05$ is reached in an element.

5.1.3 Results

Note that the initial imperfections of the columns were considered in the same way as in the previous section.

As Farah Hjeir noted in his thesis, it is necessary to reinforce the two columns and the two diagonals in pink in the figure 4.13 to find a new equilibrium configuration under the total loss of the column.

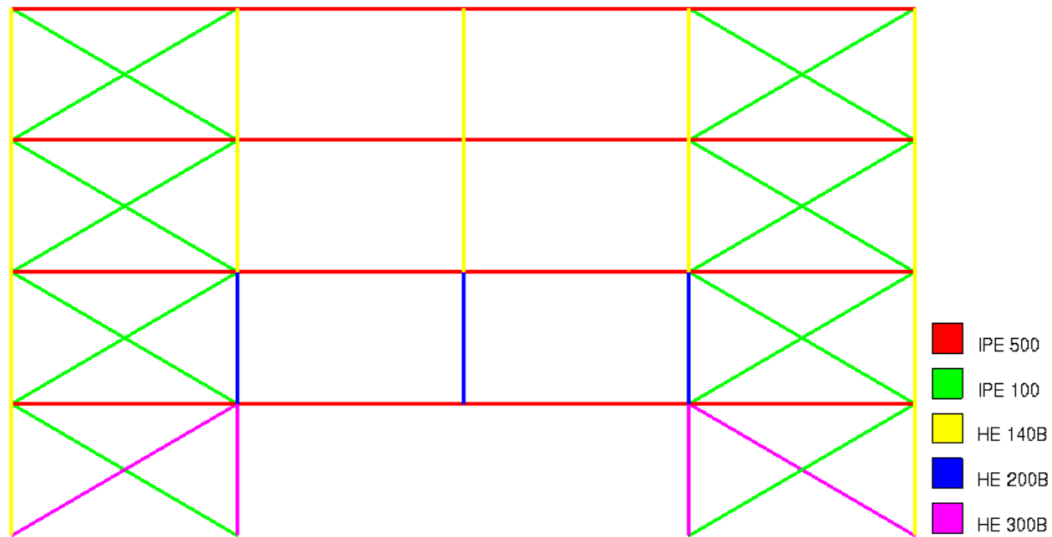


Figure 4.13: Element geometries to allow the loss of the central column

The relation between the vertical displacement at the top of the lost column and the load factor is thus that presented in Figure 4.14. The load factor λ is equal to N/N_0 , where N is the force applied downwards simulating the loss of the column and N_0 is the initial compression force in the column which will be lost (see Figure 4.15). In addition, the reaction in the support replacing the lost column is therefore $R = N_0 - N = N_0 - \lambda N_0$, and $\lambda = (N_0 - R)/N_0$.

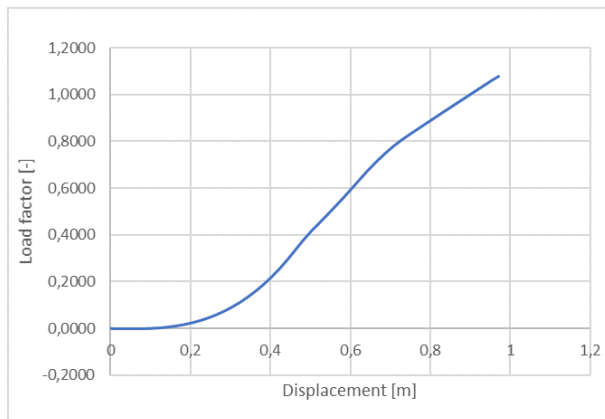


Figure 4.14: Load factor - vertical displacement relationship

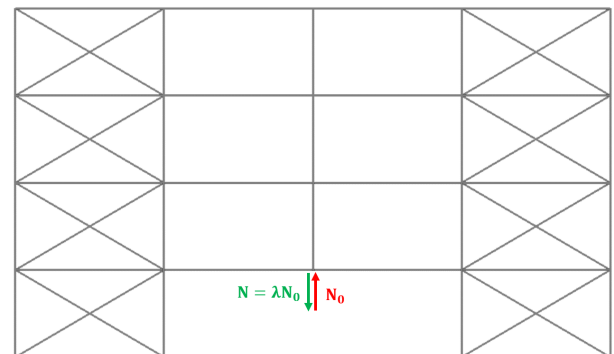


Figure 4.15: Representation of the load factor

A load factor of 1.08 is reached. The displacement at the top of the lost column is then worth 0.97m. Since the load factor reached is greater than 1, the structure is able to find a new equilibrium configuration if the column considered is entirely lost.

5.1.4 Results analysis

The plastic zones when the load factor is 1.08 are shown in Figure 4.16 below.

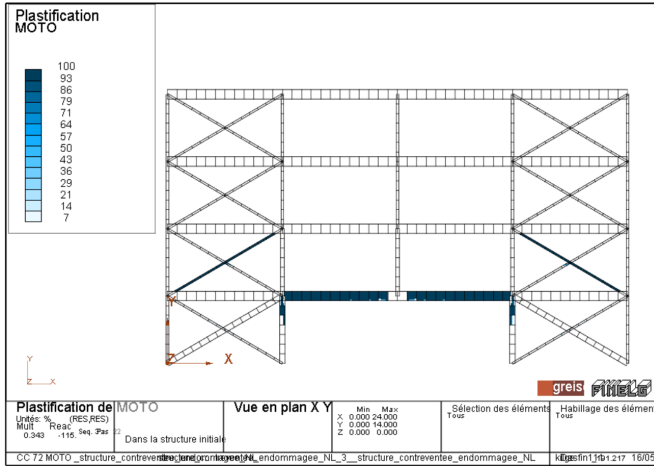


Figure 4.16: Plastic zones at the time of failure

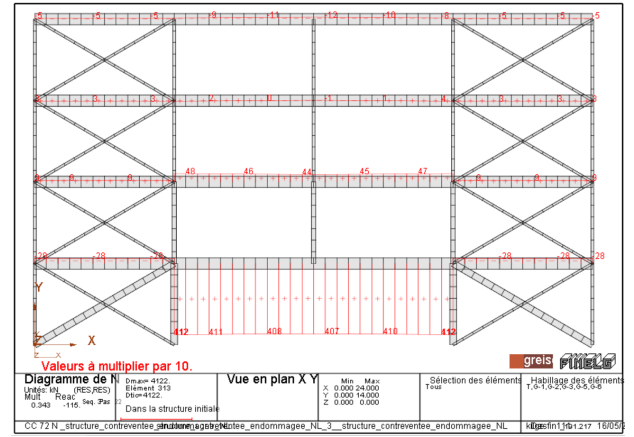


Figure 4.17: Axial forces in the beams at the time of failure

The ruin appears in one of the HE300B columns. Indeed, these columns are stressed in compression and in bending due to the effects of second-order and to the membrane forces, in constant increase, which have developed in the beams of the DAP. There therefore appears an area highly stressed in compression (plastic zone in Figure 4.16 for each column).

At the time of the failure, there is also a significant plastic zone in the beams just above the lost column. These beams are stressed by the following forces :

$$N_{Ed} = 4120 \text{ kN (see Figure 4.17)} \quad (4.1)$$

$$M_{Ed} = 3 \text{ kNm} \quad (4.2)$$

The beams hardly work anymore in bending. The bending forces have disappeared and significant membrane forces have developed.

The axial resistance of these beams is $N_{pl,Rd} = A \cdot f_y = 115.5 \cdot 10^2 \cdot 355 \text{ kN} = 4100.25 \text{ kN}$.

This resistance is slightly lower than the effort N_{Ed} . This is explained by the fact that the constitutive law of the elements is bi-linear, which slightly overestimates the resistance of the elements, as explained previously.

Then, as shown in Figure 4.17, a compression force (of -120 kN) appears in the beams of the top storey.

When the structure loses a column, it deforms. If the structure is not braced, the IAP is not very rigid and deforms a lot (see Figure 4.18). From then on, the IAP will move horizontally and sag on the DAP, which is called the arc effect. This induces compression forces in the beams of the top storeys if the structure is high enough. On the other hand, if the structure is braced and that the IAP is very rigid, it will not deform and there will be no arc effect (see Figure 4.19). The beams will then be all stressed in tension.

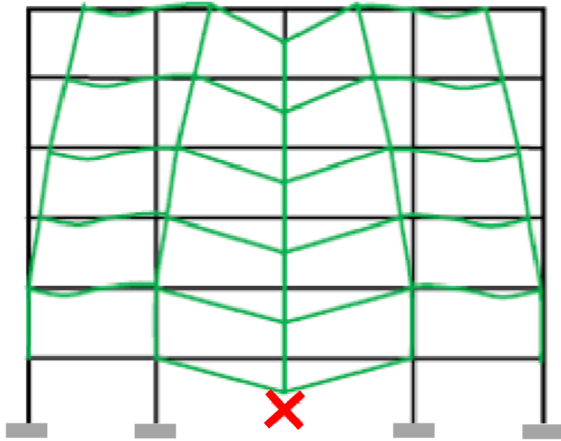


Figure 4.18: Deformation of a non-braced structure losing a column

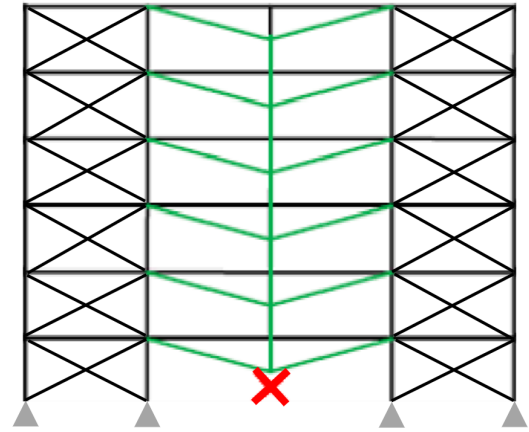


Figure 4.19: Deformation of a braced structure losing a column

In the present case, the structure is braced but the rigidity of the IAP is not significant enough to avoid an arc effect. Indeed, the deformation of the structure at the time of failure is shown in Figure 4.20. It can be seen that the IAP sags a little on the DAP. This is why a compression force (nevertheless very low) appears in the beam of the top storey.

Note also that the bracing elements working in compression of the first two storeys are strongly deformed due to the second-order effects. However, the compressive forces are very low and these elements resist.

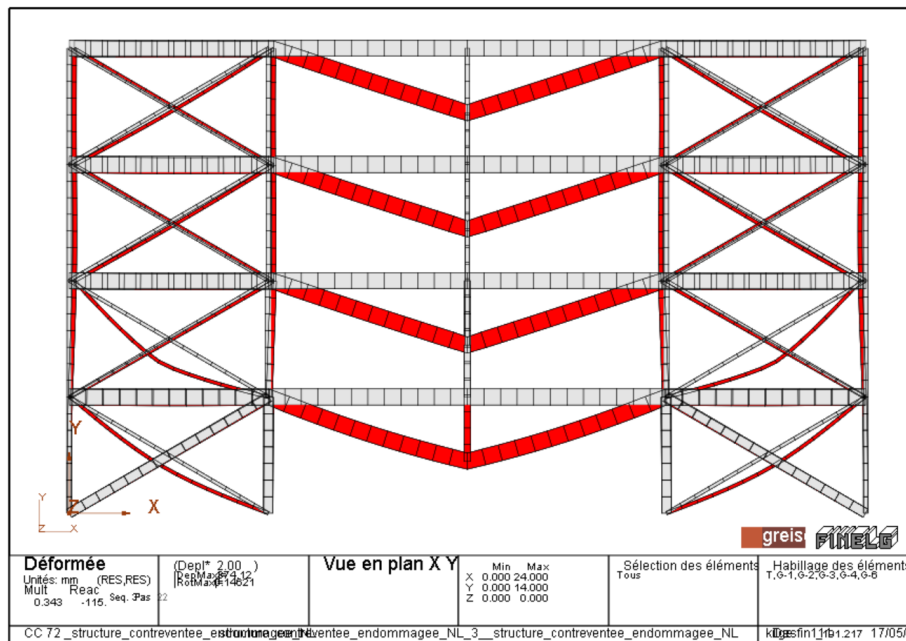


Figure 4.20: Deformed at the time of ruin

5.1.5 Assumptions about joints

According to the results above, the structure is able to find a new equilibrium configuration if the column is lost. However, remember that an assumption was made: the joints were assumed to be fully resistant.

However, the forces in the beams when the load factor is worth 1, and therefore that the column is completely lost, are represented in Figure 4.21 below. In the beams located just above the lost

column, the tensile forces are of the order of 4120 kN. This means that the joints connecting the beams of the first storey of the DAP to the HE300B columns must be able to take up a tensile force of 4120 kN.

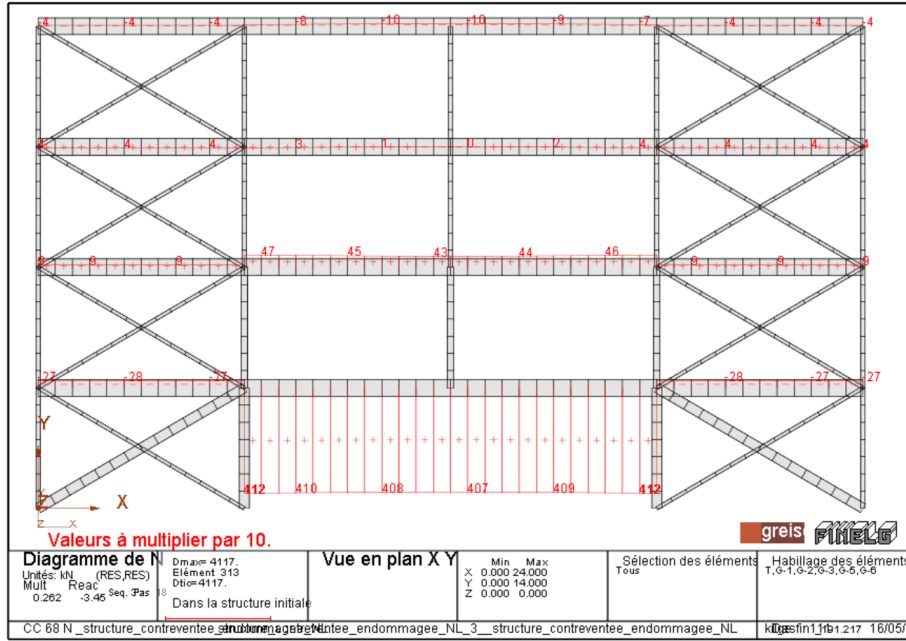


Figure 4.21: Axial forces in beams when the column is completely lost ($\lambda = 1$)

Different joint configurations will be considered to see if this assumption is acceptable or what would be the influence if the joints are not fully resistant and infinitely ductile.

As shown in Figure 4.21, significant membrane forces develop in the beams located just above the lost column, but in the upper beams, the membrane forces are much lower. Therefore, by using partial strength joints, there could be a distribution of forces towards the beams of the upper storeys, and the structure could still find a new equilibrium configuration.

5.2 With joints having the resistance specified by the tying method proposed by the Eurocode

First, the joints will have the resistance specified by the tying method present in Eurocode to assess the relevance of this method.

5.2.1 Calculation of tying force

The tying method proposed by the Eurocode indicates that each continuous tie, including its end connections, should be capable of sustaining a design tensile load:

For internal ties:

$$T_i = 0.8 \cdot (g_k + \Psi \cdot q_k) \cdot s \cdot L \text{ or } 75 \text{ kN} \quad (4.3)$$

For perimeter ties:

$$T_p = 0.4 \cdot (g_k + \Psi \cdot q_k) \cdot s \cdot L \text{ or } 75 \text{ kN} \quad (4.4)$$

Where,

- s is the (average) spacing of ties
- L is the span of considered tie
- Ψ is the factor according to the accidental load combination

- g_k is the permanent characteristic load applied on the considered floor
- q_k is the variable characteristic load applied on the considered floor

In the present case, only internal joints will be modeled. According to the tying method, their resistance must, therefore, be as follows:

$$T_i = 0.8 \cdot (g_k + \psi \cdot q_k) \cdot s \cdot L = 0.8 \cdot (15.412 + 0.5 \cdot 3) \cdot 6 \cdot 6 = 487.06 \text{ kN} \quad (4.5)$$

5.2.2 Joint design

The joints which are at the ends of the horizontal ties, and which are therefore concerned by the tying method, are represented by a red point in Figure 4.22.

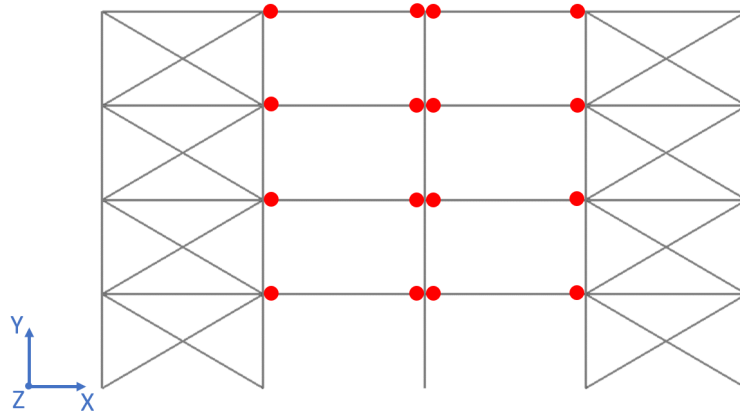


Figure 4.22: Designed joints

It will be assumed that these connections have exactly the tensile strength required by the tying method, $N_u = 487.06 \text{ kN}$. Then, as explained in the previous chapter, the tying method does not indicate the ductility of the joints. These will therefore be assumed to be infinitely ductile (i.e., with infinite elongation capacity), which is very safe.

The law of behavior in traction of these joints will consequently be that presented in Figure 4.23. The stiffness is assumed to be infinite until reaching 487.96 kN . Then the behavior is supposed to be perfectly plastic with an infinite elongation capacity.

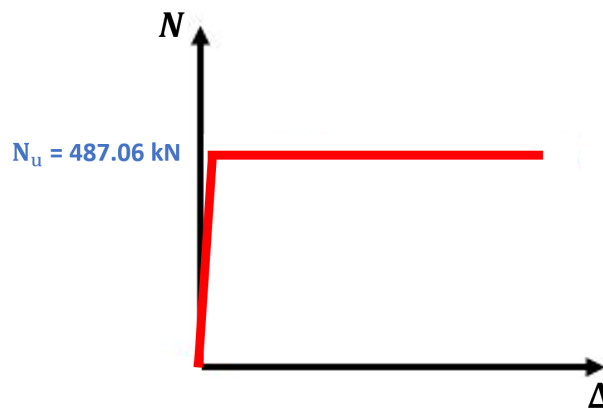


Figure 4.23: Law of behavior of joints in traction

5.2.3 Joint modeling

The joints were modeled in *FINELG* by elements of type 200. The integration of this type of element in *FINELG* is explained in [22].

Type 200 elements are unidirectional spring elements. They are attached to two nodes and act along or around a fixed direction defined in the global axes. The springs can, therefore, be translational or rotational, and the behavior of the springs can be elastic, elastic-perfectly plastic, or even multi-linear.

Joints are assumed to be dimensionless. Consequently, the two nodes to which the springs are fixed are two superimposed nodes.

Elements of type 200 will, therefore, be placed on the model at the places marked with a red point in Figure 4.22. In these places, all the elements described below will be put in place (the system of axes used to describe them is presented in Figure 4.22):

- A horizontal translational spring element, which extends along the X-axis. This element follows the rigid-perfectly plastic law described in Figure 4.23. Note that the behavior of this spring is assumed to be the same in tension as in compression, but this does not pose a problem because it will not be stressed in compression.
- Elements of translational springs which follow an elastic law with very high rigidity, along the axes Y and Z.
- Elements of rotational springs which follow an elastic law with very high rigidity, around the axes Y and X.

Around the Z-axis, the rotation is free because the joints are supposed to be simple joints.

A critical remark must be made concerning this joint modeling. The springs are defined according to the global axes. Consequently, the law of behavior in traction introduced remains along the horizontal axis. This means that the tensile strength of a joint N_{Rd} is reached when the horizontal projection of the tensile force in the beam fixed to this joint is equal to N_{Rd} . The axial force in the beams can, therefore, exceed N_{Rd} . This modeling slightly overestimates the resistance of the joints because they will yield later than in reality, for a resultant of forces greater than N_{Rd} .

5.2.4 Results

Note that the behavior law of steel and the method to simulate the loss of the column remain the same as for the case without taking into account the resistance of the joints.

The structure studied is shown in Figure 4.24. Specific geometries have been reinforced to reach a load factor of 1 (and therefore find a new equilibrium configuration after the complete loss of the column).

Previously, when the joints were supposed to be fully resistant, the bracing elements of the first storey working in traction had to be reinforced with HE300B profiles because the axial force in the beams of the first storey was significant. Now, since the tensile strength of the joints is limited, the axial force in the beams of the first storey will be less, and the forces will be better distributed between the storeys. Indeed, once the tensile strength is reached in the joints of the first storey, there will be a distribution of the forces towards the beams of the upper storeys. Consequently, the bracing system is reinforced over its entire height but with less significant reinforcement than previously.

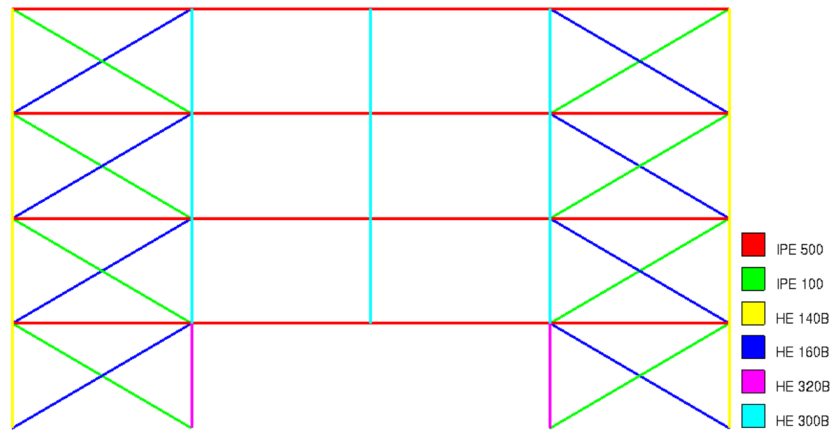


Figure 4.24: Element geometries

The relation between the load factor and the vertical vertical displacement at the top of the lost column obtained is presented in Figure 4.25. It can be seen that a load factor of 1.07 is reached for a vertical displacement at the top of the lost column of 2.12m.

Then, at the time of failure, when the load factor reaches 1.07, several results are presented.

Firstly, Figure 4.26 shows the deformation of the structure at failure, and Figure 4.27 indicates the plastic zones at failure. As before, the failure appears because $\epsilon_u = 0.05$ is reached in one of the two columns with a plastic zone. These columns are stressed in compression and in bending due to the second-order effects and to the membrane forces.

Then, Figure 4.28 shows the axial force in the beams at failure. It can be seen that the membrane forces in the beams of the DAP are identical for all the storeys. Indeed, once the axial force in the joints of the first stage has reached $N_{Rd} = 487.06$ kN, the forces will be distributed to the beams of the upper storeys. At the end, the axial forces in the joints of all the storeys will have reached $N_{Rd} = 487.06$ kN, and the joints will lengthen indefinitely.

Also, it can be seen that the membrane forces in the beams of the DAP are greater than $N_{Rd} = 487.06$ kN. Indeed, as explained, to reach a horizontal force in the joints of 487.06 kN, the axial force in the beams will be greater than 487.06 kN. In addition, the higher the vertical displacement at the top of the lost column, the more the axial force in the beams will increase. However, the horizontal projection will not exceed $N_{Rd} = 487.06$ kN.

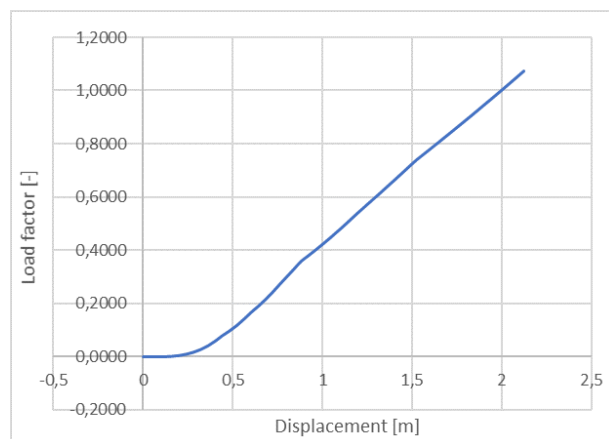


Figure 4.25: Load factor - vertical displacement at the top of the lost column relationship

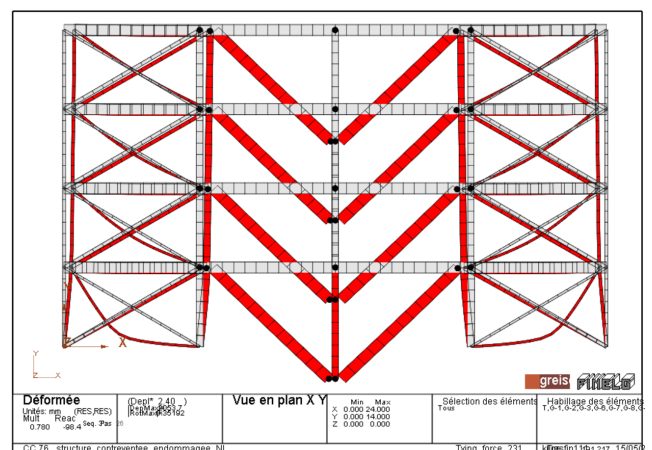


Figure 4.26: Deformed at the time of failure

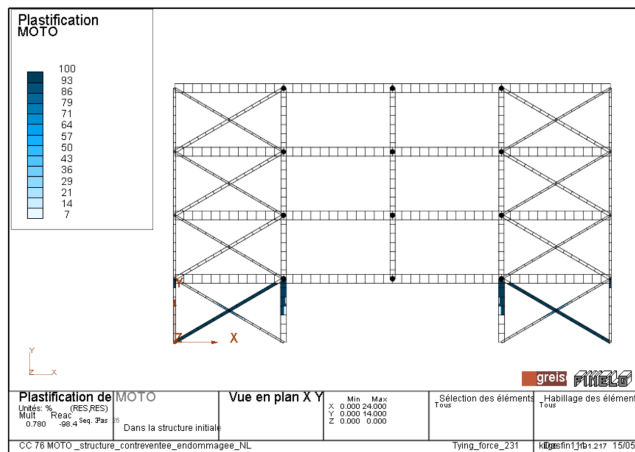


Figure 4.27: Plastic zones at the time of failure

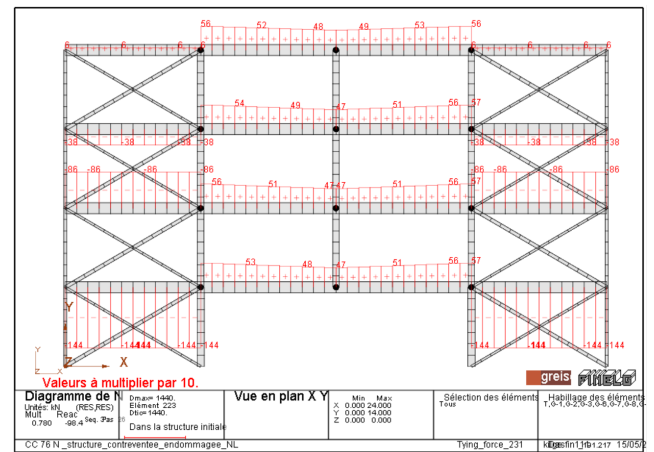


Figure 4.28: Axial forces in beams at the time of failure

When the load factor is 1, the elongations in the joints are presented in Table 4.1. The elongations in the joints of the same storey are all identical. In addition, as can be seen, the higher the storey, the lower the elongation because the later the resistance of the joints $N_{Rd} = 487.06$ kN was reached.

| Elongation in joints | |
|------------------------|-------|
| 1 st storey | 96 mm |
| 2 nd storey | 83 mm |
| 3 rd storey | 72 mm |
| 4 th storey | 63 mm |

Table 4.1: Horizontal elongations for a load factor of 1

5.2.5 Results interpretation

A load factor greater than 1 is reached, which means that the structure is able to find a new equilibrium configuration when the column is completely lost. This result was expected. Indeed, since the ductility of the joints has been considered infinite, the elongation of the beams of the DAP will be concentrated in the joints, and the structure will be able to undergo a very significant displacement at the top of the lost column (provided that the IAP does not yield before, but it can be reinforced accordingly). This is why the displacement at the top of the lost column exceeds 2m in the present case. However, the higher the vertical displacement, the higher the vertical component of the membrane forces (as illustrated in Figure 4.29 below). Consequently, when this vertical component is sufficiently large, it will counterbalance the gravitational loads which are applied to the structure, and the structure will find a new equilibrium configuration.

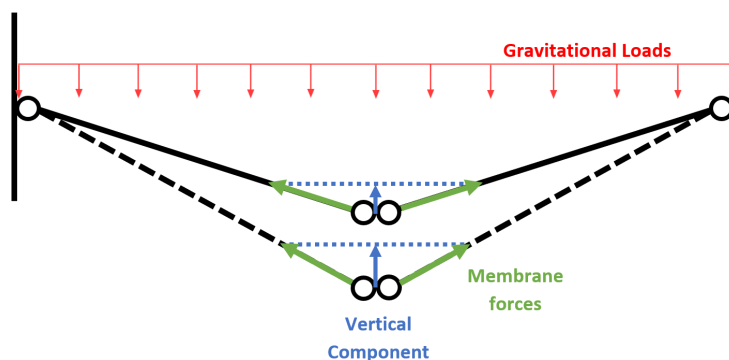


Figure 4.29: Balance of efforts

These results may suggest that the resistance obtained using the tying method is sufficient to ensure the robustness of the structure against the loss of the column considered (provided that the IAP is sufficiently resistant). However, in reality, the joints will have a finite elongation capacity, which will be of the order of a few centimeters maximum. But, for a load factor of 1, the elongation in the joints of the first storey is worth 9.6 cm (see Table 4.1), and the elongations in the joints of the other storeys are also very important. A normally designed joint is unlikely to withstand such an elongation.

Several configurations of joints will, therefore, be studied to see if one of them would have the properties necessary to ensure the robustness of the structure against the loss of the column considered.

5.3 With header plate connections sized to ULS

The first beam-column connection studied is a header plate connection type. This type of connection is shown in Figure 4.30. A plate is welded to the beam web, and this plate is then bolted to a flange of the column.

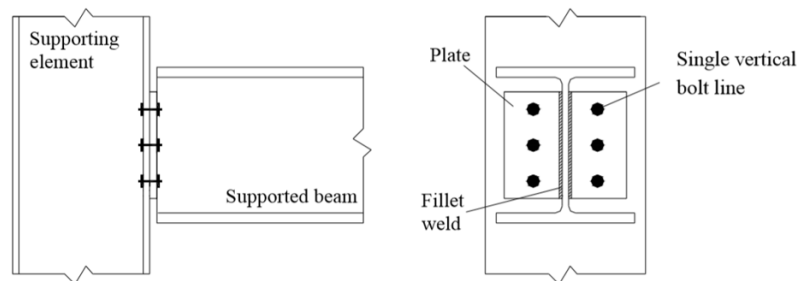


Figure 4.30: Example of a header plate connection

First, the joints will be dimensioned to take up the forces under the load combination at the ULS when the structure is intact, i.e., without taking into account the scenario of a column loss in the sizing. This will allow to see if the joints are capable of ensuring robustness without taking any particular measures. If this is not the case, better properties should be given to the joints to ensure the equilibrium of the structure for the damage scenario considered.

5.3.1 Joint design

The beam-column joints concerning the beams of the DAP (see red dots in Figure 4.31) will, therefore, be dimensioned this time to take up the forces obtained at the ends of these beams under the load combination at ULS when the structure is intact. Under these conditions, the beams of the DAP are not stressed by axial forces ($N_{Ed} = 0$ kN). The only force appearing at the ends of the beams is a shear force being worth $V_{Ed} = 277$ kN. This force is the same for the ends of the beams on each storey, except for the top storey, but the joints will be assumed to be the same as for the lower storeys.

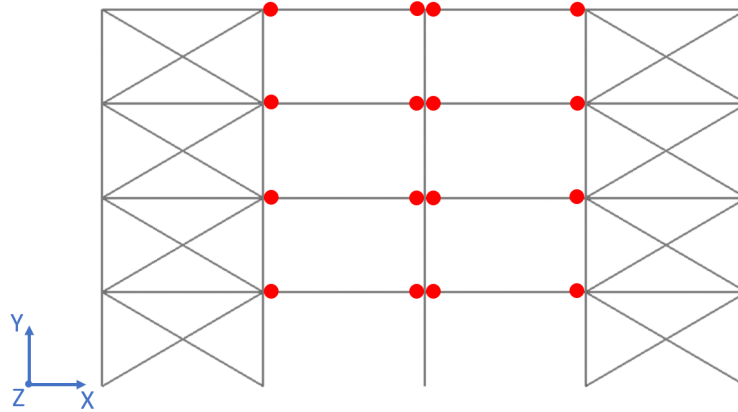


Figure 4.31: Designed joints

The connections have been dimensioned in accordance with the European recommendations for the design of simple joints in steel structures [23], and the calculation is detailed in the Annex A. The configuration obtained to take up the effort $V_{Ed} = 277$ kN is shown in Figures 4.32, 4.33 and 4.34 below.

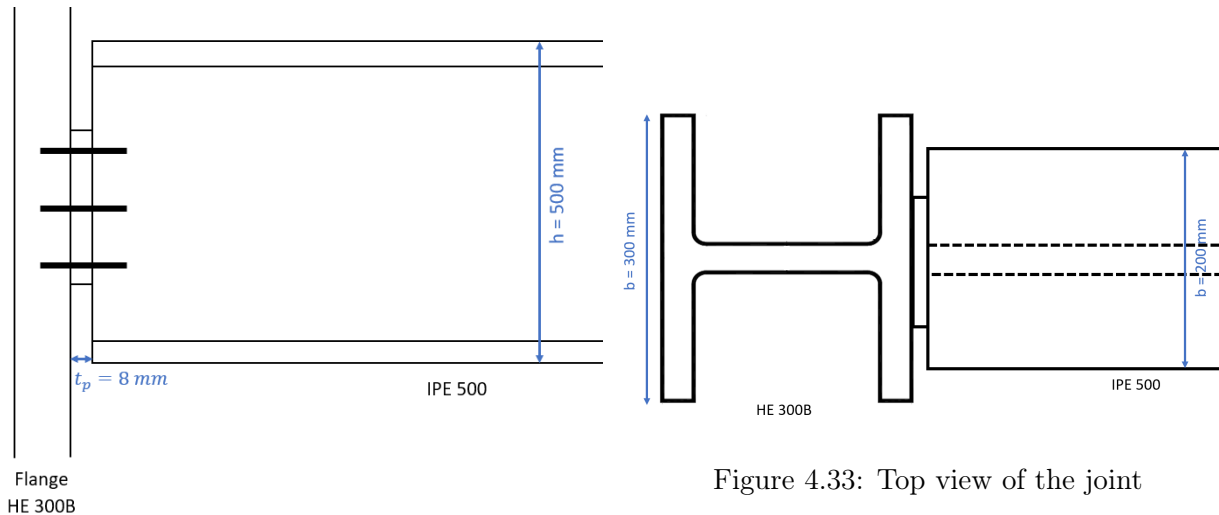


Figure 4.33: Top view of the joint

Figure 4.32: Longitudinal view of the joint

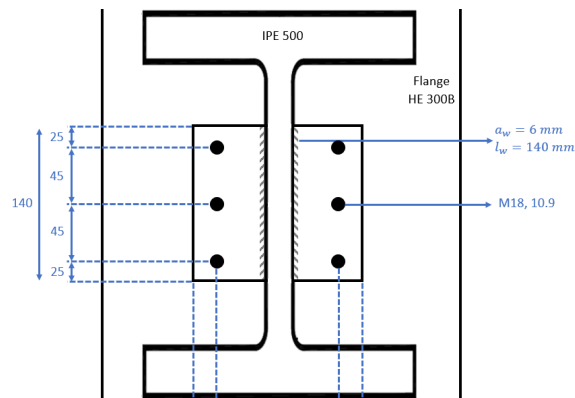


Figure 4.34: Front view of the joint

This configuration ensures a shear strength $V_{Rd} = 292.68$ kN. Also, the design tensile strength is $N_{Rd} = 506.87$ kN, and the ultimate tensile strength is $N_u = 661.98$ kN.

It should also be noted that this joint configuration respects the ductility criteria and the rotation criteria, which allow to model the joint as a simple joint (i.e., with zero rigidity in rotation).

However, such a joint does not have an infinite deformation capacity. The elongation capacity of the joint was calculated using the formulas giving the stiffnesses of the components present in Eurocode 3 Part 1-8 and by following an analytical method proposed by M. Jaspart in a calculation note provided. This calculation is also presented in the Annex A. The elongation capacity of the joint obtained is $\Delta_u = 2.86\text{mm}$.

The law of behavior of the joint in tension can thus be approximated by the bi-linear law represented in Figure 4.35 below.

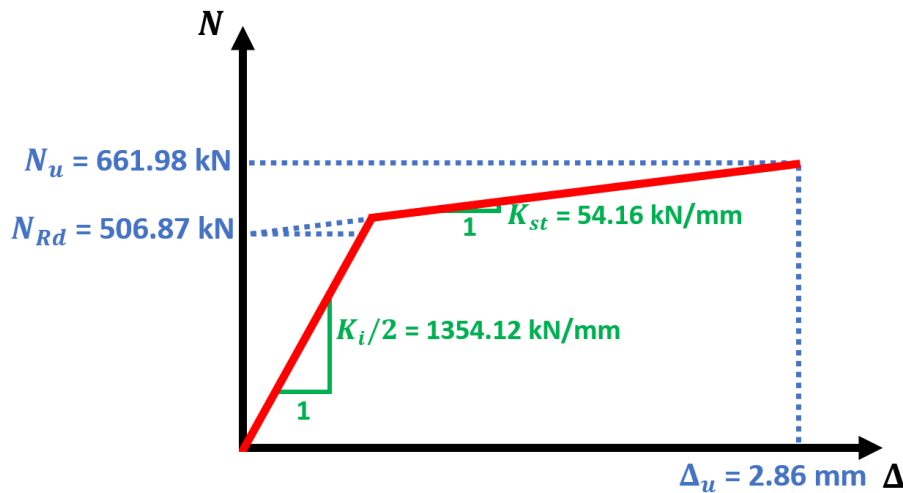


Figure 4.35: Law of behavior of the joint in traction

Note that a HE300B profile column was considered for the dimensioning of the joint because a HE300B profile must be used at the foot of the columns next to the lost column. The geometry of the column does not influence the resistance but very slightly influences the ductility of the joint. To be consistent, a HE300B profile will, therefore, be used over the entire height of the columns concerned by the dimensioned joints.

5.3.2 Joint modeling

The joints were again modeled in *FINELG* by elements of type 200 (see [22]). As a reminder, the behavior of the springs can be elastic, elastic-perfectly plastic, or even multi-linear, but the behavior will always be identical in tension and compression. Also, it is possible to set an elongation limit value for an element of type 200. Once this value is exceeded, the force and the stiffness of the element are then removed.

Then, as before, the joints are assumed to be dimensionless. From then on, the two nodes to which the springs are attached are two superimposed nodes.

However, now, two different models will be studied. These models are shown in Figures 4.36 and 4.37, where the red dots represent the places where elements of type 200 will be put in place.

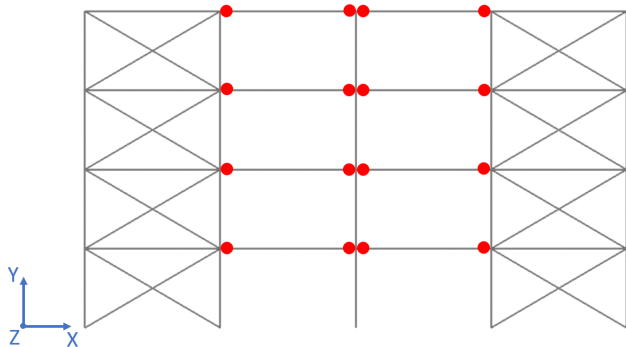


Figure 4.36: Model 1

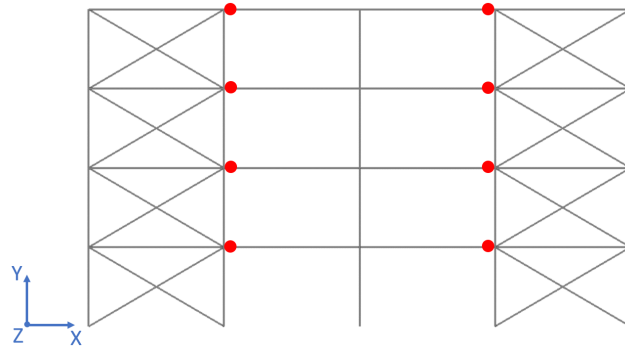


Figure 4.37: Model 2

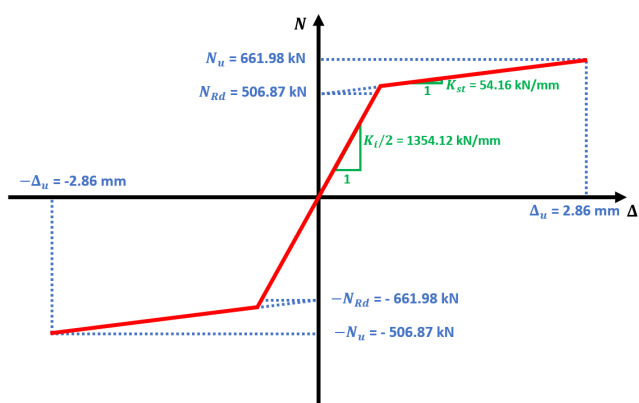


Figure 4.38: Behavior law of a horizontal extensional spring modeling the axial behavior of a single joint

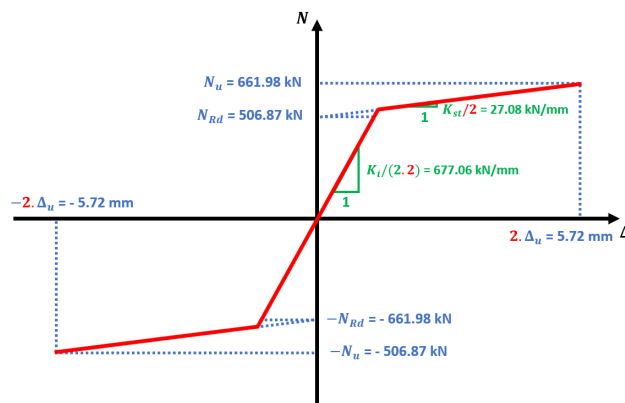


Figure 4.39: Behavior law of a horizontal extensional spring modeling the axial behavior of two joints

For the first model (Figure 4.36), the elements of type 200 are placed in the same places as before. Each set of springs therefore represents a beam-column joint. The horizontal spring elements, which extend along the X-axis, follow the behavior law represented in Figure 4.38. This law is identical to that presented in Figure 4.35, except that the behavior in compression is supposed the same as in tension (assumption always made by the elements of type 200 as explained previously). However, this is not disturbing because, during the loading, the beams will be very little stressed in compression and the compression force will never exceed N_{Rd} .

However, this model has a limitation. When the support compaction (simulating the loss of the column) increases, the membrane forces develop. At a specific time, the elongation in the horizontal spring elements of the first storey will reach the elongation limit $\Delta_u = 2.86\text{mm}$. At this time, these spring elements will instantly lose their stiffness and resistance. Therefore, a mechanism is created at each of the two beams on the first storey of the DAP, and the program stops. Indeed, since the horizontal spring elements placed at each end of these beams no longer have any stiffness, the beams can move freely in the horizontal direction, and the software detects a pivot.

This model, therefore, allows to trace the response of the structure following the loss of the column only until the joints of the first storey fail. It does not allow the progressive collapse of all the storeys of the DAP to appear. In reality, once the ruin of the first storey is reached, the ruin of the other storeys will follow quickly. Still, it could nevertheless be that the maximum load factor reaches its maximum after the ruin of several storeys. It therefore seems interesting to be able to trace the response of the structure to the complete ruin of the DAP.

To do this, a second model was studied (see Figure 4.37). For this second model, the elements

of type 200 are only installed at one end of the DAP beams. Each set of springs, therefore, models two joints, and a horizontal extensional spring element models the axial behavior of two joints. Consequently, the law of behavior of an element of horizontal extensional spring is that represented in Figure 4.39. The extension capacity of the spring is equivalent to the extension capacity $2\Delta_u$ of two joints. On the other hand, resistances N_{Rd} and N_u do not change. Consequently, the rigidities $K_i/2$ and K_{st} are divided by 2.

With this second model, when the elements of horizontal springs of the first storey will reach their limit of elongation $2\Delta_u$, there will be no appearance of local mechanisms at each beam of the first storey of the DAP because the beams remain held horizontally on one side. The program will continue to run. From then on, the progressive collapse of all the storeys will be able to be observed, and the program will stop when the failure of all storeys is reached and a global DAP mechanism is created (provided that the IAP does not yield before).

This second model is nevertheless less exact than the first since the two joints of a beam are modeled at only one end of it. This is why the two models will be studied. Thus, the second model can be validated by comparing it to the first.

For each of the two models, elements of type 200 (defined in the global axes) will, therefore, be put in place at the places marked with a red point on Figures 4.36 and 4.37. In these places, the elements described below will be put in place :

- A horizontal translational spring element, which extends along the X-axis. This element follows the bi-linear law shown in Figure 4.38 or in Figure 4.39 depending on the model studied .
- A vertical translational spring element, which extends along the Y-axis. This element follows an elastic-perfectly plastic law, with a very high elastic stiffness and a resistance equal to $V_{Rd} = 292.68$ kN. For this element, no strain limit has been set because the resistance V_{Rd} will never be exceeded, and the joint will not deform in shear.
- A translational spring element which follows an elastic law with very high rigidity, along the Z-axis.
- Elements of rotational springs which follow an elastic law with very high rigidity, around the axes Y and X.

Around the Z-axis, the rotation is free because the joints are simple joints.

The same remark as previously can be made about this joint modeling. Since the springs are defined according to the global axes, the law of behavior in traction introduced will remain according to the horizontal axis. Consequently, the tensile strength of a joint N_u will be reached when the horizontal projection of the tensile force in the beam fixed to this joint will be equal to N_u . This modeling therefore slightly overestimates the resistance of the joints which will yield for a resultant of the forces greater than N_u .

However, since the elongation capacity of the joints is now limited, the vertical displacement at the top of the lost column will be less and the resistance will be less overestimated than for joints having the resistance specified by the tying method.

Note also that the beam-column joints of the IAP were not modeled when they could have been added easily to the model. Indeed, due to the progressive collapse of the beams of the DAP, the beams of the IAP will undergo significant compressive forces. However, the elements 200 used to model the joints have the same behavior in tension as in compression. It would therefore not be wise to place elements 200 with the properties of the joint in tension at the level of the beams of

the IAP. Also, the compressive strength of the joints has not been calculated because it is assumed to be sufficient.

5.3.3 Results

The structure studied is shown in Figure 4.40. Certain elements were reinforced compared to the initial structure dimensioned to the ultimate limit states (ULS) and the service limit states (SLS) in order to avoid a premature ruin of an element of the IAP by plastic strain (i.e., by reaching the limit of deformation ϵ_u) before reaching the complete collapse of the DAP due to the successive failures of the joints of each storey. Also, as explained above, since the feet of the columns close to the lost column had to be reinforced with HE300B profiles, the joints were dimensioned with HE300B columns. Therefore, to be consistent, HE300B profiles were used over the entire height (what will be the case in reality to avoid costly continuity joints).

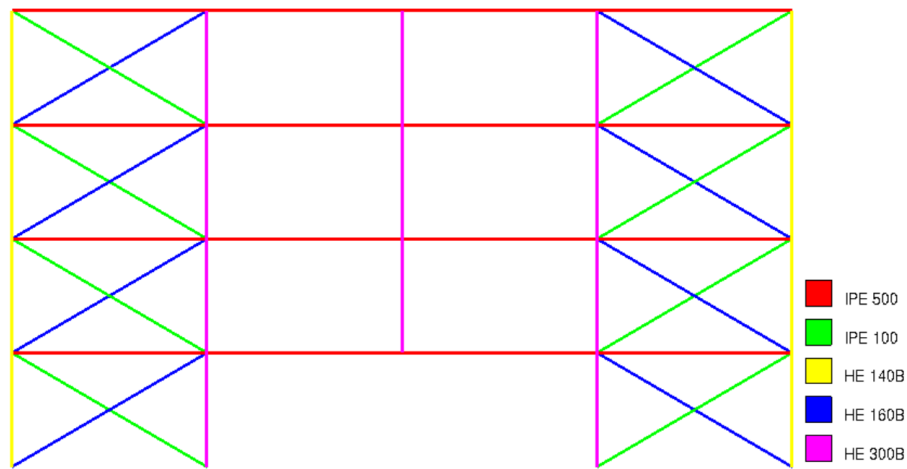


Figure 4.40: Element geometries

The relation between the load factor and the vertical displacement at the top of the lost column is then that presented in Figure 4.41. Two curves are shown in this Figure. The blue curve is the response obtained with the first model, for which the joints are modeled at the two ends of each beam of the DAP. As explained above, this curve stops when the joints of the first storey have failed because a mechanism then appears in the beams of the first storey of the DAP. Then, the orange curve is the response obtained with the second model, for which the two joints of a beam are modeled at the same end of it as explained previously. As for this curve, it stops when the joints of the four storeys have failed and a global mechanism is created in the DAP.

It can be seen that the two curves are perfectly superimposed. The responses obtained with each of the two models are therefore equivalent.

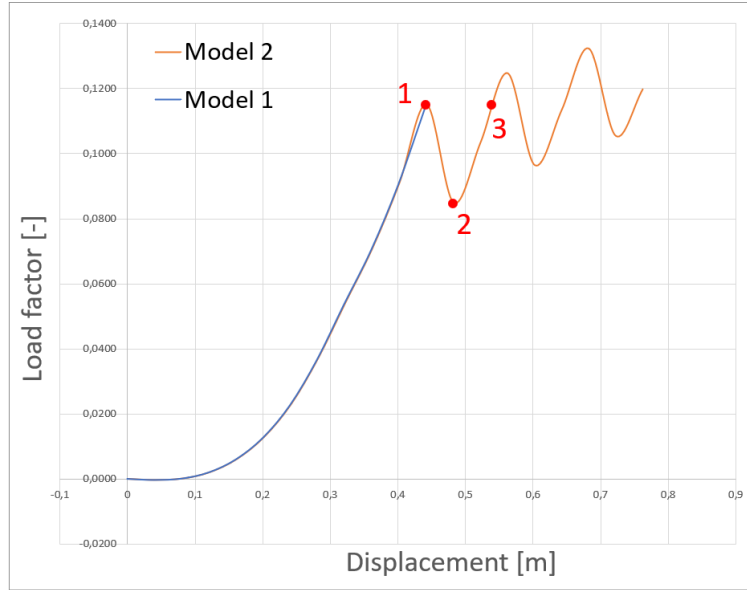


Figure 4.41: Load factor - vertical displacement at the top of the lost column relationship

On the orange curve, sudden drops can be seen. These appear because the joints of each storey successively reach the limit elongation Δ_u .

For example, just before the first drop (point 1 in Figure 4.41), the force in the horizontal springs of the first storey almost reached $N_u = 661.98$ kN (see Figure 4.42), and these springs have already lengthened. The reaction in the support representing the lost column is worth 1170 kN (Figure 4.43).

Then, just after the first drop (point 2 in Figure 4.41), the elongation in the horizontal springs of the first storey reached $2 \cdot \Delta_u = 2 \cdot 2.86$ mm (and the effort reached $N_u = 661.98$ kN). Consequently, these springs no longer have any stiffness and no longer take up any effort. The axial force in the beams of the first storey then suddenly disappears (Figure 4.44), and the reaction in the support representing the lost column suddenly increases (Figure 4.45), which causes the load factor to drop.

In reality, the joints of the first floor have yielded and the beams of the first floor are lost. This loss is however "authorised" by the standard. Indeed, as explained in the first chapter, robustness is ensured as long as the damage is not disproportionate compared to the cause which is at the origin of it. This definition is very subjective but it may be considered acceptable to lose the beams on the first storey. This is why it can be interesting to see if a load factor of 1 can be reached even if the beams of the first storey are lost.

After the loss of the beams on the first storey, the efforts taken up by the lost beams will have to be redistributed towards the beams on the upper storeys. At point 3 (see Figure 4.41), the reaction in the support representing the lost column again reaches 1170 kN (Figure 4.47), and the load factor is then the same as at point 1. The axial forces in the beams at point 3 are presented in Figure 4.46. It can be seen that, between points 1 and 3, the axial force in the beams of the second storey went from 400 kN to 623 kN and the axial force in the beams of the third storey went from 78 kN to 321 kN.

Then, in the same way, the joints of the upper storeys will successively reach the limit elongation $\Delta_u = 2.86$ mm, instantly losing all stiffness and resistance, and at the end of the curve, the four storeys of the DAP are collapsed.

In the present case, the ruin is therefore detected because the joints at the ends of the beams

CHAPTER 4. STUDY OF A STRUCTURE SUBJECT TO A LOSS OF COLUMN

of the DAP have all failed and the DAP has completely collapsed. However, the load factor can still increase before reaching the limit deformation ϵ_u in an element of the IAP.

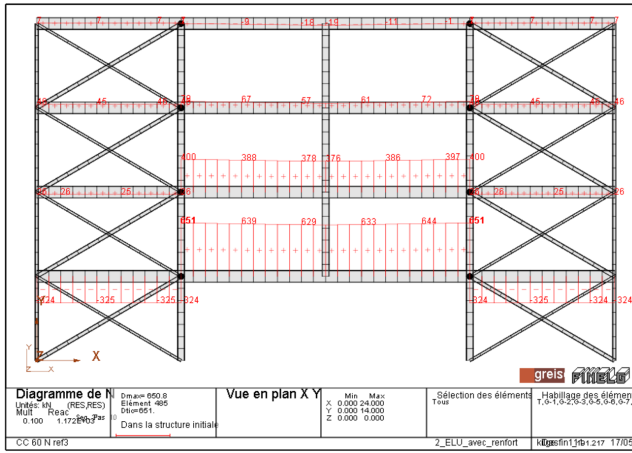


Figure 4.42: Axial force in beams at point 1

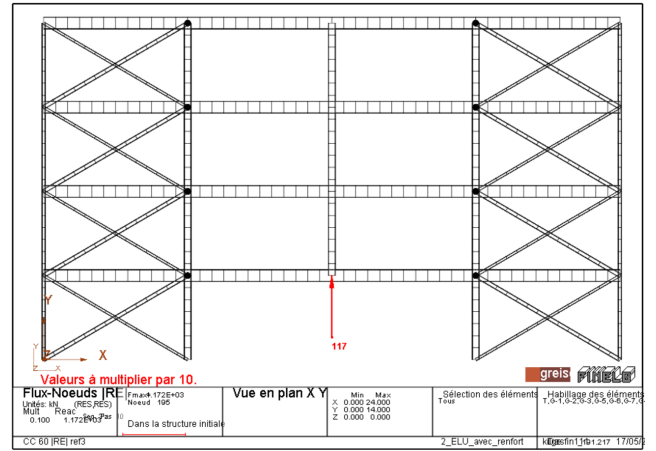


Figure 4.43: Support reaction representing the lost column in point 1

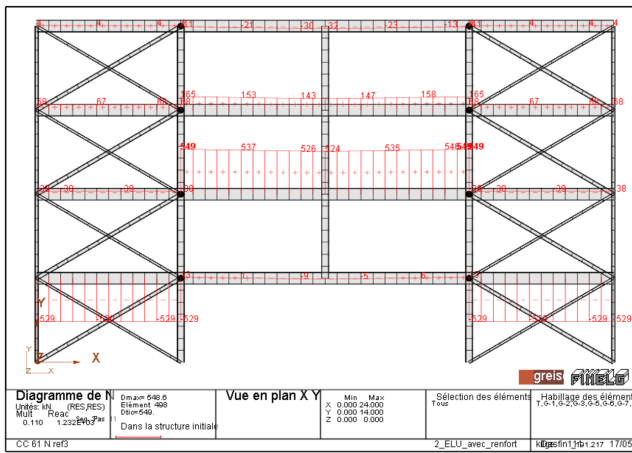


Figure 4.44: Axial force in beams at point 2

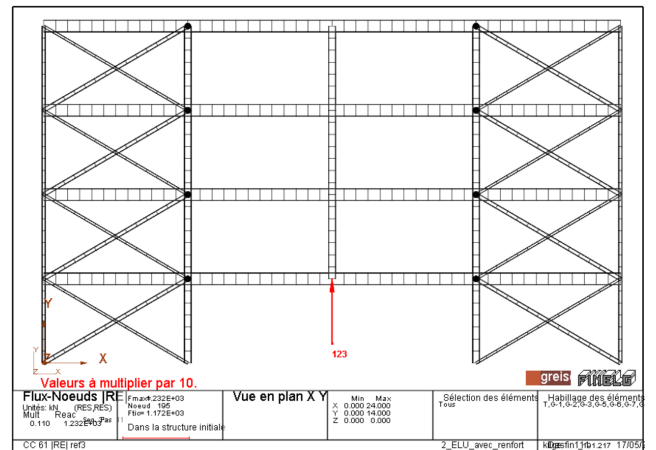


Figure 4.45: Support reaction representing the lost column in point 2

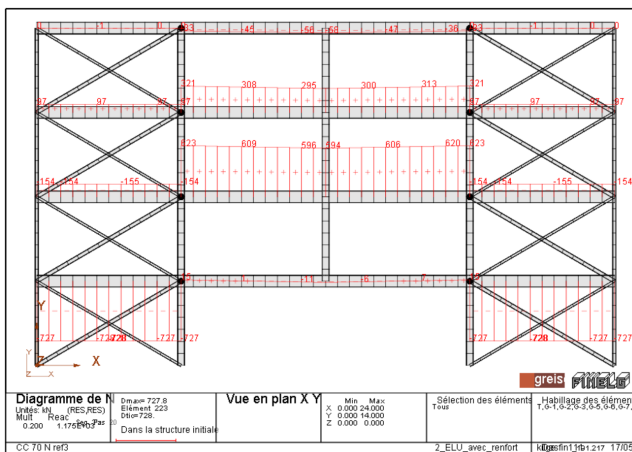


Figure 4.46: Axial force in beams at point 3

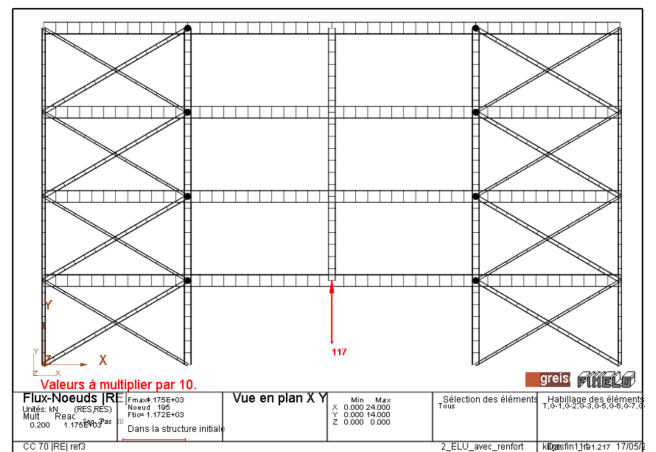


Figure 4.47: Support reaction representing the lost column in point 3

Finally, it can be seen in Figure 4.41 that the load factor reaches its maximum just before losing the beams of the third floor. The maximum reached is then 0.13.

The maximum is reached after losing several storeys because the elongation capacity of the joints is rather low ($\Delta_u = 2.86$ mm). Once the horizontal force has reached $N_{Rd} = 506.87$ kN in the joints of the first storey, these lose a lot of rigidity (the rigidity becomes K_{st}) and begin to deform strongly. When the load factor increases, the forces will then increase mainly in the beams of the upper storeys whose rigidity of the joints is higher (the rigidity of these is worth $K_i/2$). However, since the elongation capacity of the joints is low, the efforts will not have time to increase much in the beams of the upper storeys before the joints of the first storey fail. Consequently, at the loss of the joints of the first storey, the force in the beams of the upper storeys remains relatively low. This explains the fact that the load factor will further increase and reach a greater value when the second storey joints are lost. Similarly, the load factor at the loss of the joints of the third storey will be greater. However, after having lost the joints of the third storey, the efforts in the joints of the fourth storey increase suddenly and these joints are lost quickly.

5.3.4 Conclusion about header plate connections sized at ULS

The header plate connections dimensioned to take up the stresses under loading at the ultimate limit state (ELU), when the structure is intact, do not have sufficient axial strength and elongation capacity to find a new equilibrium configuration and avoid the progressive collapse of the directly affected part (DAP). Indeed, the maximum load factor reached is worth 0.13, which is much less than 1.

However, these joints respect the resistance criterion specified by the tying method. As a reminder, this criterion said that each tie, including its end connections, must be able to take up a tensile force $T_i = 487.06$ kN. In the present case, the tensile strength of the joints is $N_u = 661.98$ kN and the criterion is thus well respected. But, the ductility of the joints is very low and that is why the maximum load factor reached is very low. This first joint configuration already seems to show that the tensile strength proposed by the tying method is too low and that the ductility greatly influences the results.

Since this joint configuration does not allow to find a new equilibrium configuration, the joints must therefore be dimensioned for the scenario of the loss of the column considered. However, header plate connections are simple joints, designed to take up shear forces mainly. It is therefore not guaranteed to find a joint configuration which ensures robustness in case of column loss.

5.4 With header plate connections with the best possible properties

Now, the header plates connections will, therefore, be dimensioned to ensure robustness against the loss of the column considered. For the joints to be fully resistant, they must be able to take up a tensile force of 4120 kN, as explained during the study without taking into account the resistance of the joints (Figure 4.21). However, it is not possible to find a configuration of the header plate connection allowing to take up such an effort.

Therefore, the best possible properties will be given to the joints to see if this type of joint can allow avoiding a progressive collapse of the DAP due to the loss of the column considered, or whether another type of joint more suitable for high tensile forces should be considered.

5.4.1 Joint design

The design method envisaged is as follows. The joint configuration was chosen to have the best possible tensile strength N_u . This maximum possible strength is worth $N_u = 2014.59$ kN and is limited by the component *beam web in tension*. To increase this resistance, it would therefore be necessary to use beams with an upper profile. Then, the elongation capacity of the joint was

optimised, taking care to keep a maximum resistance $N_u = 2014.59$ kN.

It will thus be checked whether, for the maximum resistance, the elongation capacity obtained is sufficient or, if this is not the case, what elongation capacity is necessary.

The configuration imagined is that presented in Figures 4.48, 4.49 and 4.50 below.

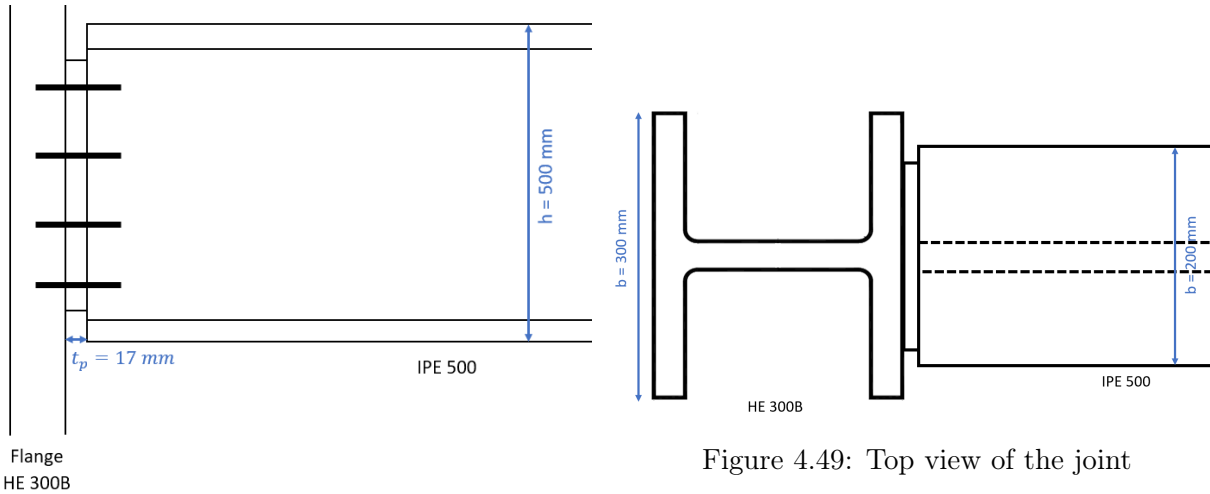


Figure 4.48: Longitudinal view of the joint

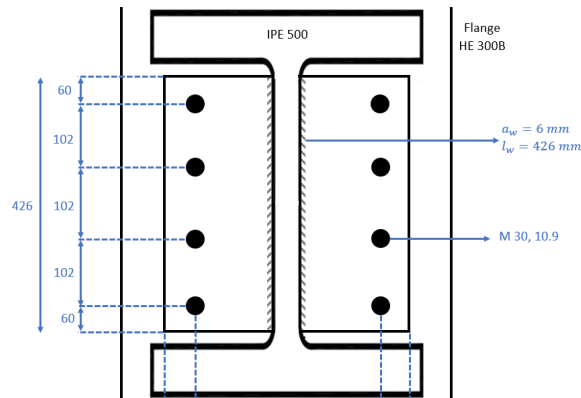


Figure 4.50: Front view of the joint

This joint configuration has a shear strength $V_{Rd} = 890.59$ kN. Also, the properties of the joint in tension are represented in Figure 4.51.

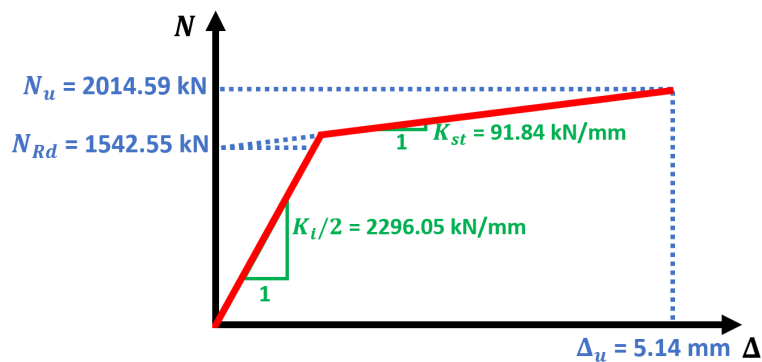


Figure 4.51: Law of behavior of the joint in traction

The axial strength and the shear strength were calculated following the procedure described in [23], and the deformation capacity was calculated using the formulas giving the stiffnesses of the components present in Eurocode 3 Part 1-8 and using an analytical method proposed by Mr. Jaspart in a calculation note provided. The calculations are presented in the Annex B.

5.4.2 Joint modeling

The joints are modeled with elements of type 200, exactly in the same way as for the header plate connections dimensioned at the ultimate limit state (ULS). In addition, as before, the two models shown in Figures 4.52 and 4.53 will be studied. The laws of behavior of the horizontal spring elements (modeling the behavior in traction of the joints) for each of the two models are then presented respectively on Figures 4.54 and 4.55.

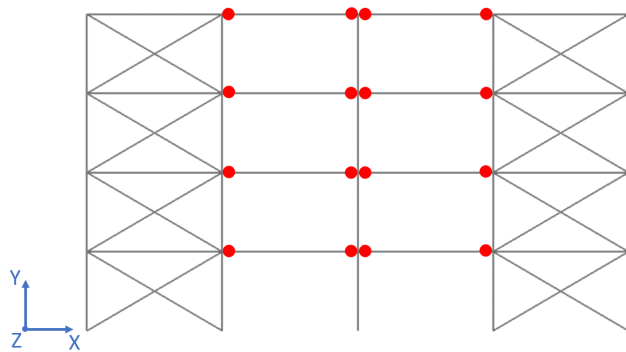


Figure 4.52: Model 1

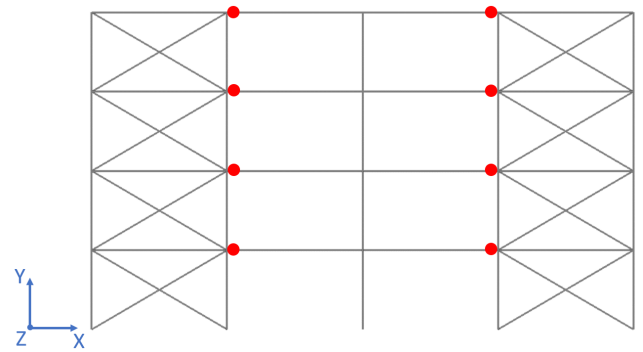


Figure 4.53: Model 2

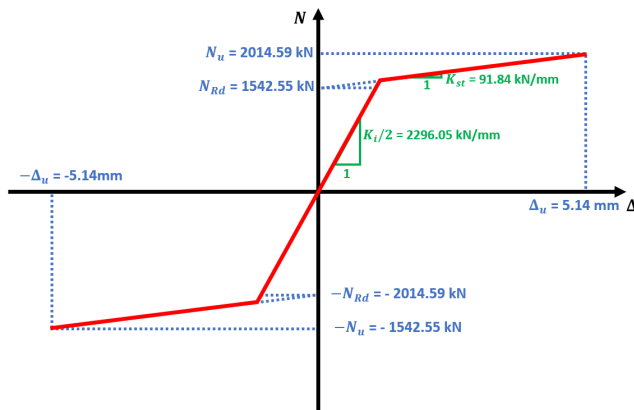


Figure 4.54: Behavior law of a horizontal extensional spring modeling the axial behavior of a single joint

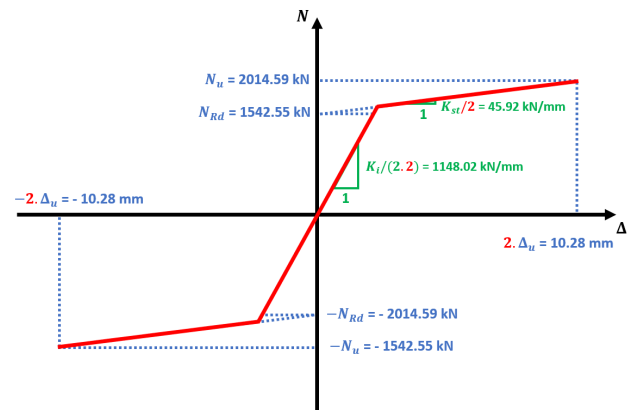


Figure 4.55: Behavior law of a horizontal extensional spring modeling the axial behavior of two joints

5.4.3 Results

To avoid a premature failure by plastification by reaching the deformation limit ϵ_u in an element before reaching the complete progressive collapse of the DAP due to the successive failures of the joints, the geometries considered are those presented in the Figure 4.56 below.

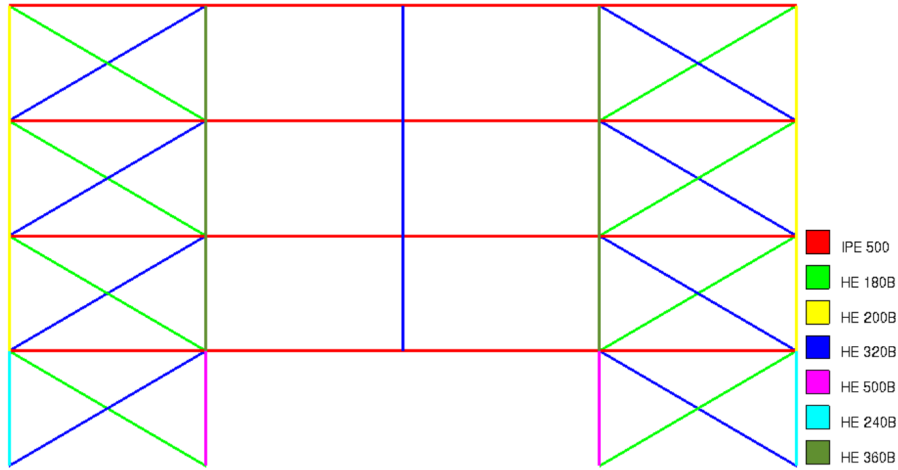


Figure 4.56: Element geometries

The relationship between the load factor and the vertical displacement at the top of the lost column for the imagined joint configuration is described in Figure 4.57.

As before, the blue curve is the curve obtained with the first model (for which the joints are modeled at the two ends of each beam of the DAP), which stops when the joints of the first storey have failed. And the orange curve is the curve obtained with the second model (for which the two joints of a beam are modeled at the same end of it), which stops when the joints of the four storeys have failed. The three sudden drops appearing on the orange curve correspond to the successive losses of the joints of the first three storeys, and the curve stops when the joints of the last storey fail and the DAP is entirely lost. Also, it can be seen that the two curves are superimposed again perfectly, the second model, therefore, seems valid.

The maximum value reached by the load factor is 0.51, which is much lower than the unit meaning that the structure has found a new equilibrium configuration. Consequently, the properties of the joints are not sufficient. It is necessary either to increase the tensile strength of the joints (which is currently worth $N_u = 2014.59$ kN), or to increase the elongation capacity of the joints (which currently is worth $\Delta_u = 5.14$ mm).

The resistance given to the joints, $N_u = 2014.59$ kN, is the maximum possible resistance. It has therefore been calculated, for the design tensile strength $N_{Rd} = 1542.55$ kN and the ultimate tensile strength $N_u = 2014.59$ kN, what is the elongation capacity Δ_u necessary to reach a load factor of 1. To do this, the rigidity $K_i/2$ was taken equal to 2296.05 kN/mm and it is the hardening rigidity K_{st} which will vary. It has been obtained that the elongation capacity necessary to reach a load factor of 1 is then equal to $\Delta_u = 15$ mm. Indeed, as shown in Figure 4.58, for such an elongation capacity, the load factor reaches 1.01.

However, a configuration of header plate connection having a resistance $N_u = 2014.59$ kN and an elongation capacity $\Delta_u = 15$ mm does not exist. It is not possible to increase the elongation capacity of the joint without highly reducing its resistance. To obtain an elongation capacity of 15 mm, the resistance of the joint must then be worth no more than $N_u = 846$ kN, which is too low (because for such resistance the elongation capacity should be higher than 15 mm to reach a load factor of 1) and the directly affected part (DAP) collapses completely.

The only possibility for the joints to have sufficient properties would be to install IPE 750 profile beams to increase the resistance of the component *beam web in tension* and therefore increase the resistance of the joint. This solution nevertheless seems too expensive and hardly possible.

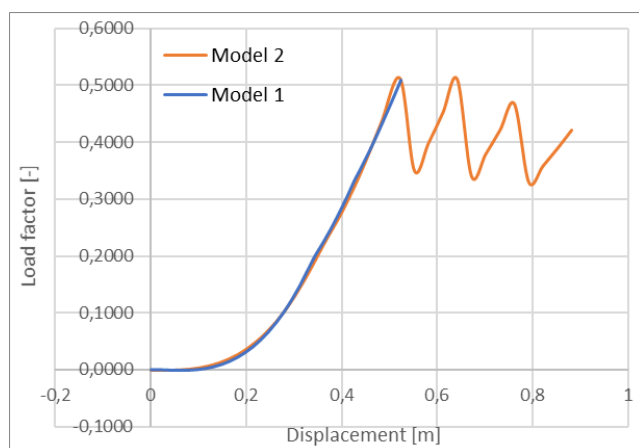


Figure 4.57: Relation between the load factor and the displacement at the top of the lost column for $\Delta_u = 5.14\text{mm}$

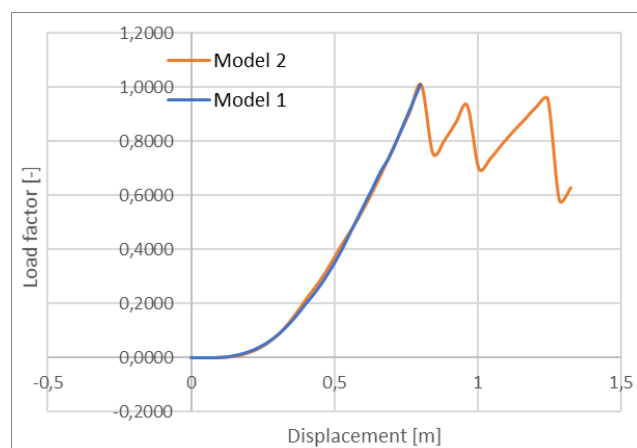


Figure 4.58: Relation between the load factor and the displacement at the top of the lost column for $\Delta_u = 15\text{mm}$

Finally, it can be seen that, unlike the joints dimensioned at ULS, the maximum load factor is each time reached before the loss of the joints of the first storey.

Indeed, this time, the elongation capacity is greater ($\Delta_u = 5.14\text{mm}$ then $\Delta_u = 15\text{mm}$). As explained previously, once the resistance has reached N_{Rd} in the joints of the first storey, these lose a lot of rigidity (the rigidity becomes K_{st}) and start to deform strongly. When the load factor increases, the forces will then increase mainly in the beams of the upper storeys whose rigidity of the joints is higher (the rigidity of these is worth $K_i/2$). As in the present case the elongation capacity of the joints is greater, the efforts will have time to increase more significantly in the beams of the upper storeys before the failure of the joints of the first storey. This explains the fact that once the joints of the first storey have failed, the progressive collapse will take place more quickly.

In Figure 4.58, the joints of the second storey fail so quickly after losing those of the first storey that the load factor re-increases a little before losing the joints of the third storey.

5.4.4 Conclusion about header plate connections

It can be concluded that it is not possible to find a configuration of the header plate connection having both sufficient tensile strength and ductility to find a new equilibrium configuration and avoid a progressive collapse of the DAP.

As already explained, the joints with a header plate are simple joints designed to take up shear forces mainly. Their tensile strength and their elongation capacity are then too low to take up the membrane forces developed in the beams of the DAP during the loss of the column considered.

Also, the columns were considered to work along their strong axis so the joints are fixed to the column flange. If the secondary frame of a 3D structure had been studied and therefore the columns had been considered to work along their weak axis, the joints would have been fixed to the column web. However, the column web in tension has lower resistance and the properties of the joints would have been less good. Consequently, regardless of the orientation of the columns, header plate connections do not have sufficient properties to ensure robustness.

Other types of simple joints could, however, be studied before generalising the conclusion and being able to say that the simple joints do not make it possible to ensure robustness against the loss of the column considered. Fin plate connections (another type of simple joint) have, therefore, been designed in accordance with the European recommendations for the design of simple joints in steel structures (see [23]). However, this type of joint has poorer tensile properties than header

plate connections and was soon abandoned.

Finally, this study again shows the inconsistency of the tying method proposed by Eurocode. The resistance of the joints is, in this case, much higher than the resistance specified by the tying method:

$$N_u = 2014.59\text{kN} \gg T_i = 487.06\text{kN} \quad (4.6)$$

According to the tying method, the header plate connections dimensioned at ULS make it possible to ensure the redistribution of efforts within the structure and to find a new equilibrium configuration. Still, even by dimensioning the header plate connections so that they have the best possible properties, this is not the case.

Also, it may be interesting to note that when using header plate connections, the greatest possible elongation capacity for a resistance fixed to the tying force of 487.06 kN is 24 mm, which is much less than the 96 mm required to reach a load factor of 1.

This again highlights two problems with the tying method: the specified tensile strength is far too low, and the method does not take ductility into account while it is essential.

5.5 With flush end-plate connections with the best possible properties

Since simple joints such as header plate connections and fin plate connections do not have sufficient properties, another type of joint will be studied: flush end-plate connections. An example of a flush end-plate connection is shown in Figure 4.59. For flush end-plate connections, unlike header plate connections, the plate is also welded to the beam flanges. This type of joint generally has a specific stiffness in rotation and is generally classified as semi-rigid. However, it is sometimes used in braced structures.

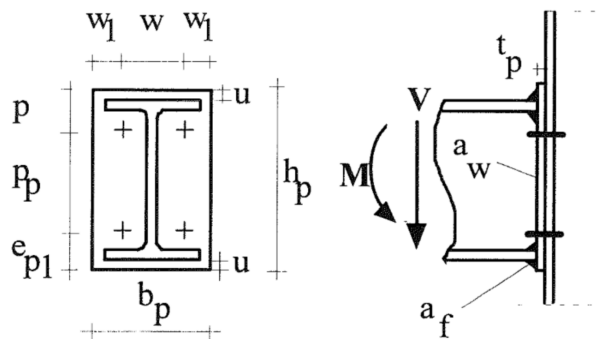


Figure 4.59: Example of flush end-plate connection

5.5.1 Joint design

As in the previous cases, the joints designed concern the beam-column joints in relation to the beams of the DAP. Also, the design strategy is the same as for header plate connections with the best possible properties. The joint configuration was chosen to have the best possible tensile strength N_u . Then, the elongation capacity of the joint was optimised, taking care to keep the maximum resistance. It will then be checked whether, for the maximum resistance, the elongation capacity obtained is sufficient or, if this is not the case, what elongation capacity is necessary.

The joints were this time sized using the joint calculation software *COP*. This software is useful to directly obtain the shear strength, the flexural strength and the rotational stiffness of the designed joint configuration. Then, the software provides the stiffness, the design tensile strength, and the effective length/width of each component taking into account the group effects. By assembling the components, it is possible to obtain the design tensile strength of the joint N_{Rd} . Also, using the effective lengths obtained and the formulas of Eurocode 3 Part 1-8, it is possible to calculate

the ultimate tensile strength of the joint N_u and then the elongation capacity Δ_u .

The designed joint configuration is shown in Figure 4.60 below.

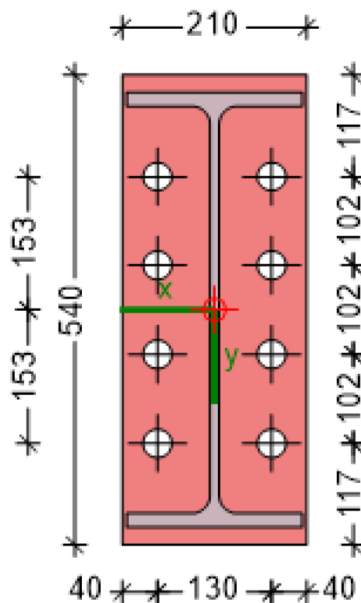


Figure 4.60: End plate

This configuration has the following properties :

| | | | | |
|------------------------------|------------------|---|--------------------|---------|
| Plastic moment resistance | $M_{pl,Rd}$ | = | 336.8 | kNm |
| Elastic moment resistance | $M_{el,Rd}$ | = | 224.5 | kNm |
| Initial rotational stiffness | $S_{j,ini}$ | = | $7.306 \cdot 10^4$ | kNm/rad |
| Rotational stiffness | $S_{j,ini}/\eta$ | = | $3.653 \cdot 10^4$ | kNm/rad |
| Shear resistance | V_{Rd} | = | 613.6 | kN |
| Design tensile strength | N_{Rd} | = | 1508 | kN |
| Ultimate tensile strength | N_u | = | 1969.3 | kN |
| Elongation capacity | Δ_u | = | 8.28 | mm |

Also, the constitutive law in tension of the joint is represented in Figure 4.61. Note that the tensile strength is slightly lower than that of header plate connection but that the elongation capacity is greater.

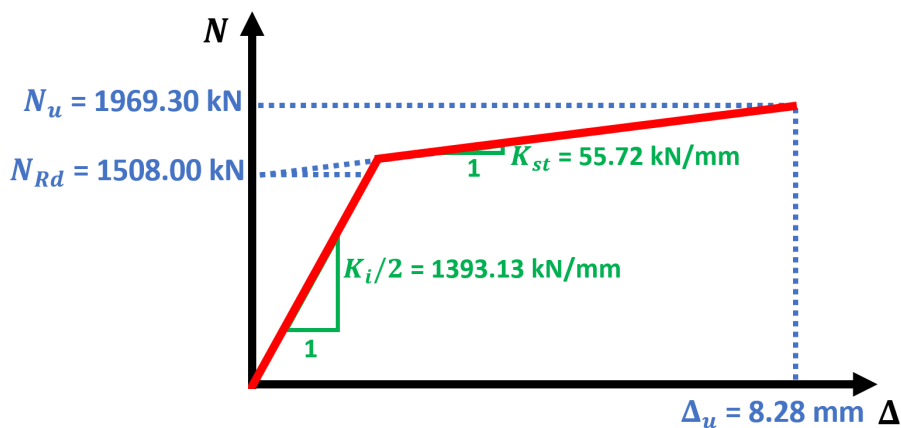


Figure 4.61: Law of behavior in traction of the joint

More details on the geometry of the joint and the resistance of each component are given in the

Annex C. Note that this joint configuration present a ductile ruin.

5.5.2 Joint modeling

The joints are again modeled with elements of type 200, and the same two models as presented above will be studied. These models are presented in Figures 4.62 and 4.63.

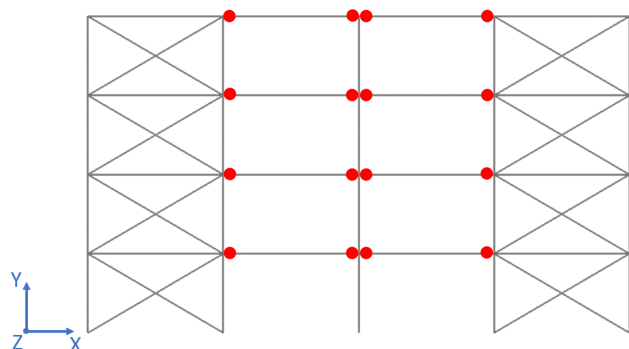


Figure 4.62: Model 1

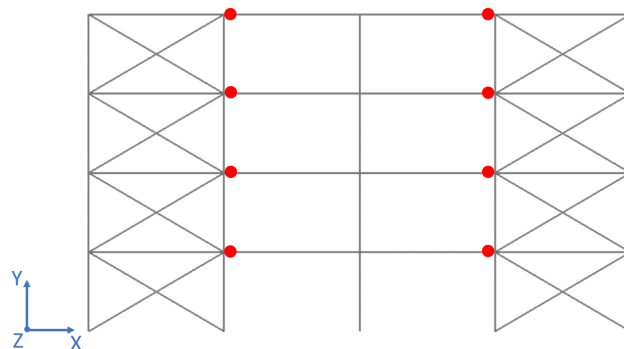


Figure 4.63: Model 2

However, a strong assumption will be made in the present case. Indeed, the configuration of the flush end-plate connection studied is semi-rigid, therefore bending forces will appear in the joints. Consequently, when the membrane forces develop, there will be an M-N interaction in the joints. The resistance and the deformation capacity of the joints must, therefore, take account of the M-N interactions. To do this, it would be necessary to use non-linear coupled springs, which does not yet exist in *FINELG*. Another student is doing his Master thesis on this subject. This is why it will be assumed that the joints are simple (i.e., their rotational resistance is zero) and that they are therefore not subjected to any bending force. This assumption is very safe, but in the second time, a more precise approach will be presented.

For each of the two models, the following elements of type 200, defined in the global axes, will therefore be set up at the places marked with a red point on Figures 4.62 and 4.63 :

- A horizontal translational spring element, which extends along the X-axis. This element follows the bi-linear law shown in Figure 4.64 or Figure 4.65 depending on the model studied.
- A vertical translational spring element, which extends along the Y-axis. This element follows an elastic-perfectly plastic law, with a very high elastic stiffness and a resistance equal to $V_{Rd} = 613.6$ kN. For this element, no strain limit has been set because the resistance V_{Rd} will never be exceeded and the joint will not deform in shear.
- A translational spring element which follows an elastic law with very high rigidity, along the Z-axis.
- Elements of rotational springs which follow an elastic law with very high rigidity, around the axes Y and X.

Around the Z-axis, the rotation is free because the joints will be assumed to be simple joints, as explained.

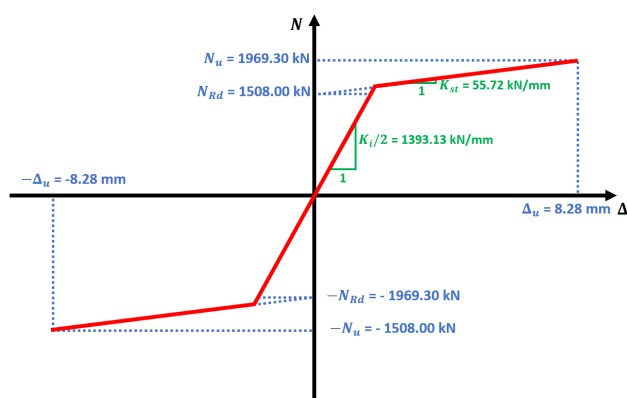


Figure 4.64: Behavior law of a horizontal extensional spring modeling the axial behavior of a single joint

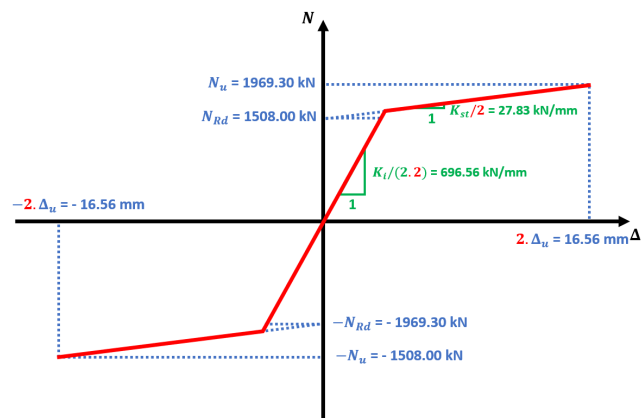


Figure 4.65: Behavior law of a horizontal extensional spring modeling the axial behavior of two joints

5.5.3 Results

The geometries considered are the same as for the header plate connections having the best possible properties (see Figure 4.66). These geometries were chosen so that there is no ruin by plastification by reaching the limit of deformation ϵ_u in an element before having the complete progressive collapse of the DAP.

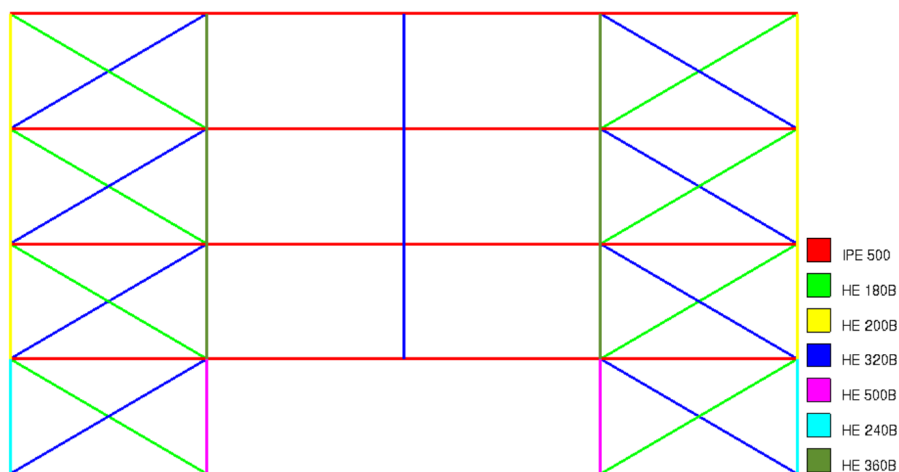


Figure 4.66: Element geometries

The relationship between the load factor and the vertical displacement at the top of the lost column obtained is then presented in Figure 4.67.

As before, the curves obtained with each of the two models overlap perfectly. Using the second model, the progressive collapse of the DAP can be seen. Indeed, each drop of the orange curve corresponds to the loss of one storey of the DAP, and the curve stops when the four storeys are lost.

It can be seen that with the flush end-plate connection studied, a load factor of 0.61 is reached while with the header plate connection, a load factor of only 0.51 is reached. In fact, the tensile strength is slightly lower than that of header plate connections but the elongation capacity is more significant, which makes it possible to reach a higher load factor. Also, a very safe hypothesis (assuming simple joints) has been made. Without this assumption, it is therefore possible that the flush end-plate connection allows to achieve a load factor of 1.

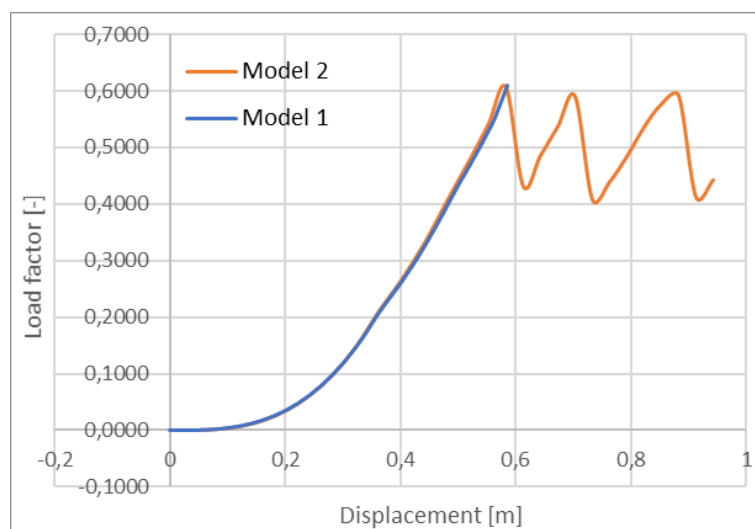


Figure 4.67: Relationship between the load factor and the vertical displacement at the top of the lost column

5.5.4 Second approach

A second, less secure approach will, therefore, be carried out to see if a load factor of 1 can be reached.

For the joints (which are semi-rigid) to behave like hinges, plastic hinges must have formed in the joints. As explained in the previous chapter, the response of a structure subject to the loss of a column can be divided into three phases (see Figure 4.68). The membrane forces begin to develop only in the third phase (from point (4) in Figure 4.68), when plastic hinges have formed at the ends of each beam of the DAP and that a plastic mechanism was formed in the DAP. Indeed, it is only when a plastic mechanism is formed in the DAP that significant deformations and displacements will appear in the DAP and that membrane forces will result.

To be less safe and more precise, it would therefore be interesting to calculate the value of the effort simulating the progressive loss of the column for which this plastic mechanism develops in the directly affected part (i.e., the effort at point (4) in Figure 4.68). Then this value can be added to the effort that the structure can support during the activation of the membrane efforts.

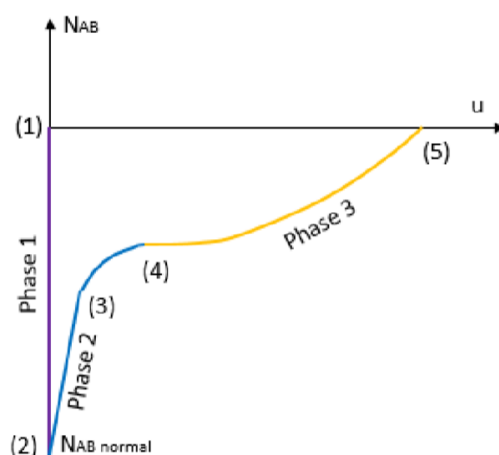


Figure 4.68: Typical relationship between axial force in the lost column and vertical displacement at the top of the lost column

The value of the effort for which a plastic mechanism develops in the directly affected part can be calculated quickly using the kinematic method. Indeed, this method allows to calculate

analytically, for a given structure and an identified plastic mechanism, the load necessary for this plastic mechanism to appear.

In the present case, the plastic mechanism has 16 plastic hinges and is shown in Figure 4.69.

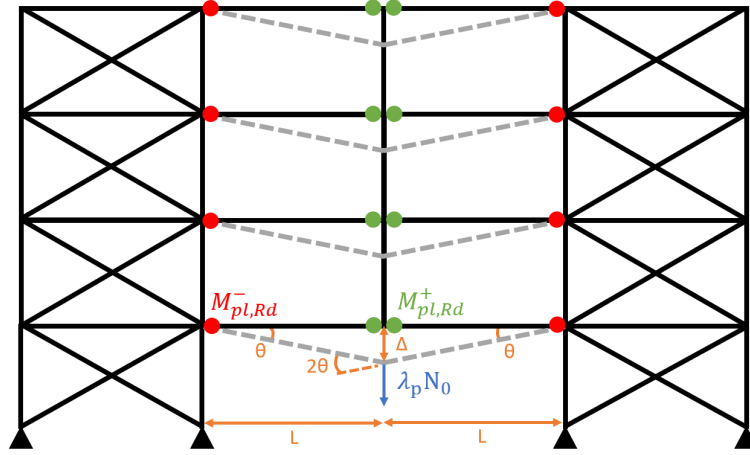


Figure 4.69: Plastic mechanism

For this plastic mechanism, the interior work is worth:

$$W_i = 8 \cdot M_{pl,Rd}^+ \cdot \theta + 8 \cdot M_{pl,Rd}^- \cdot \theta \quad (4.7)$$

In addition, the exterior work is worth:

$$W_e = \lambda_p \cdot N_0 \cdot \Delta = \lambda_p \cdot N_0 \cdot \theta \cdot L \quad (4.8)$$

Therefore,

$$W_i = W_e \Leftrightarrow 8 \cdot M_{pl,Rd}^+ \cdot \theta + 8 \cdot M_{pl,Rd}^- \cdot \theta = \lambda_p \cdot N_0 \cdot \theta \cdot L \Leftrightarrow \lambda_p \cdot N_0 = \frac{8 \cdot M_{pl,Rd}^+ + 8 \cdot M_{pl,Rd}^-}{L} \quad (4.9)$$

Since the designed assembly is symmetrical, $M_{pl,Rd}^+ = M_{pl,Rd}^- = 336.8$ kNm. So there comes:

$$\lambda_p \cdot N_0 = \frac{16 \cdot 336.8}{6} = 898.13 \text{ kN} \quad (4.10)$$

The force $\lambda_p \cdot N_0$ is the force simulating the loss of the column, where N_0 is the initial compression force in the column which will be lost (see Figure 4.70). N_0 is 1334 kN. Therefore, the load factor λ_p is equal to $898.13/1334 = 0.67$. This factor is quite large, so it was crucial to take it into account.

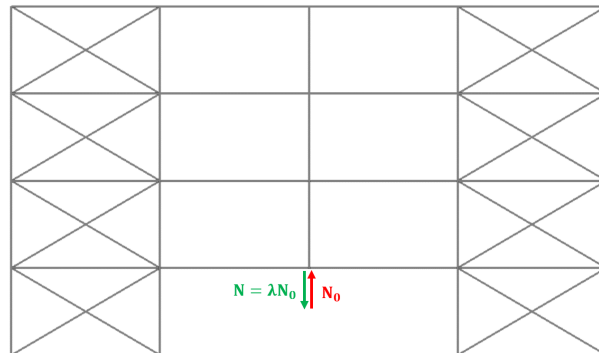


Figure 4.70: Representation of the load factor

This factor λ_p can also be calculated numerically by making a small modification to the first model studied (the model for which the joints are modeled at the two ends of each beam).

Around the Z-axis, where the rotation was free, it is possible to place a rotational spring element which follows an elastic-perfectly plastic law, with an elastic stiffness $S_{j,ini}/\eta = 3.653 \cdot 10^4$ kNm/rad and a resistance equal to $M_{pl,Rd} = 336.8$ kN.

Therefore, using this new model, it is possible to obtain the reaction in the support replacing the lost column at the moment when the bending moment reaches $M_{pl,Rd} = 368.8$ kN at all the ends of the beams of the DAP, as shown in Figure 4.71.

This support reaction, which is equivalent to $\lambda_p \cdot N_0 - N_0$, is worth 436 kN. Therefore,

$$\lambda_p = \frac{1334 - 436}{1334} = 0.67 \quad (4.11)$$

The value λ_p obtained is the same as that obtained by the kinematic method.

In addition, at this time, as shown in Figure 4.72, the membrane forces are not yet developed in the beams of the DAP, which are stressed by slight compression.

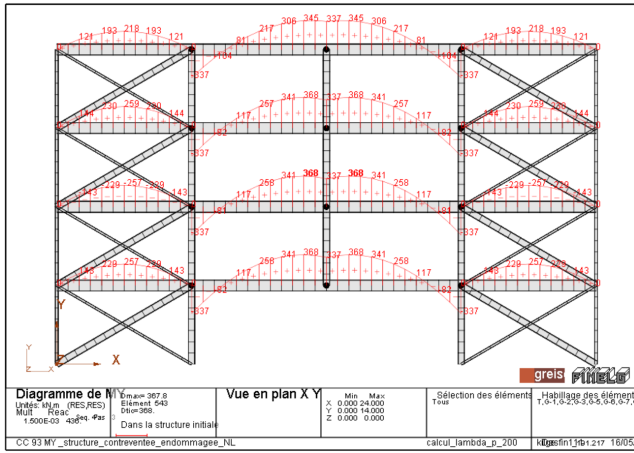


Figure 4.71: Bending moments in the beams at the time of the formation of the plastic mechanism

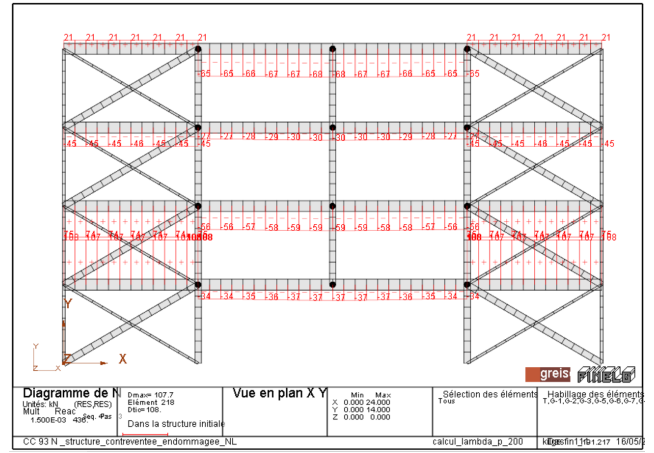


Figure 4.72: Normal forces in the beams at the time of the formation of the plastic mechanism

Now that the value of the load factor for which the plastic mechanism is formed is known, it is necessary to add this value to the load factor that the structure can support after the formation of the plastic mechanism. The curve giving the relationship between the load factor and the vertical displacement at the top of the lost column obtained by assuming the joints as simple joints (Figure 4.67) will be moved from $\lambda_p = 0.67$. The new curve obtained is presented in Figure 4.73.

It can be seen that a load factor of 1.28 is now reached. The load factor reached is therefore higher than unity. This means that with the configuration of the flush end-plate connection studied, the structure is able to find a new equilibrium configuration after the total loss of the column considered.

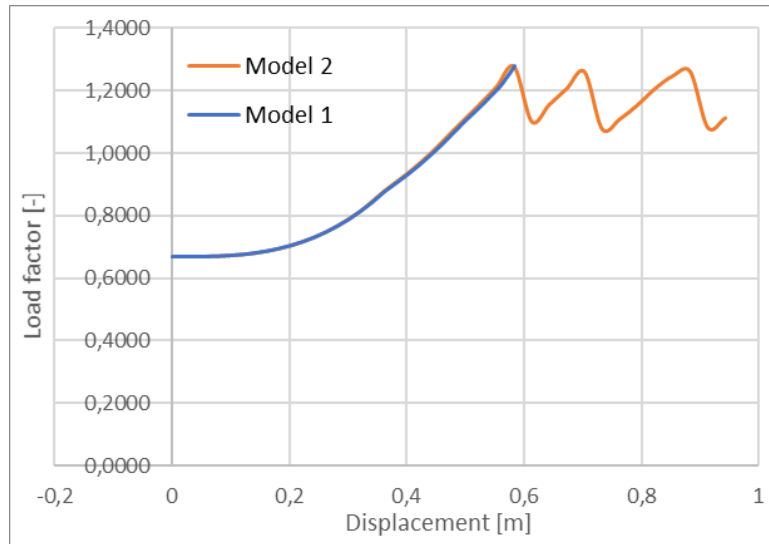


Figure 4.73: New relationship between the load factor and the vertical displacement at the top of the lost column

Then, the axial forces in the beams at the moment when the load factor is worth 1 are presented in Figure 4.74 below.

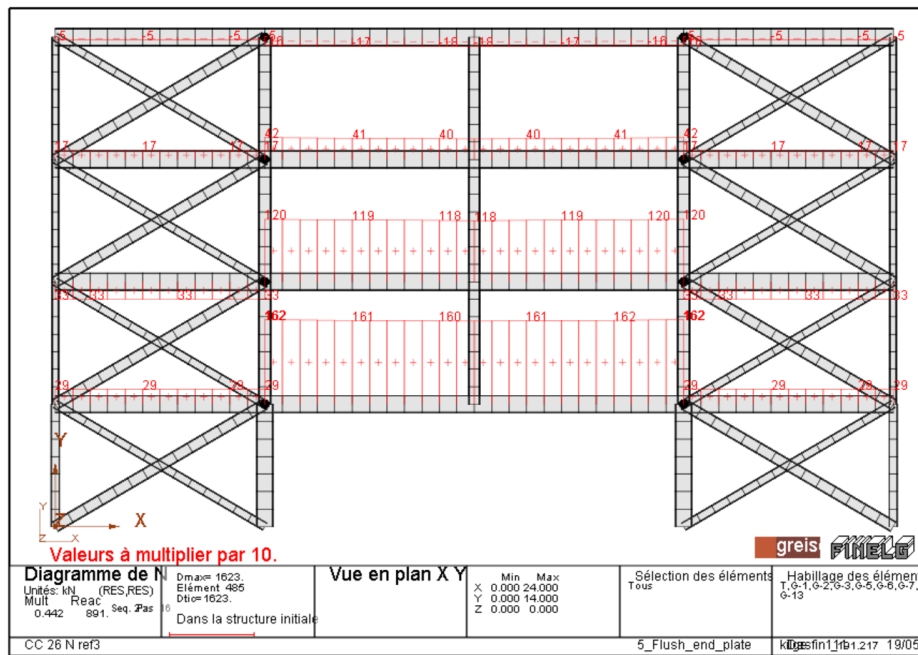


Figure 4.74: Axial force in beams for a load factor of 1

It can be seen that the tensile forces in the beams of the first two storeys greatly exceed the resistance required by the tying method. As a reminder, this resistance was worth 487.06 kN.

5.5.5 Conclusion about flush end-plate connections

It can be concluded that it is possible to design a configuration of flush end-plate connection which ensures the robustness against the loss of the column considered.

The fact that this type of joint has a certain rigidity in rotation and that it is necessary to develop a plastic mechanism before developing membrane forces has a very beneficial effect. Indeed, the value of the load factor for the plastic mechanism to form is relatively large ($\lambda_p = 0.67$) and

makes it possible to reach a load factor greater than 1.

However, again, the resistance specified by the tying method is too low. Even though the load factor is already relatively high before membrane forces develop, the membrane forces reach 1620 kN. Moreover, for a configuration of flush end-plate connection of tensile strength equal to $T_i = 487.06$ kN, the flexural strength would be much lower. Therefore, the load factor for a plastic mechanism to form would also be much lower and the membrane forces will develop earlier.

6 Parametric study

Now a parametric study will be carried out. The number of storeys and the number of spans will vary to observe their influence on the demand for strength and ductility of the joints.

As already explained, in his Master's thesis [20], Farah Hjeir has already carried out a parametric study to identify the structural requirements necessary to ensure the robustness of a structure losing one of its columns. He studied several structures by varying the number of storeys and the number of spans of a framed structure. Also, he first considered the case of non-braced structures with rigid joints and then the case of braced structures with simple joints. However, in the context of his study, he considered that the joints were fully resistant and infinitely ductile.

This study will therefore not focus on the reinforcements required in the elements to achieve a load factor of 1 and ensure robustness. It will focus on the requirements for joints, which have not yet been studied. To do this, the structures studied have been reinforced so that no element of the indirectly affected part (IAP) yields by plastification before reaching a complete collapse of the directly affected part (DAP). In this way, if the load factor reaches its maximum after one or more storeys are lost, as was the case for the header plate connections sized at the ultimate limit state (ULS), this maximum can be identified. The structures dimensioned at ULS and SLS and the reinforcements they have undergone are presented in the Annex D.

The reference joint configuration for this study will be the header plate connection configuration with the best possible properties presented above. The header plate connection was chosen rather than the flush end-plate connection because this type of joint is a simple joint. Therefore, its behavior can be modeled without having to make assumptions and the response of the structure obtained will be exact.

As a reminder, this joint configuration has the tensile properties shown in Figure 4.75.

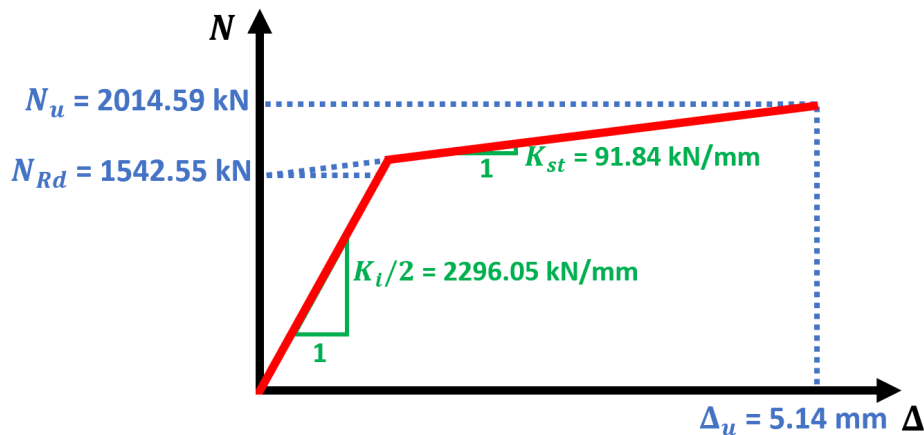


Figure 4.75: Law of behavior in traction of the joint

First, for different values of the number of spans and the number of storeys, it will be studied which maximum load factor is reached with this joint configuration.

Then, it will be studied, for the design tensile strength $N_{Rd} = 1542.55$ kN and the ultimate tensile strength $N_u = 2014.59$ kN, what is the elongation capacity necessary to reach a load factor of 1. The rigidity $K_i/2$ will be assumed to be fixed, and it is the rigidity K_{st} which will vary with the elongation capacity Δ_u .

6.1 Variation of the number of spans

The results obtained by varying the number of spans are presented in Table 4.2 below. Note that the maximum load factor is always reached just before the joints of the first storey fail. Indeed, as soon as the joints on the first storey have failed, the collapse of the DAP takes place very quickly.

| Number of spans | Load factor reached with $\Delta_u = 5.14$ mm | Joint elongation capacity required to reach a load factor of 1 |
|-----------------|---|--|
| 4 | 0.51 | 15 mm |
| 5 | 0.52 | 14 mm |
| 6 | 0.56 | 12.5 mm |
| 7 | 0.59 | 10.5 mm |
| 8 | 0.62 | 9.5 mm |

Table 4.2: Variation of the number of spans

It can be seen that, for the reference joint configuration, no structure reaches a load factor of 1. However, the greater the number of spans, the greater the load factor achieved and the more robust the structure is against the loss of the column considered.

Indeed, as summarized in Figure 4.76, the greater the number of spans and the further the bracing system is from the lost column. Consequently, the indirectly affected part (IAP) is less rigid, it deforms more and it sags more on the directly affected part (DAP).

For the same load factor, the horizontal displacement of the IAP is therefore greater, the vertical displacement of the DAP is also greater and the membrane forces in the beams of the DAP must be less to balance the gravity loads.

As a result, the membrane forces will reach the strength of the joints less quickly and the joints will yield less quickly. Therefore, the maximum load factor reached is higher. Also, obviously, since the load factor achieved is higher, the demand for additional ductility to reach a load factor of 1 is lower. This explains why the elongation capacity required to reach a load factor of 1 is lower, as presented in Table 4.2.

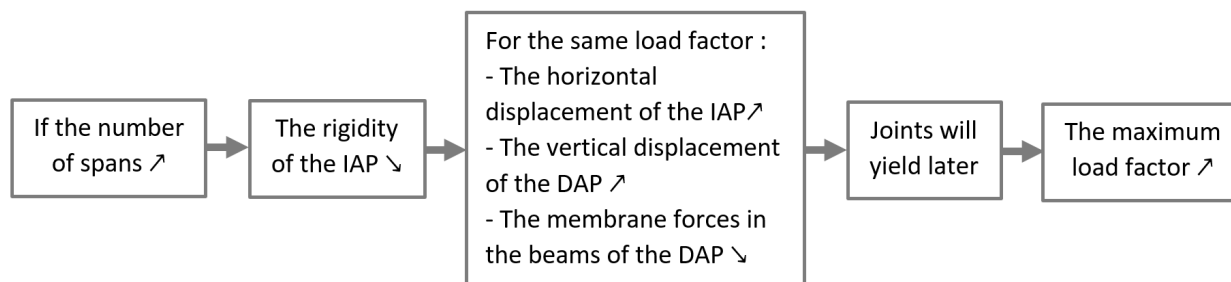


Figure 4.76: Consequences of increasing the number of spans

6.2 Variation of the number of storeys

The results obtained by varying the number of storeys are presented in Table 4.3 below. As with the previous structures, the maximum load factor is always reached just before the joints of the first storey fail.

| Number of storeys | Load factor reached with $\Delta_u = 5.14$ mm | Joint elongation capacity required to reach a load factor of 1 |
|-------------------|---|--|
| 4 | 0.51 | 15 mm |
| 5 | 0.41 | 18.5 mm |
| 6 | 0.33 | 22 mm |
| 7 | 0.30 | 26 mm |
| 8 | 0.26 | 29.5 mm |

Table 4.3: Variation of the number of storeys

Also, unlike the number of spans, for the reference joint configuration, the greater the number of storeys, the lower the load factor and the less the structure is robust at the loss of the column considered.

Indeed, as summarized in Figure 4.77, the greater the number of storeys, the greater the efforts taken up by the columns at the foot of the structure, and therefore the greater the initial effort in the column that will be lost. Consequently, for the same load factor (i.e., for the same percentage of loss of the column), the forces to be redistributed to the rest of the structure are higher and the membrane forces in the beams of the DAP are therefore higher. As a result, the ruin of the joints is reached more quickly and the maximum load factor reached is lower. For an 8-storey structure, the gravity loads are two times greater (approximately because the last floor is not subjected to the same loads as the others) than for a 4-storey structure so the load factor reached is two times lower.

Also, since the load factor achieved is lower, the demand for additional ductility to reach a load factor of 1 is greater. This explains why the elongation capacity required to reach a load factor 1 is greater, as presented in Table 4.3.

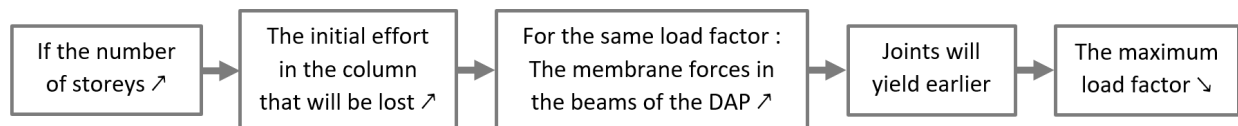


Figure 4.77: Consequences of increasing the number of storeys

7 Conclusion of the study

This study has demonstrated several things.

Firstly, the results obtained highlight two problems concerning the tying method currently proposed by Eurocode.

The first problem is that the tying resistance specified by this method for horizontal ties in the case of a framed structure is much too low to reach an equilibrium configuration and avoid a progressive collapse of the DAP if a column is lost. Indeed, if the joints have exactly the tensile strength obtained by this method, i.e., 487.06 kN, they must have an elongation capacity of 96 mm to reach a load factor of 1. However, none of the joints studied has such a ductility. The tensile strength must, therefore, be higher.

Then, the second problem is that this method does not take into account the ductility whereas this highly influences the degree of robustness reached. This has been demonstrated with the case of header plates connections having the best possible properties. For a tensile strength $N_u = 2014.59$ kN, an elongation capacity of 5.14 mm allows to reach a load factor of 0.51 while an elongation capacity of 15 mm allows to reach a load factor of 1.01. The influence of ductility was also highlighted in the context of the parametric study.

These inconsistencies concerning the tying method mean that, by using this method, it can be thought that certain joints make it possible to ensure robustness against the loss of a column when this is not the case. For example, the header plate connections dimensioned to take up the efforts under the combination of loads at the ultimate limit state (when the structure is intact) have a tensile strength $N_u = 661.98$ kN higher than the strength of 487.06 kN specified by the tying method. However, it has been shown that the load factor achieved with this joint configuration is much less than 1 (it is 0.13). Also, even giving the best possible properties to header plate connections, it is not possible to obtain a load factor of 1.

Then, following the results obtained, several conclusions about the types of joints studied can be drawn.

First, simple joints such as head plate connections and fin plate connections, originally designed to primarily take up shear forces, do not have sufficient tensile properties to take up the membrane forces that develop in the DAP when a column is lost. Therefore, if a structure should be robust against the loss of a column, another type of joint should be used.

Then, the study of the case with flush end-plate connections, which are semi-rigid joints, highlighted the fact that having to develop plastic hinges in the joints and a complete plastic mechanism in the DAP before membrane efforts develop has a very beneficial effect on the degree of robustness achieved. The higher the flexural strength of the joints, the more beneficial it will be.

Chapter 5

General conclusion

1 Conclusion

This work has been divided into two main parts.

Firstly, an important period was devoted to becoming aware of the research and development work carried out in recent years on the concept of robustness. This made it possible to develop approaches for dealing with the problem of robustness in steel and composite structures, based on the tools available for the strategies proposed by Eurocode 1 Part 1-7. These strategies are presented in Figure 5.1.

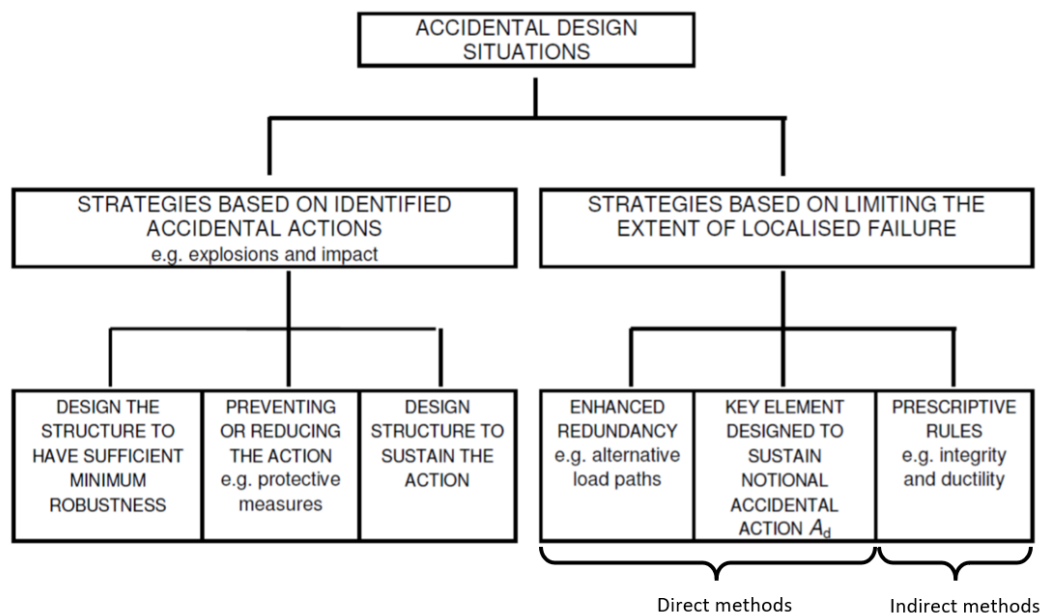


Figure 5.1: The strategies to be considered for exceptional design situations according to the Eurocode 1 Part 1-7

As a reminder, the approaches developed concerned all the strategies presented in Figure 5.1, except the first two. Indeed, the strategy consisting of designing the structure to have sufficient minimum robustness refers to the category of strategies based on limiting the extent of localised failure, while the strategy of preventing or reducing the action simply requires taking protective measures. No sizing procedure is necessary when choosing one of these strategies.

Also, the prescriptive tying method was considered as a possible approach if the alternative load paths method is chosen rather than as a strategy in its own right.

Consequently, the flowchart represented in Figure 5.2 was imagined. For the strategy of alternative load paths, it can be seen that three approaches are possible: the prescriptive approach, the analytical approach and the numerical approach. Then, for the key element method, two approaches are possible: the primary structure approach and the fuse approach. Finally, for the strategy of designing the structure to sustain the action, approaches were developed for an impact loading and an blast loading.

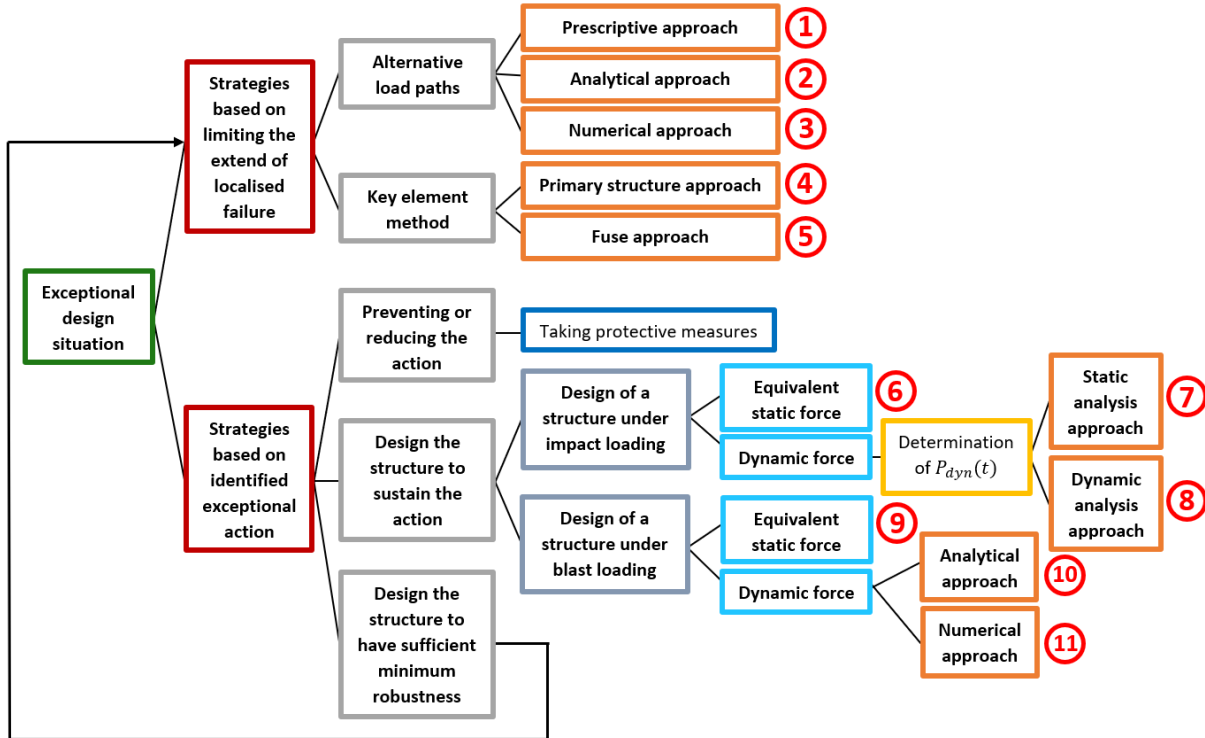


Figure 5.2: Development of approaches for exceptional design situations

For each of the approaches mentioned (and numbered) in Figure 5.2 above, the tools it requires to use, the limits it presents, and the analysis and verification steps to be followed have been presented. The procedure to be followed and the limitations for each of the approaches numbered in Figure 5.2 are recalled hereafter, in order, in Figures 5.3 to 5.8.

These approaches seem solid and coherent, even if some have limitations, except the prescriptive approach for the strategy of the alternative load paths. Indeed, this approach requires having recourse to the tying method which presents several inconsistencies, and a more realistic approach is being developed.

The second part of the work, therefore, focused on this tying method. The objective of this second part was to identify the limits of the method currently proposed by Eurocode, to assess its relevance and the degree of robustness actually achieved by following this method. To do this, a structure subjected to the loss of a column was analysed by giving different properties to the beam-column joints of the DAP. First, these joints had the resistance specified by the tying method, then different joint configurations were studied. This made it possible to highlight two problems concerning the current tying method : the specified resistance is too low to find a new equilibrium configuration if a column is lost, and the method does not take into account the ductility of the elements and the joints while this greatly influences the degree of robustness achieved, as has been demonstrated.

Finally, this second part also showed that simple joints such as header plate connections and fin plate connections do not allow to take up the membrane forces and ensure robustness if a column

is lost. On the other hand, structures with beam-column joints such as flush end-plates, which have a certain rigidity, must develop a plastic mechanism of the DAP before they can develop membrane forces. This can have a very beneficial effect and can lead to reaching a new equilibrium configuration if a column is lost. If it is desirable that a structure be robust against the loss of a column, the choice of the type of joints is therefore very important.

2 Perspectives

The development of different approaches for the strategies presented in the Eurocode made it possible to take stock of what is available and possible to do at present. Indeed, the research and development work carried out in recent years has been grouped around a global philosophy. This highlighted the design and treatment approaches to the robustness problem that it is currently possible to follow. Still, it also highlighted the limits of the tools currently available and the work carried out. Therefore, in the future, new research and development work to improve current tools and reduce their limitations will undoubtedly be carried out. This is already the case with the analytical model developed at the University of Liège to obtain the response of a structure undergoing the loss of a column, for example. This model is continuously undergoing improvements.

Also, the approaches developed within the framework of this work constitute a first development which could be improved in the future. These approaches can be further refined. Indeed, they are based on the documents and research work that have been read, but other documents currently available can provide additional information. In addition, they can possibly be supplemented by approaches for other types of load, such as, for example, a fire not provided for in the initial design, or exceptional loads of natural cause such as an earthquake (not provided in the initial design) or a tsunami. Then, current approaches can be improved in parallel with the development of calculation tools.

Finally the study of the structure undergoing the loss of a column was carried out to highlight the problems of the tying method currently proposed by Eurocode and contributes to the development of a new more coherent method. After this study, it becomes clear that the ductility will have to be taken into account in new approaches and that the specified resistance will have to be higher because the degree of robustness achieved with the current method is far too low.

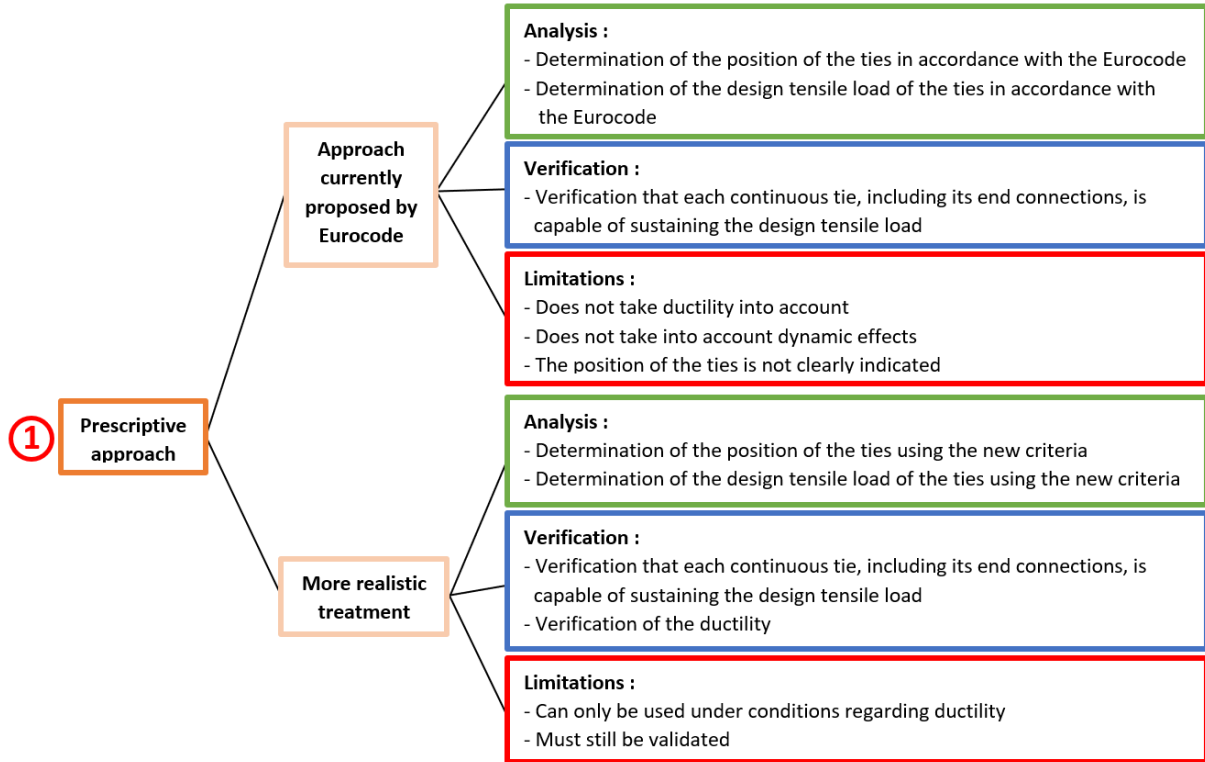


Figure 5.3: Procedure by opting for the prescriptive approach after having chosen the alternative load paths strategy

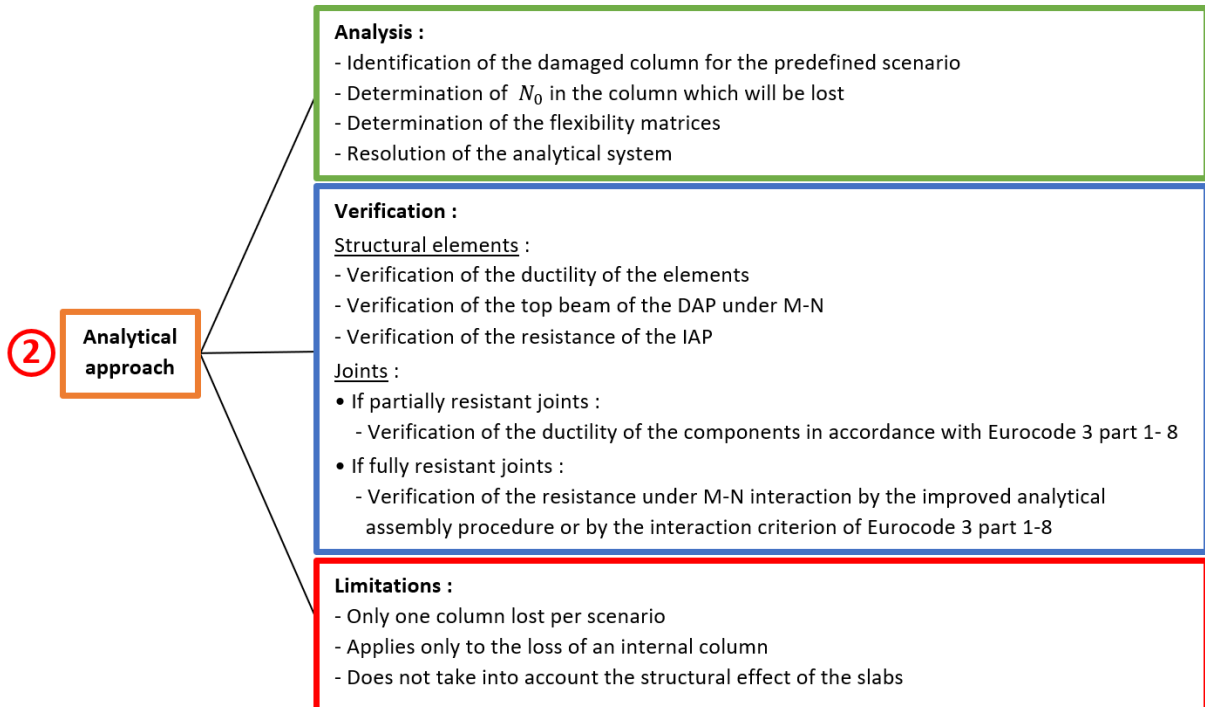


Figure 5.4: Procedure by opting for the analytical approach after having chosen the alternative load paths strategy

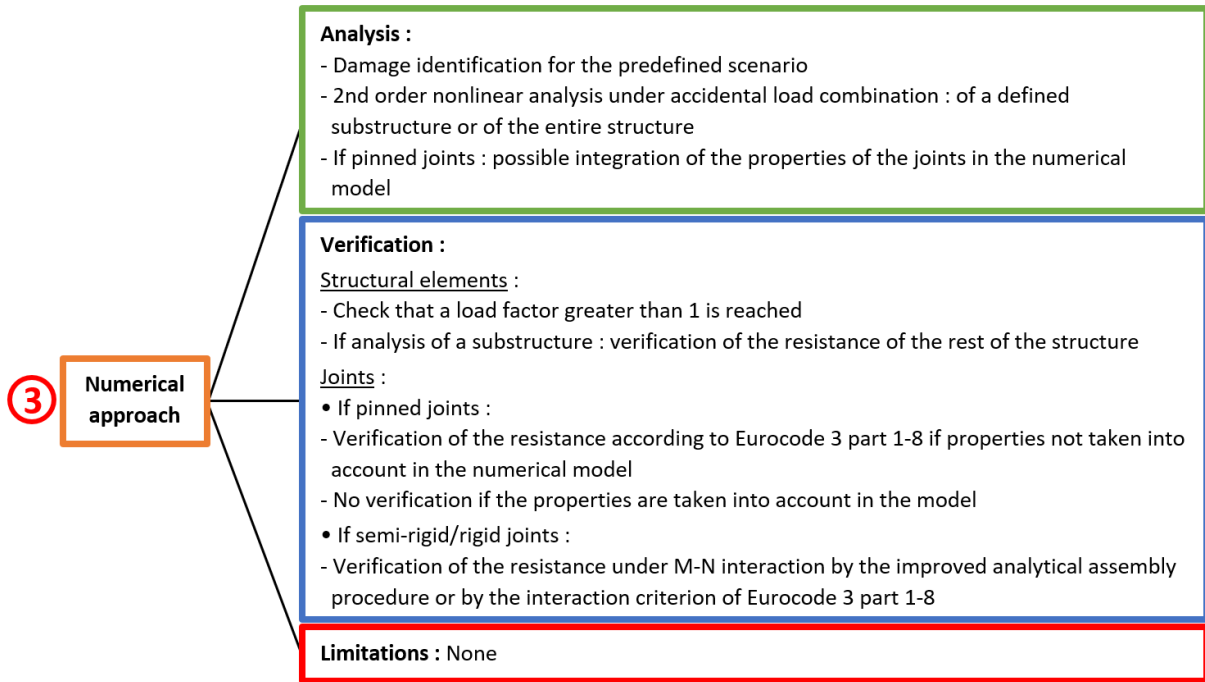


Figure 5.5: Procedure by opting for the numerical approach after having chosen the alternative load paths strategy

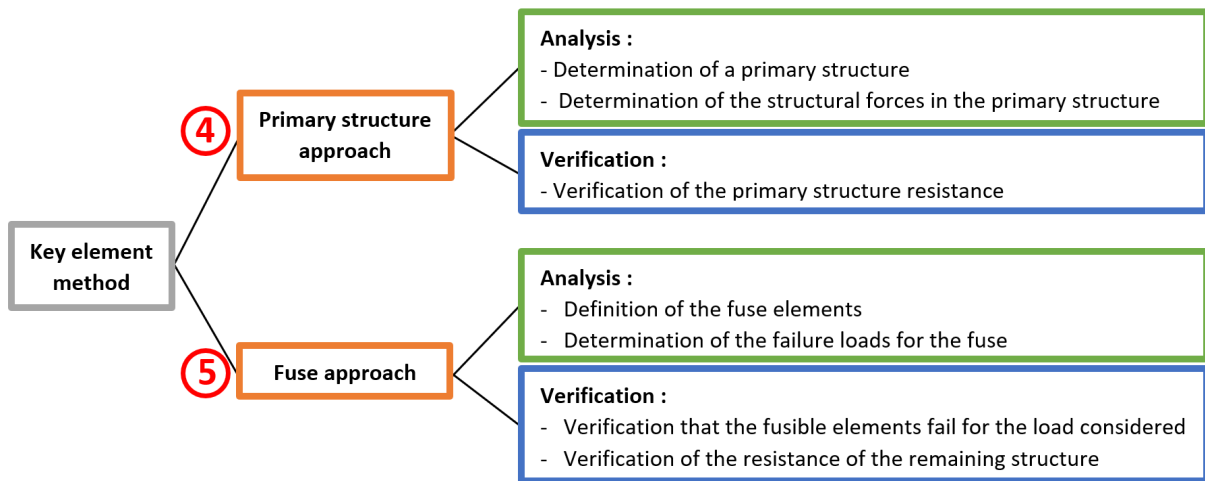


Figure 5.6: Procedures for possible approaches by opting for the key element strategy

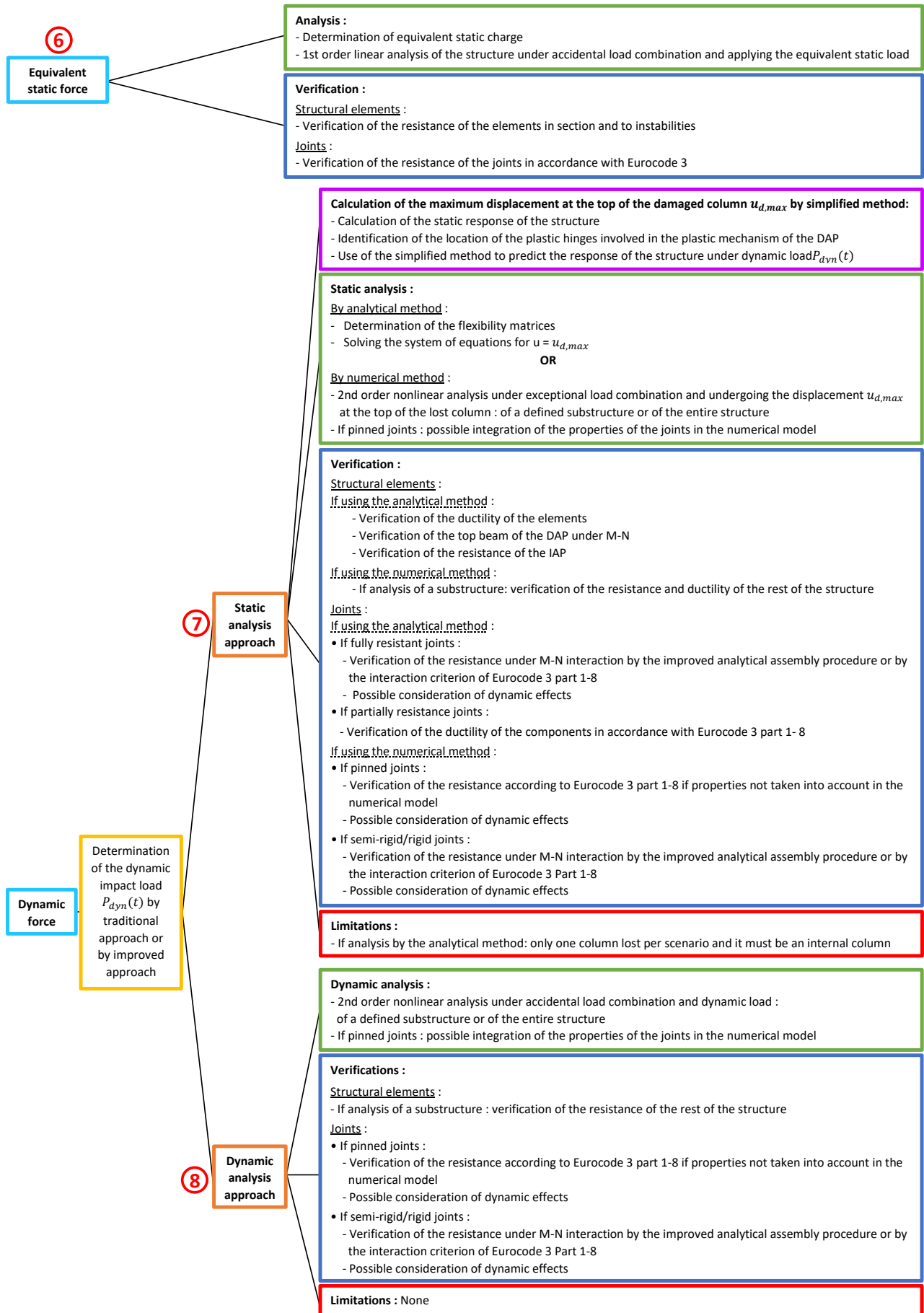


Figure 5.7: Procedures for possible approaches to design the structure under impact loading

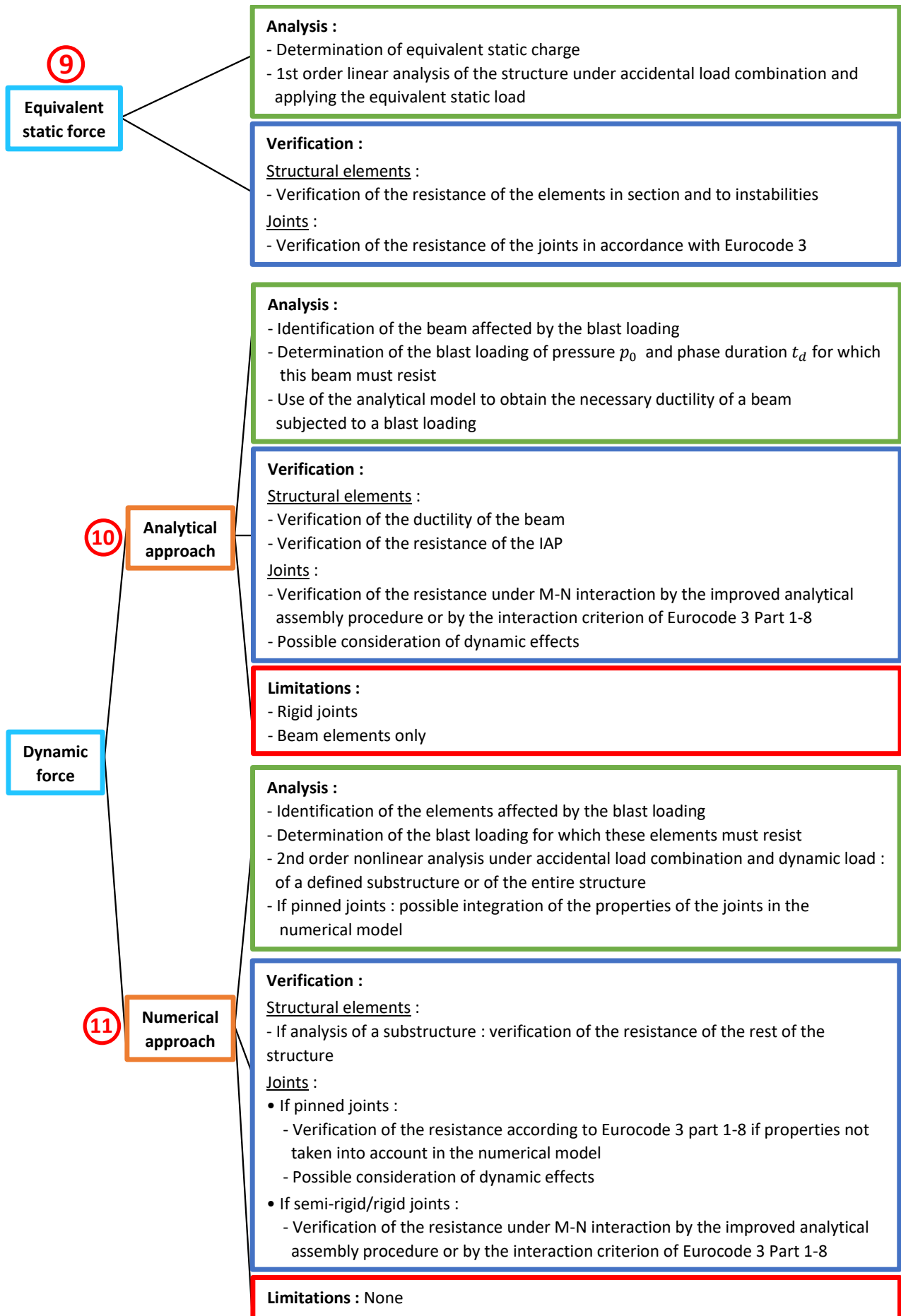


Figure 5.8: Procedures for possible approaches to design the structure under blast loading

Annexes

A Sizing of header plate connections at ULS

The header plates connections have been dimensioned following the procedure described in [23]. The calculations are detailed below for the joint configuration dimensioned under the combination of loads at the ultimate limit state (ULS) when the structure is intact.

A.1 Main joint data

Configuration : Beam to column flange

Column : HE 300B S355

Beam : IPE 500 S355

Header plate : 140 x 100 x 8, S355

A.2 Detailed characteristics

Column HE 300B, S355

| | | | | |
|-------------------------|----------|---|-------|----------|
| Depth | h_c | = | 300 | mm |
| Thickness of the web | t_{cw} | = | 11 | mm |
| Width | b_c | = | 300 | mm |
| Thickness of the flange | t_{cf} | = | 19 | mm |
| Root radius | r | = | 27 | mm |
| Area | A | = | 149,1 | cm^2 |
| Inertia | I_y | = | 25170 | cm^4 |
| Yield strength | f_{yc} | = | 355 | N/mm^2 |
| Ultimate strength | f_{uc} | = | 510 | N/mm^2 |

Beam IPE 500, S355

| | | | | |
|-------------------------|----------|---|-------|----------|
| Depth | h_b | = | 500 | mm |
| Thickness of the web | t_{bw} | = | 10,2 | mm |
| Width | b_b | = | 200 | mm |
| Thickness of the flange | t_{bf} | = | 16 | mm |
| Root radius | r | = | 21 | mm |
| Area | A | = | 115,5 | cm^2 |
| Shear area | A_v | = | 59,9 | cm^2 |
| Inertia | I_y | = | 48200 | cm^4 |
| Yield strength | f_{yb} | = | 355 | N/mm^2 |
| Ultimate strength | f_{ub} | = | 510 | N/mm^2 |
| Length | L | = | 6000 | mm |

Header plate 140 x 100 x 8, S355

| | | | | |
|-------------------|----------|---|-----|----------|
| Vertical gap | g_v | = | 30 | mm |
| Depth | h_p | = | 140 | mm |
| Width | b_p | = | 100 | mm |
| Thickness | t_p | = | 8 | mm |
| Yield strength | f_{yp} | = | 355 | N/mm^2 |
| Ultimate strength | f_{up} | = | 510 | N/mm^2 |

Direction of load transfer (1)

| | | | | |
|-------------------------------------|------------|---|----|-------|
| Number of bolts rows | n_1 | = | 3 | bolts |
| Edge distance to first bolt row | e_{11} | = | 25 | mm |
| Pitch between bolts rows 1 and 2 | $p_{1[1]}$ | = | 45 | mm |
| Pitch between bolts rows 2 and 3 | $p_{1[2]}$ | = | 45 | mm |
| Distance from last bolt row to edge | e_{1n} | = | 25 | mm |

Direction perpendicular to load transfer (2)

| | | | | |
|-------------------------------------|----------|---|----|-------|
| Number of bolts rows | n_2 | = | 2 | bolts |
| Edge distance to first bolt row | e_{21} | = | 25 | mm |
| Pitch between bolts rows 1 and 2 | $p_{2'}$ | = | 50 | mm |
| Distance from last bolt row to edge | e_{2n} | = | 25 | mm |
| Distance from last bolt row to edge | e_{2s} | = | 25 | mm |

Bolts M18, 10.9

| | | | | |
|----------------------------|--------------|---|-------|----------|
| Tensile stress area | A_s | = | 201 | mm^2 |
| Diameter of the shank | d | = | 16 | mm |
| Diameter of the holes | d_0 | = | 18 | mm |
| Head height | h_D | = | 12.40 | mm |
| Nut height | h_N | = | 15.80 | mm |
| Outer diameter of a washer | ϕ_{ext} | = | 34 | mm |
| Yield strength | f_{yb} | = | 900 | N/mm^2 |
| Ultimate strength | f_{ub} | = | 1000 | N/mm^2 |

Welds

| | | | | |
|------------------------------|-------|---|-----|----|
| Throat thickness of the weld | a_w | = | 6 | mm |
| Length of the weld | l_w | = | 140 | mm |

Safety factors

| | | |
|---------------|---|------|
| γ_{M0} | = | 1.00 |
| γ_{M2} | = | 1.25 |
| γ_{Mu} | = | 1.10 |

A.3 Applied forces

| | | | |
|----------|---|-----|----|
| V_{Ed} | = | 277 | kN |
| N_{Ed} | = | 0 | kN |

A.4 Ductility and rotation requirements

To apply the following design rules, certain inequalities concerning the rotation requirements and the ductility requirements must be satisfied.

Rotation requirements

1)

$$h_p \leq d_b \Leftrightarrow 140\text{mm} \leq 426\text{mm} \rightarrow Ok \quad (5.1)$$

2)

$$\phi_{available} \geq \phi_{required} \Leftrightarrow 0.044 \geq 0.005 \rightarrow Ok \quad (5.2)$$

Because,

$$- \phi_{available} = t_p/h_e = 8/180 = 0.044$$

$$- \phi_{required} = \frac{\gamma_p L^3}{24EI} = \frac{56.472 \cdot 6000^3}{24 \cdot 210000 \cdot 48200 \cdot 10^4} = 0.005$$

Ductility requirements

1)

$$\frac{d}{t_p} \geq 2.8 \sqrt{\frac{f_{yp}}{f_{ub}}} \Leftrightarrow 2 \geq 1.67 \rightarrow Ok \quad (5.3)$$

2)

$$a \geq \frac{\beta_w f_{ybw} \gamma_{M2}}{\sqrt{2} f_{ubw} \gamma_{M0}} t_{bw} \Leftrightarrow 6 \text{ mm} \geq 5.65 \text{ mm} \rightarrow Ok \quad (5.4)$$

A.5 Calculation of the shear resistance**Bolts in shear**

$$V_{Rd,1} = 0.8 \cdot n \cdot F_{v,Rd} = 385.92 \text{ kN} \quad (5.5)$$

Because,

$$- n = 6$$

$$- F_{v,Rd} = \alpha_v A f_{ub} / \gamma_{M2} = 80.4 \text{ kN}$$

Header plate in bearing

$$V_{Rd,2} = n \cdot F_{b,Rd} = 317.53 \text{ kN} \quad (5.6)$$

Because,

$$- n = 6$$

$$- \alpha_b = \min(\alpha_1 ; \alpha_2 ; \alpha_3 ; 1) = \min(e_1/(3 \cdot d_0) ; p_1/(3 \cdot d_0) - 1/4 ; f_{ub}/f_{up}) = \min(0.46 ; 0.58 ; 1.96) = 0.46$$

$$- k_1 = \min(2.8 \cdot e_2/d_0 - 1.7 ; 2.5) = 2.19$$

$$- F_{b,Rd} = k_1 \cdot \alpha_b \cdot d \cdot t_p \cdot f_{up} / \gamma_{M2} = 52.92 \text{ kN}$$

Column flange in bearing

$$V_{Rd,3} = n \cdot F_{b,Rd} = 950.22 \text{ kN} \quad (5.7)$$

Because,

$$- n = 6$$

$$- \alpha = \min(\alpha_1 ; \alpha_2 ; \alpha_3 = \min(p_1/(3 \cdot d_0) - 1/4 ; f_{ub}/f_{ucf} ; 1) = \min(0.58 ; 1.96 ; 1) = 0.58$$

$$- k_1 = \min(1.4 \cdot p_2/d_0 - 1.7 ; 2.8 \cdot e_{2s}/d_0 - 1.7 ; 2.5) = 2.19$$

$$- F_{b,Rd} = k_1 \cdot \alpha_b \cdot d \cdot t_{cf} \cdot f_{ucf} / \gamma_{M2} = 158.37 \text{ kN}$$

Cross-section of the header plate in shear

$$V_{Rd,4} = 2 \cdot F_{v,Rd} = 361.50 \text{ kN} \quad (5.8)$$

$$\text{Because, } F_{v,Rd} = h_p \cdot t_p \cdot f_{yp} / (1.27 \cdot \sqrt{3} \cdot \gamma_0) = 180.75 \text{ kN}$$

Net section of the header plate in shear

$$V_{Rd,5} = 2 \cdot F_{v,Rd} = 324.13 \text{ kN} \quad (5.9)$$

Because,

- $A_{v,net} = t_p \cdot (h_p - n_1 \cdot d_0) = 688 \text{ mm}^2$
- $F_{v,Rd} = A_{v,net} \cdot f_{up} / (\sqrt{3} \cdot \gamma_{M2}) = 162.06 \text{ kN}$

Shear block of the header plate

$$V_{Rd,6} = 2 \cdot F_{eff,Rd} = 334 \text{ kN} \quad (5.10)$$

Because,

- $A_{nt} = t_p \cdot (e_2 - d_0/2) = 128 \text{ mm}^2$
- $A_{nv} = t_p \cdot (h_p - e_1 - (n_1 - 0.5) \cdot d_0) = 560 \text{ mm}^2$
- $F_{eff,Rd} = F_{eff,1,Rd} = \frac{f_{up} \cdot A_{nt}}{\gamma_{M2}} + \frac{1}{\sqrt{3}} \cdot f_{yp} \cdot \frac{A_{nv}}{\gamma_{M0}} = 167 \text{ kN}$

Header plate in bending

$$V_{Rd,7} = \infty \quad (5.11)$$

Beam web in shear

$$V_{Rd,8} = F_{v,Rd} = t_{bw} \cdot h_p \cdot \frac{f_{ybw}}{\gamma_{M0} \cdot \sqrt{3}} = 292.68 \text{ kN} \quad (5.12)$$

Joint shear resistance

$$V_{Rd} = \min_{i=1}^8 V_{Rd,i} = 292.68 \text{ kN} \quad (5.13)$$

A.6 Calculation of ultimate tensile strength**Bolts in tension**

$$N_{u,1} = n \cdot B_{t,u} = 1096.36 \text{ kN} \quad (5.14)$$

Because,

- $n = 6$
- $B_{t,u} = f_{ub} \cdot A_s / \gamma_{Mu} = 182.73 \text{ kN}$

Header plate in bending

$$N_{u,2} = \min(F_{hp,u,1}, F_{hp,u,2}) = 661.98 \text{ kN} \quad (5.15)$$

Because,

- $m_p = (p_2' - t_w - 2 \cdot 0.8 \cdot a \cdot 2^{0.5}) / 2 = 13.11 \text{ mm}$
- $n_p = \min(e_2; 1.25 \cdot m_p) = 16.39 \text{ mm}$
- $m_{u,p} = \frac{t_p^2 \cdot f_{up}}{4 \cdot \gamma_{Mu}} = 7418.18 \text{ Nmm/mm}$
- $l_{eff,p,t,1} = l_{eff,p,t,2} = h_p = 140 \text{ mm}$
- $F_{hp,u,1} = \frac{(8 \cdot n_p - 2 \cdot e_w) \cdot l_{eff,p,t,1} \cdot m_{u,p}}{2 \cdot m_p \cdot n_p - e_w \cdot (m_p + n_p)} = 661.98 \text{ kN}$
- $F_{hp,u,2} = \frac{2 \cdot l_{eff,p,t,2} \cdot m_{u,p} + n \cdot B_{t,u} \cdot n_p}{m_p + n_p} = 679.5 \text{ kN}$

Supporting member in bending

Resistance assumed to be sufficient.

Beam web in tension

$$N_{u,4} = t_w \cdot h_p \cdot f_{ubw} / \gamma_{Mu} = 662.07 \text{ kN} \quad (5.16)$$

Welds

Conditions for full-strength behaviour of the welds are fulfilled.

Ultimate tensile strength

$$N_u = \min_{i=1}^4 N_{u,i} = 661.98 \text{ kN} \quad (5.17)$$

A.7 Calculation of design tensile strength**Bolts in tension**

$$N_{Rd,1} = n \cdot B_{t,Rd} = 868.32 \text{ kN} \quad (5.18)$$

Because,

$$- n = 6$$

$$- B_{t,Rd} = 0.9 f_{ub} \cdot A_s / \gamma_{M2} = 144.72 \text{ kN}$$

Header plate in bending

$$N_{Rd,2} = \min(F_{hp,Rd,1}, F_{hp,Rd,2}) = 506.87 \text{ kN} \quad (5.19)$$

Because,

$$- m_p = (p'_2 - t_w - 2 \cdot 0.8 \cdot a \cdot 2^{0.5}) / 2 = 13.11 \text{ mm}$$

$$- n_p = \min(e_2; 1.25 \cdot m_p) = 16.39 \text{ mm}$$

$$- m_{Rd,p} = \frac{t_p^2 \cdot f_{yp}}{4 \cdot \gamma_{M0}} = 5680 \text{ Nmm/mm}$$

$$- l_{eff,pt,1} = l_{eff,pt,2} = h_p = 140 \text{ mm}$$

$$- F_{hp,Rd,1} = \frac{(8 \cdot n_p - 2 \cdot e_w) \cdot l_{eff,p,t,1} \cdot m_{u,p}}{2 \cdot m_p \cdot n_p - e_w \cdot (m_p + n_p)} = 506.87 \text{ kN}$$

$$- F_{hp,Rd,2} = \frac{2 \cdot l_{eff,p,t,2} \cdot m_{u,p} + n \cdot B_{t,Rd} \cdot n_p}{m_p + n_p} = 536.31 \text{ kN}$$

Supporting member in bending

Resistance assumed to be sufficient.

Beam web in tension

$$N_{Rd,4} = t_w \cdot h_p \cdot f_{ybw} / \gamma_{M0} = 506.94 \text{ kN} \quad (5.20)$$

Welds

Conditions for full-strength behaviour of the welds are fulfilled.

Design tensile strength

$$N_{Rd} = \min_{i=1}^4 N_{Rd,i} = 506.87 \text{ kN} \quad (5.21)$$

A.8 Calculation of the tensile rigidity and the elongation capacity of the joint

The constitutive law of a joint in tension is represented in Figure 5.10.

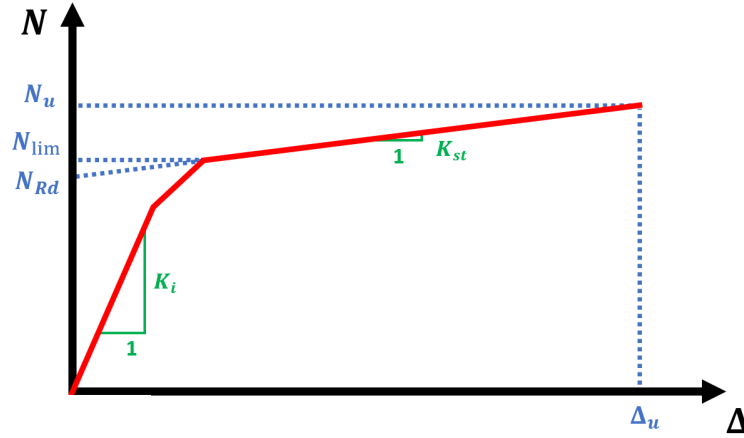


Figure 5.9: Law of behavior in traction of a joint

Calculation of tensile stiffness

$$K_i = \frac{E \cdot k_{ib} \cdot k_{ihp}}{k_{ihp} + k_{ib}} = 2708.24 \text{ kN/mm} \quad (5.22)$$

Because,

$$- k_{ihp} = \frac{0.9 \cdot l_{eff} \cdot t_p^3}{m_p^3} = 28.62 \text{ mm}$$

$$- k_{ib} = \frac{1.6 \cdot A_s \cdot n_1}{t_c + t_{cf} + 0.5 \cdot (h_N = h_D)} = 23.47 \text{ mm}$$

$$K_{st} = K_i / 50 = 54.16 \text{ kN/mm} \quad (5.23)$$

Calculation of the elongation capacity

$$\Delta_u = \frac{N_u - N_{Rd}}{K_{st}} = 2.86 \text{ mm} \quad (5.24)$$

B Sizing of header plate connections with the best possible properties

The calculations are this time detailed for the configuration of the header plate connection designed to have the best possible properties.

B.1 Main joint data

Configuration : Beam to column flange

Column : HE 300B S355

Beam : IPE 500 S355

Header plate : 426 x 180 x 17, S355

B.2 Detailed characteristics

Column HE 300B, S355

| | | | | |
|-------------------------|----------|---|-------|----------|
| Depth | h_c | = | 300 | mm |
| Thickness of the web | t_{cw} | = | 11 | mm |
| Width | b_c | = | 300 | mm |
| Thickness of the flange | t_{cf} | = | 19 | mm |
| Root radius | r | = | 27 | mm |
| Area | A | = | 149,1 | cm^2 |
| Inertia | I_y | = | 25170 | cm^4 |
| Yield strength | f_{yc} | = | 355 | N/mm^2 |
| Ultimate strength | f_{uc} | = | 510 | N/mm^2 |

Beam IPE 500, S355

| | | | | |
|-------------------------|----------|---|-------|----------|
| Depth | h_b | = | 500 | mm |
| Thickness of the web | t_{bw} | = | 10,2 | mm |
| Width | b_b | = | 200 | mm |
| Thickness of the flange | t_{bf} | = | 16 | mm |
| Root radius | r | = | 21 | mm |
| Area | A | = | 115,5 | cm^2 |
| Shear area | A_v | = | 59,9 | cm^2 |
| Inertia | I_y | = | 48200 | cm^4 |
| Yield strength | f_{yb} | = | 355 | N/mm^2 |
| Ultimate strength | f_{ub} | = | 510 | N/mm^2 |
| Length | L | = | 6000 | mm |

Header plate 426 x 180 x 17, S355

| | | | | |
|-------------------|----------|---|-----|----------|
| Vertical gap | g_v | = | 40 | mm |
| Depth | h_p | = | 426 | mm |
| Width | b_p | = | 180 | mm |
| Thickness | t_p | = | 17 | mm |
| Yield strength | f_{yp} | = | 355 | N/mm^2 |
| Ultimate strength | f_{up} | = | 510 | N/mm^2 |

Direction of load transfer (1)

| | | | | |
|-------------------------------------|------------|---|-----|-------|
| Number of bolts rows | n_1 | = | 4 | bolts |
| Edge distance to first bolt row | e_{11} | = | 60 | mm |
| Pitch between bolts rows 1 and 2 | $p_{1[1]}$ | = | 102 | mm |
| Pitch between bolts rows 2 and 3 | $p_{1[2]}$ | = | 102 | mm |
| Distance from last bolt row to edge | e_{1n} | = | 60 | mm |

Direction perpendicular to load transfer (2)

| | | | | |
|-------------------------------------|----------|---|-----|-------|
| Number of bolts rows | n_2 | = | 2 | bolts |
| Edge distance to first bolt row | e_{21} | = | 40 | mm |
| Pitch between bolts rows 1 and 2 | $p_{2'}$ | = | 100 | mm |
| Distance from last bolt row to edge | e_{2n} | = | 40 | mm |
| Distance from last bolt row to edge | e_{2s} | = | 40 | mm |

Bolts M30, 10.9

| | | | | |
|----------------------------|--------------|---|-------|----------|
| Tensile stress area | A_s | = | 561 | mm^2 |
| Diameter of the shank | d | = | 30 | mm |
| Diameter of the holes | d_0 | = | 33 | mm |
| Head height | h_D | = | 19.75 | mm |
| Nut height | h_N | = | 25.60 | mm |
| Outer diameter of a washer | ϕ_{ext} | = | 56 | mm |
| Yield strength | f_{yb} | = | 900 | N/mm^2 |
| Ultimate strength | f_{ub} | = | 1000 | N/mm^2 |

Welds

| | | | | |
|------------------------------|-------|---|-----|----|
| Throat thickness of the weld | a_w | = | 6 | mm |
| Length of the weld | l_w | = | 426 | mm |

Safety factors

| | | |
|---------------|---|------|
| γ_{M0} | = | 1.00 |
| γ_{M2} | = | 1.25 |
| γ_{Mu} | = | 1.10 |

B.3 Ductility and rotation requirements

To apply the following design rules, certain inequalities concerning the rotation requirements and the ductility requirements must be satisfied.

Rotation requirements

1)

$$h_p \leq d_b \Leftrightarrow 426mm \leq 426mm \rightarrow Ok \quad (5.25)$$

2)

$$\phi_{available} \geq \phi_{required} \Leftrightarrow 0.459 \geq 0.005 \rightarrow Ok \quad (5.26)$$

Because,

$$\begin{aligned} - \phi_{available} &= t_p/h_e = 17/37 = 0.0459 \\ - \phi_{required} &= \frac{\gamma_p L^3}{24EI} = \frac{56.472 \cdot 6000^3}{24 \cdot 210000 \cdot 48200 \cdot 10^4} = 0.005 \end{aligned}$$

Ductility requirements

1)

$$\frac{d}{t_p} \geq 2.8 \sqrt{\frac{f_{yp}}{f_{ub}}} \Leftrightarrow 1.76 \geq 1.67 \rightarrow Ok \quad (5.27)$$

2)

$$a \geq \frac{\beta_w f_{ybw} \gamma_{M2}}{\sqrt{2} f_{ubw} \gamma_{M0}} t_{bw} \Leftrightarrow 6 \text{ mm} \geq 5.65 \text{ mm} \rightarrow Ok \quad (5.28)$$

B.4 Calculation of the joint shear resistance

Bolts in shear

$$V_{Rd,1} = 0.8 \cdot n \cdot F_{v,Rd} = 1436.16 \text{ kN} \quad (5.29)$$

Because,

$$\begin{aligned} - n &= 8 \\ - F_{v,Rd} &= \alpha_v A f_{ub} / \gamma_{M2} = 224.4 \text{ kN} \end{aligned}$$

Header plate in bearing

$$V_{Rd,2} = n \cdot F_{b,Rd} = 1708.97 \text{ kN} \quad (5.30)$$

Because,

$$- n = 8$$

$$- \alpha_b = \min(\alpha_1 ; \alpha_2 ; \alpha_3 ; 1) = \min(e_1/(3 \cdot d_0) ; p_1/(3 \cdot d_0) - 1/4 ; f_{ub}/f_{up}) = \min(0.61 ; 0.78 ; 1.96) = 0.61$$

$$- k_1 = \min(2.8 \cdot e_2/d_0 - 1.7 ; 2.5) = 1.69$$

$$- F_{b,Rd} = k_1 \cdot \alpha_b \cdot d \cdot t_p \cdot f_{up}/\gamma_{M2} = 213.62 \text{ kN}$$

Column flange in bearing

$$V_{Rd,3} = n \cdot F_{b,Rd} = 2459.16 \text{ kN} \quad (5.31)$$

Because,

$$- n = 8$$

$$- \alpha = \min(\alpha_1 ; \alpha_2 ; \alpha_3 = \min(p_1/(3 \cdot d_0) - 1/4 ; f_{ub}/f_{ucf} ; 1) = \min(0.78 ; 1.96 ; 1) = 0.78$$

$$- k_1 = \min(1.4 \cdot p_2/d_0 - 1.7 ; 2.8 \cdot e_{2s}/d_0 - 1.7 ; 2.5) = 1.69$$

$$- F_{b,Rd} = k_1 \cdot \alpha_b \cdot d \cdot t_{cf} \cdot f_{ucf}/\gamma_{M2} = 307.39 \text{ kN}$$

Cross section of the header plate in shear

$$V_{Rd,4} = 2 \cdot F_{v,Rd} = 2337.5 \text{ kN} \quad (5.32)$$

$$\text{Because, } F_{v,Rd} = h_p \cdot t_p \cdot f_{yp}/(1.27 \cdot \sqrt{3} \cdot \gamma_0) = 1168.75 \text{ kN}$$

Net section of the header plate in shear

$$V_{Rd,5} = 2 \cdot F_{v,Rd} = 2354.65 \text{ kN} \quad (5.33)$$

Because,

$$- A_{v,net} = t_p \cdot (h_p - n_1 \cdot d_0) = 4998 \text{ mm}^2$$

$$- F_{v,Rd} = A_{v,net} \cdot f_{up}/(\sqrt{3} \cdot \gamma_{M2}) = 1177.32 \text{ kN}$$

Shear block of the header plate

$$V_{Rd,6} = 2 \cdot F_{eff,Rd} = 2071.63 \text{ kN} \quad (5.34)$$

Because,

$$- A_{nt} = t_p \cdot (e_2 - d_0/2) = 399.5 \text{ mm}^2$$

$$- A_{nv} = t_p \cdot (h_p - e_1 - (n_1 - 0.5) \cdot d_0) = 4258.5 \text{ mm}^2$$

$$- F_{eff,Rd} = F_{eff,1,Rd} = \frac{f_{up} \cdot A_{nt}}{\gamma_{M2}} + \frac{1}{\sqrt{3}} \cdot f_{yp} \cdot \frac{A_{nv}}{\gamma_{M0}} = 1035.82 \text{ kN}$$

Header plate in bending

$$V_{Rd,7} = \infty \quad (5.35)$$

Beam web in shear

$$V_{Rd,8} = F_{v,Rd} = t_{bw} \cdot h_p \cdot \frac{f_{ybw}}{\gamma_{M0} \cdot \sqrt{3}} = 890.59 \text{ kN} \quad (5.36)$$

Joint shear resistance

$$V_{Rd} = \min_{i=1}^8 V_{Rd,i} = 890.59 \text{ kN} \quad (5.37)$$

B.5 Calculation of ultimate tensile strength

Bolts in tension

$$N_{u,1} = n \cdot B_{t,u} = 4080 \text{ kN} \quad (5.38)$$

Because,

$$- n = 8$$

$$- B_{t,u} = f_{ub} \cdot A_s / \gamma_{Mu} = 510 \text{ kN}$$

Header plate in bending

$$N_{u,2} = \min(F_{hp,u,1}, F_{hp,u,2}) = 2130.97 \text{ kN} \quad (5.39)$$

Because,

$$- m_p = (p'_2 - t_w - 2 \cdot 0.8 \cdot a \cdot 2^{0.5}) / 2 = 38.11 \text{ mm}$$

$$- n_p = \min(e_2; 1.25 \cdot m_p) = 40 \text{ mm}$$

$$- m_{u,p} = \frac{t_p^2 \cdot f_{up}}{4 \cdot \gamma_{Mu}} = 33497.73 \text{ Nmm/mm}$$

$$- l_{eff,p,t,1} = l_{eff,p,t,2} = h_p = 426 \text{ mm}$$

$$- F_{hp,u,1} = \frac{(8 \cdot n_p - 2 \cdot e_w) \cdot l_{eff,p,t,1} \cdot m_{u,p}}{2 \cdot m_p \cdot n_p - e_w \cdot (m_p + n_p)} = 2130.97 \text{ kN}$$

$$- F_{hp,u,2} = \frac{2 \cdot l_{eff,p,t,2} \cdot m_{u,p} + n \cdot B_{t,u} \cdot n_p}{m_p + n_p} = 2454.69 \text{ kN}$$

Supporting member in bending

Resistance assumed to be sufficient.

Beam web in tension

$$N_{u,4} = t_w \cdot h_p \cdot f_{ubw} / \gamma_{Mu} = 2014.59 \text{ kN} \quad (5.40)$$

Welds

Conditions for full-strength behaviour of the welds are fulfilled.

Ultimate tensile strength

$$N_u = \min_{i=1}^4 N_{u,i} = 2014.59 \text{ kN} \quad (5.41)$$

B.6 Calculation of design tensile strength

Bolts in tension

$$N_{Rd,1} = n \cdot B_{t,Rd} = 3231.36 \text{ kN} \quad (5.42)$$

Because,

$$- n = 8$$

$$- B_{t,Rd} = 0.9 f_{ub} \cdot A_s / \gamma_{M2} = 403.92 \text{ kN}$$

Header plate in bending

$$N_{Rd,2} = \min(F_{hp,Rd,1}, F_{hp,Rd,2}) = 1631.65 \text{ kN} \quad (5.43)$$

Because,

$$\begin{aligned} - m_p &= (p_2' - t_w - 2 \cdot 0.8 \cdot a \cdot 2^{0.5})/2 = 38.11 \text{ mm} \\ - n_p &= \min(e_2; 1.25 \cdot m_p) = 40 \text{ mm} \\ - m_{Rd,p} &= \frac{t_p^2 \cdot f_{yp}}{4 \cdot \gamma_{M0}} = 25648.75 \text{ Nmm/mm} \\ - l_{eff,pt,1} &= l_{eff,pt,2} = h_p = 426 \text{ mm} \\ - F_{hp,Rd,1} &= \frac{(8 \cdot n_p - 2 \cdot e_w) \cdot l_{eff,p,t,1} \cdot m_{u,p}}{2 \cdot m_p \cdot n_p - e_w \cdot (m_p + n_p)} = 1631.65 \text{ kN} \\ - F_{hp,Rd,2} &= \frac{2 \cdot l_{eff,p,t,2} \cdot m_{u,p} + n \cdot B_{t,Rd} \cdot n_p}{m_p + n_p} = 1934.5 \text{ kN} \end{aligned}$$

Supporting member in bending

Resistance assumed to be sufficient.

Beam web in tension

$$N_{Rd,4} = t_w \cdot h_p \cdot f_{ybw} / \gamma_{M0} = 1542.55 \text{ kN} \quad (5.44)$$

Welds

Conditions for full-strength behaviour of the welds are fulfilled.

Design tensile strength

$$N_{Rd} = \min_{i=1}^4 N_{Rd,i} = 1542.55 \text{ kN} \quad (5.45)$$

B.7 Calculation of the tensile rigidity and the elongation capacity of the joint

The constitutive law of an assembly in tension is represented in Figure 5.10.

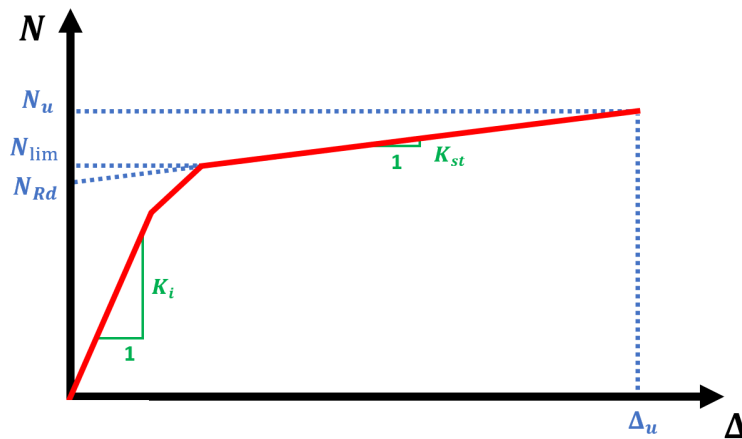


Figure 5.10: Law of behavior in traction of a joint

Calculation of tensile stiffness

$$K_i = \frac{E \cdot k_{ib} \cdot k_{ihp}}{k_{ihp} + k_{ib}} = 4592.09 \text{ kN/mm} \quad (5.46)$$

Because,

$$- k_{ihp} = \frac{0.9 \cdot l_{eff} \cdot t_p^3}{m_p^3} = 34.03 \text{ mm}$$

$$- k_{ib} = \frac{1.6 \cdot A_s \cdot n_1}{t_c + t_{cf} + 0.5 \cdot (h_N = h_D)} = 61.19 \text{ mm}$$

$$K_{st} = K_i/50 = 91.84 \text{ kN/mm} \quad (5.47)$$

Calculation of the elongation capacity

$$\Delta_u = \frac{N_u - N_{Rd}}{K_{st}} = 5.14 \text{ mm} \quad (5.48)$$

C Sizing of end-plate connections flush with the best possible properties

The dimensioning of these joints was carried out with the software *COP* and Eurocode 3 Part 1-8.

C.1 Main joint data

Configuration : Beam to column flange

Column : HE 300B S355

Beam : IPE 500 S355

Header plate : 426 x 180 x 17, S355

C.2 Detailed characteristics

Column HE 300B, S355

| | | | | |
|-------------------------|----------|---|-------|-------------------|
| Depth | h_c | = | 300 | mm |
| Thickness of the web | t_{cw} | = | 11 | mm |
| Width | b_c | = | 300 | mm |
| Thickness of the flange | t_{cf} | = | 19 | mm |
| Root radius | r | = | 27 | mm |
| Area | A | = | 149,1 | cm ² |
| Inertia | I_y | = | 25170 | cm ⁴ |
| Yield strength | f_{yc} | = | 355 | N/mm ² |
| Ultimate strength | f_{uc} | = | 510 | N/mm ² |

Beam IPE 500, S355

| | | | | |
|-------------------------|----------|---|-------|-------------------|
| Depth | h_b | = | 500 | mm |
| Thickness of the web | t_{bw} | = | 10,2 | mm |
| Width | b_b | = | 200 | mm |
| Thickness of the flange | t_{bf} | = | 16 | mm |
| Root radius | r | = | 21 | mm |
| Area | A | = | 115,5 | cm ² |
| Shear area | A_v | = | 59,9 | cm ² |
| Inertia | I_y | = | 48200 | cm ⁴ |
| Yield strength | f_{yb} | = | 355 | N/mm ² |
| Ultimate strength | f_{ub} | = | 510 | N/mm ² |
| Length | L | = | 6000 | mm |

End plate

| | | | | |
|---------------------|----------|---|-----|----------|
| End plate height | h | = | 540 | mm |
| End plate width | b | = | 210 | mm |
| End plate thickness | t_{cp} | = | 17 | mm |
| Yield strength | f_{yp} | = | 355 | N/mm^2 |
| Ultimate strength | f_{up} | = | 510 | N/mm^2 |

Direction of load transfer (1)

| | | | | |
|--------------------------|----------|---|-----|-------|
| Number of bolts rows | n_1 | = | 4 | bolts |
| Pitch between bolt rows | p_{11} | = | 102 | mm |
| Pitch between bolts rows | p_{12} | = | 102 | mm |
| Pitch between bolts rows | p_{13} | = | 102 | mm |

Direction perpendicular to load transfer (2)

| | | | | |
|----------------------------|----------|---|-----|---------|
| Number of columns | n_2 | = | 2 | columns |
| Pitch between bolt columns | p_{21} | = | 130 | mm |

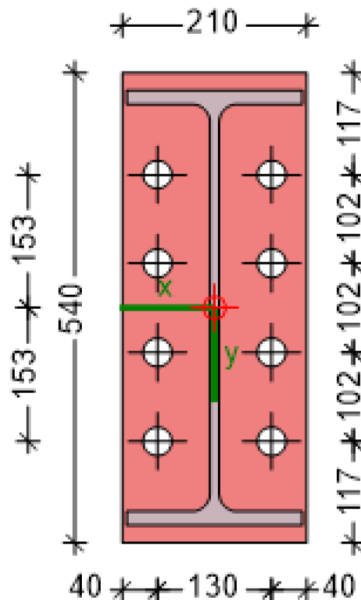


Figure 5.11: End plate

Bolts M30, 10.9

| | | | | |
|----------------------------|--------------|---|-------|----------|
| Tensile stress area | A_s | = | 561 | mm^2 |
| Diameter of the shank | d | = | 30 | mm |
| Diameter of the holes | d_0 | = | 33 | mm |
| Head height | h_D | = | 19.75 | mm |
| Nut height | h_N | = | 25.60 | mm |
| Outer diameter of a washer | ϕ_{ext} | = | 56 | mm |
| Yield strength | f_{yb} | = | 900 | N/mm^2 |
| Ultimate strength | f_{ub} | = | 1000 | N/mm^2 |

Welds

| | | | | |
|------------------|-------|---|-----|----|
| Flange weld size | a_f | = | 6 | mm |
| Web weld size | a_w | = | 426 | mm |

Safety factors

$$\begin{aligned}\gamma_{M0} &= 1.00 \\ \gamma_{M2} &= 1.25 \\ \gamma_{Mu} &= 1.10\end{aligned}$$

C.3 Ductility requirements

1)

$$\frac{d}{t_p} \geq 2.8 \sqrt{\frac{f_{yp}}{f_{ub}}} \Leftrightarrow 1.76 \geq 1.67 \rightarrow Ok \quad (5.49)$$

2)

$$a \geq \frac{\beta_w f_{ybw} \gamma_{M2}}{\sqrt{2} f_{ubw} \gamma_{M0}} t_{bw} \Leftrightarrow 6 \text{ mm} \geq 5.65 \text{ mm} \rightarrow Ok \quad (5.50)$$

C.4 Moment resistance and rotational stiffness

| | | | | |
|------------------------------|------------------|---|--------------------|---------|
| Plastic moment resistance | $M_{pl,Rd}$ | = | 336.8 | kNm |
| Elastic moment resistance | $M_{el,Rd}$ | = | 224.5 | kNm |
| Initial rotational stiffness | $S_{j,ini}$ | = | $7.306 \cdot 10^4$ | kNm/rad |
| Rotational stiffness | $S_{j,ini}/\eta$ | = | $3.653 \cdot 10^4$ | kNm/rad |

C.5 Shear resistance

$$V_{Rd} = 613.6 \text{ kN} \quad (5.51)$$

C.6 Design tensile strength**Bolts in tension**

$$N_{Rd,1} = 3231.2 \text{ kN} \quad (5.52)$$

Header plate in bending

$$N_{Rd,2} = 1508 \text{ kN} \quad (5.53)$$

Supporting member in bending

$$N_{Rd,3} = 2123 \text{ kN} \quad (5.54)$$

Beam web in tension

$$N_{Rd,4} = 2124 \text{ kN} \quad (5.55)$$

Design tensile strength

$$N_{Rd} = \min_{i=1}^4 N_{Rd,i} = 1508 \text{ kN} \quad (5.56)$$

C.7 Ultimate tensile strength**Bolts in tension**

$$N_{u,1} = 4080 \text{ kN} \quad (5.57)$$

Header plate in bending

$$N_{u,2} = 1969.30 \text{ kN} \quad (5.58)$$

Supporting member in bending

$$N_{u,3} = 2700.78 \text{ kN} \quad (5.59)$$

Beam web in tension

$$N_{u,4} = 2773.61 \text{ kN} \quad (5.60)$$

Ultimate tensile strength

$$N_u = \min_{i=1}^4 N_{u,i} = 1969.30 \text{ kN} \quad (5.61)$$

C.8 Calculation of the tensile rigidity and the elongation capacity of the joint**Calculation of tensile stiffness**

$$K_i = \frac{E \cdot k_{ib} \cdot k_{ihp}}{k_{ihp} + k_{ib}} = 2786.25 \text{ kN/mm} \quad (5.62)$$

Because,

- $k_{ihp} = 17.31 \text{ mm}$

- $k_{ib} = 56.84 \text{ mm}$

$$K_{st} = K_i/50 = 55.72 \text{ kN/mm} \quad (5.63)$$

Calculation of the elongation capacity

$$\Delta_u = \frac{N_u - N_{Rd}}{K_{st}} = 8.28 \text{ mm} \quad (5.64)$$

D Structures studied during the parametric study

The structures were initially dimensioned at ULS and SLS. Then, the structures studied have been reinforced so that no element of the indirectly affected part (IAP) yields by plastification before reaching a complete collapse of the directly affected part (DAP).

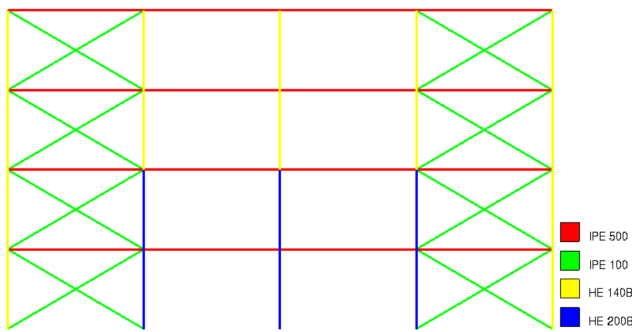


Figure 5.12: Initial geometries of a 4-storey, 4-span structure

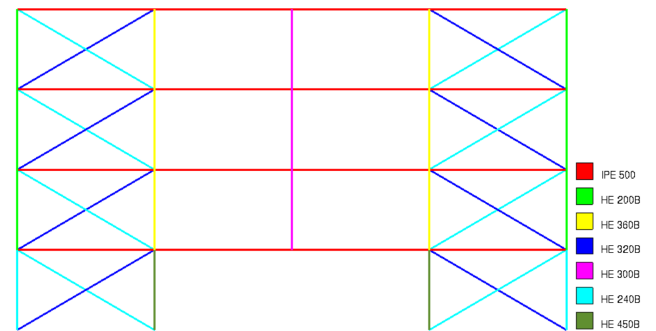


Figure 5.13: Geometries reinforced with a 4-storey, 4-span structure

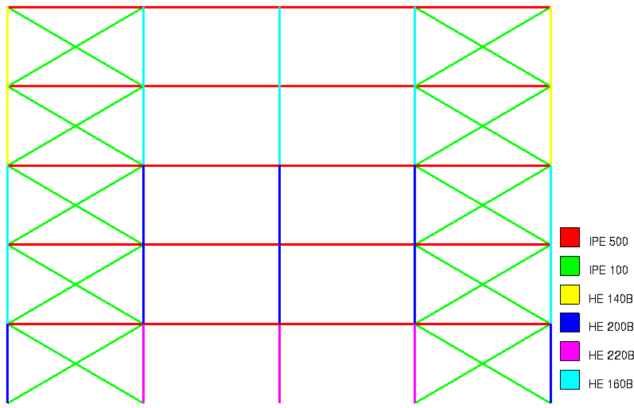


Figure 5.14: Initial geometries of a 5-storey, 4-span structure

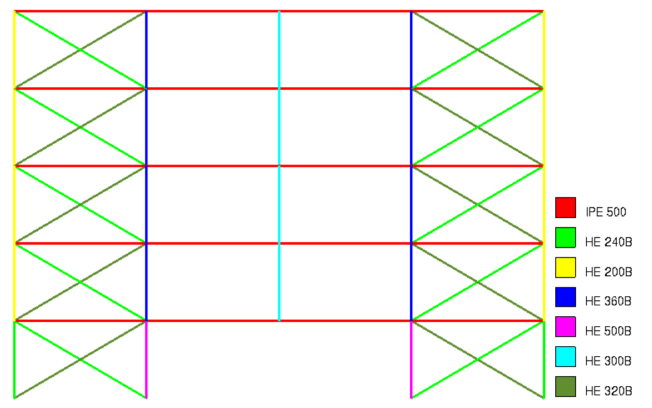


Figure 5.15: Geometries reinforced with a 5-storey, 4-span structure

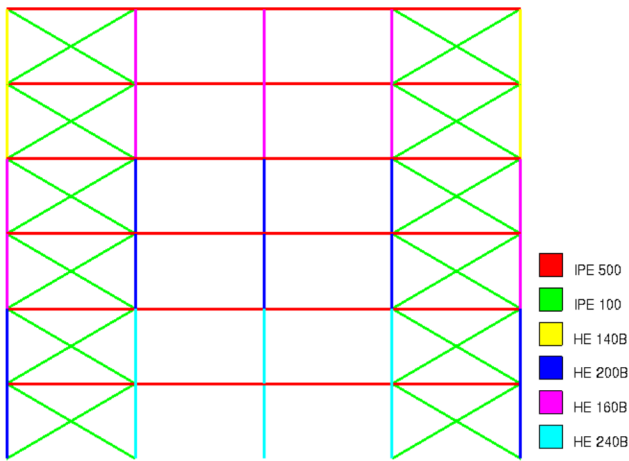


Figure 5.16: Initial geometries of a 6-storey, 4-span structure

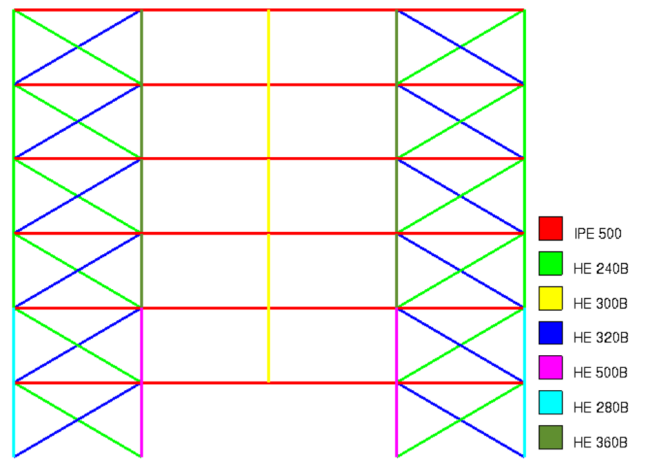


Figure 5.17: Geometries reinforced with a 6-storey, 4-span structure

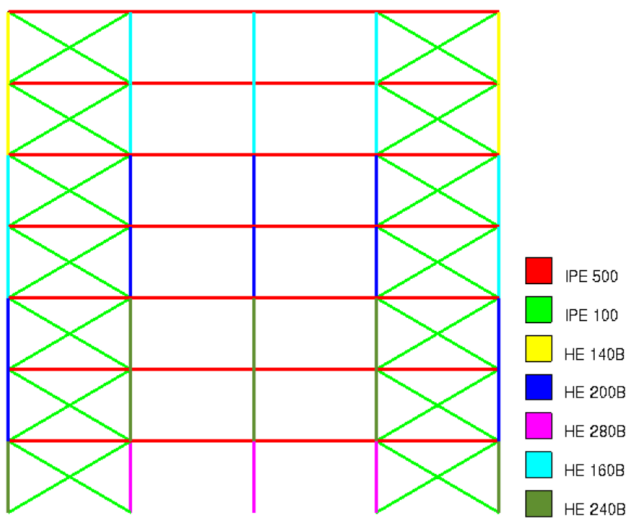


Figure 5.18: Initial geometries of a 7-storey, 4-span structure

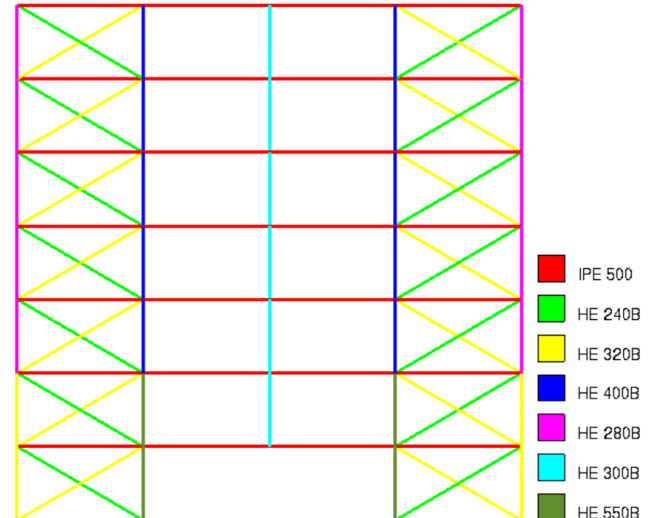


Figure 5.19: Geometries reinforced with a 7-storey, 4-span structure

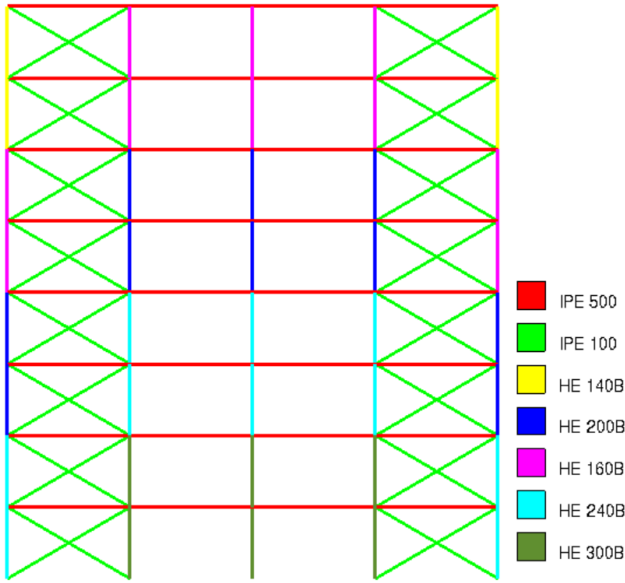


Figure 5.20: Initial geometries of a 8-storey, 4-span structure

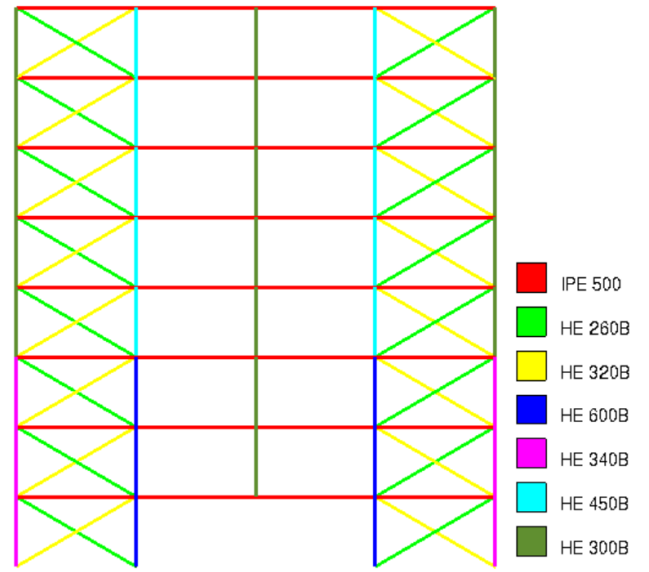


Figure 5.21: Geometries reinforced with a 8-storey, 4-span structure

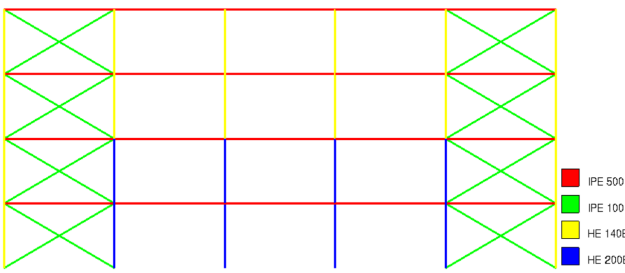


Figure 5.22: Initial geometries of a 4-storey, 5-span structure

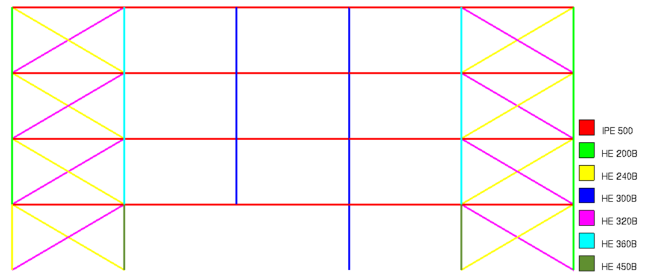


Figure 5.23: Geometries reinforced with a 4-storey, 5-span structure

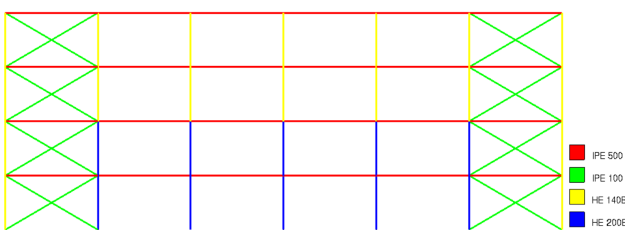


Figure 5.24: Initial geometries of a 4-storey, 6-span structure

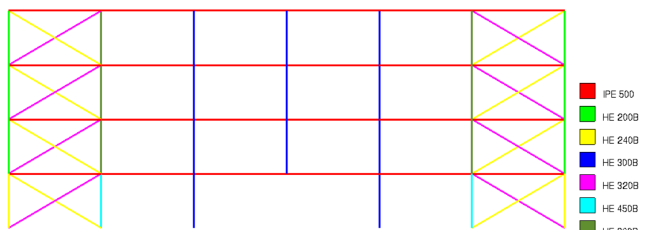


Figure 5.25: Geometries reinforced with a 4-storey, 6-span structure

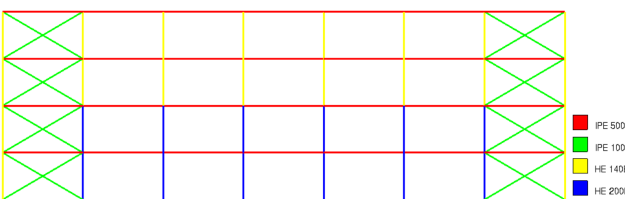


Figure 5.26: Initial geometries of a 4-storey, 7-span structure

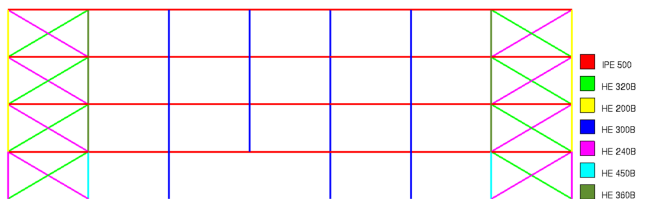


Figure 5.27: Geometries reinforced with a 4-storey, 7-span structure

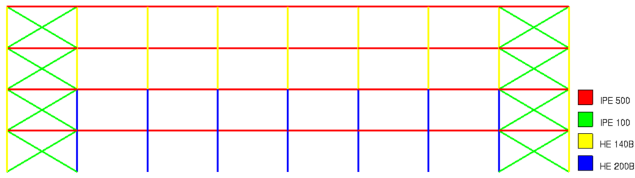


Figure 5.28: Initial geometries of a 4-storey, 8-span structure

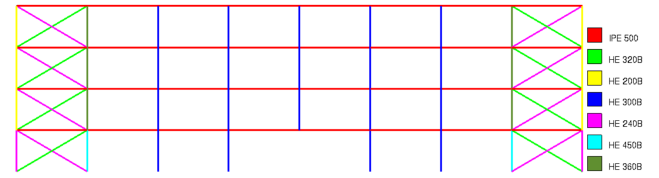


Figure 5.29: Geometries reinforced with a 4-storey, 8-span structure

Bibliography

- [1] European committee for standardization. *E1991-1-7: Actions on structures - Part 1-7: General actions - Accidental actions*. Brussels, Belgium, December 2006.
- [2] J.-F. Demonceau & B. Dewals. *Natural and technological risks in civil engineering*, Part dedicated to the robustness of the structures. University of Liège course. University of Liège, Belgium, 2019.
- [3] B. Izzudin. *Prescriptive Tying Force Requirements*. Presentation presented at a WG6 meeting. London, United Kingdom, 20th November 2019.
- [4] B. Belletti. *Regarding implementation of proposals into EN1992*. Presentation presented at a WG6 meeting. London, United Kingdom, 20th November 2019.
- [5] J.-F. Demonceau. *Steel and composite building frames: sway response under conventional loading and development of membranes effects in beams further to an exceptional action*. PhD thesis. University of Liège, Belgium, 2008.
- [6] L. N. N. Hai. *Structural response of steel composite building frames further to an impact leading to the loss of a column*. PhD thesis. University of Liege, Belgium, 2008.
- [7] C. Huvelle. *Contribution à l'étude de la robustesse des structures de bâtiments*. Master thesis. University of Liège, Belgium, 2011.
- [8] C. Huvelle, V.-L. Hoang, J.-P. Jaspart, J.-F. Demonceau, *Complete analytical procedure to assess the response of a frame submitted to a column loss*. Scientific article. Oxford, United Kingdom, 2015.
- [9] M. Jacques. *Robustness of steel frames further to a column loss: development of analytical methods for practitioners*. Master thesis. University of Liège, Belgium, 2019.
- [10] J.-F. Demonceau, F. Cerfontaine, J.-P. Jaspart. *Resistance of steel and composite connections under combined axial force and bending including group effects: Analytical procedures and comparison with laboratory tests*. Scientific article. Netherlands, 2019.
- [11] F. Cerfontaine. *Etude de l'interaction entre moment de flexion et effort normal dans les assemblages boulonnés*. PhD thesis. University of Liège, Belgium, 2003.
- [12] F. Lemaire. *Etude du comportement 3D de structures en acier ou mixtes lors de la perte d'une colonne*. Master thesis. University of Liège, Belgium, 2010.
- [13] S. Kulik. *Robustness of steel structures: consideration of coupling in a 3D structure*. Master thesis. University of Liège, Belgium, 2014.
- [14] C. Colomer Segura, L. Hamra, M. D'Antimo, J.-F. Demonceau, M. Feldmann. *Determination of Loading Scenarios on Buildings Due to Column Damage*. Scientific article. Belgium, November 2017.
- [15] J.-F. Demonceau, L. Comeliau, V.-L. Hoang, J.-P. Jaspart. *How can a steel structure survive to impact loading ? Numerical and analytical investigations*. Scientific article. Liège, Belgium, 2017.

BIBLIOGRAPHY

- [16] J.-F., H. Vanvinckenroye, M. D'Antimo, V. Denoël, J.-P. Japsart. *Beam-to-column joints, column bases and joint components under impact loading*. Scientific article. Copenhagen, Denmark, September 2017.
- [17] M. D'Antimo, M. Latour, G. Rizzano, J.-F. Demonceau, J.-P. Japsart. *Preliminary Study on Beam-To-Column Joint Under Impact Loading*. Scientific article. University of Liège, Belgium, 2018.
- [18] M. D'Antimo. *Impact characterization of innovative seismically designed connections for robustness application*. PhD thesis. University of Liège, Belgium, 2020.
- [19] L. Hamra, J.-F. Demonceau, V. Denoël. *Pressure-impulse diagram of a beam developing non-linear membrane action under blast loading*. Scientific article. Oxford, United Kingdom, December 2015.
- [20] F. Hjeir. *Robustness of steel structures further to a column loss: Identification of the structural requirements through parametrical studies*. Master thesis. University of Liège, Belgium, 2015.
- [21] F. Collin & V. de Ville de Goyet. *Non linear finite elements*. University of Liège course. University of Liège, Belgium, 2019.
- [22] *FINELG user's manual. Non-linear finite element analysis program*. Version 9.0. Chapter 8.200, *Non-linear spring - RESS2A*. Bureau Greisch & University of Liège, Belgium, 2003.
- [23] J.-P. Japsart, J.-F. Demonceau, S. Renkin, M.-L. Guillaume. *European Recommendations for the Design of Simple Joints in Steel Structures*. University of Liège, Belgium, 2009.

List of Figures

- 1.1 Ronan Point, 1968 (researchgate.net) 1
- 1.2 Oklahoma City, 1995 (ici.radio-canada.ca) 2
- 1.3 World Trade Center, 2001 (ibtimes.sg) 2

- 2.1 Strategies for exceptional situations 5
- 2.2 Key element version 1 [2] 7
- 2.3 Key element version 2 [2] 8

- 3.1 Flowchart for strategies based on limiting the extent of localised failure 10
- 3.2 Procedure by opting for the prescriptive approach 12
- 3.3 Column loss scenario 13
- 3.4 $N_{AB} - u$ relationship [2] 13
- 3.5 Appearance of a first plastic hinge 14
- 3.6 Formation of a plastic mechanism 14
- 3.7 Substructure 15
- 3.8 Determination of flexibility matrices [8] 16
- 3.9 Modeling of plastic hinges in the beam [9] 17
- 3.10 Horizontal shift of the substructure 18
- 3.11 Criterion of the resistance of a joint under M-N proposed by Eurocode 3 Part 1-8 [2] 23
- 3.12 Modeling of a single-sided joint [10] 23
- 3.13 Procedure by opting for the analytical approach 24
- 3.14 Simulation of the loss of column - Step 1 [2] 25
- 3.15 Simulation of the loss of column - Step 2 [2] 25
- 3.16 Procedure by opting for the numerical approach 26
- 3.17 Possible approaches by opting for the key element strategy 28
- 3.18 Possible approaches to design under impact loading 28
- 3.19 Procedure by opting for the equivalent static force approach 29
- 3.20 Traditional approach [14] 30
- 3.21 Improved approach [14] 31
- 3.22 Load simulating the loss of a column 32
- 3.23 Type 1 response [15] 32
- 3.24 Type 2 response [15] 32
- 3.25 Calculation of the generalised mass [15] 34
- 3.26 Example of type 1 response [15] 35
- 3.27 Example of type 2 response [15] 35
- 3.28 Procedure by opting for the dynamic force and static analysis approach 38
- 3.29 Procedure by opting for the dynamic force approach and dynamic analysis 39
- 3.30 Possible approaches to design under blast loading 39
- 3.31 Procedure by opting for the equivalent static force approach 40
- 3.32 Description of the problem [19] 41
- 3.33 Evolution of pressure over time during for a blast [2] 41
- 3.34 Evolution of the terms of the energy of deformation [19] 43
- 3.35 Asymptotes [19] 44

LIST OF FIGURES

| | | |
|------|---|----|
| 3.36 | Procedure by opting for the analytical approach with dynamic force | 46 |
| 3.37 | Procedure by opting for the numerical approach with dynamic force | 47 |
| 4.1 | Structure studied | 49 |
| 4.2 | Loads | 50 |
| 4.3 | Geometries of the different elements | 51 |
| 4.4 | Spherical step method [21] | 54 |
| 4.5 | Real behavior law of steel | 54 |
| 4.6 | Elastic-perfectly plastic behavior law | 54 |
| 4.7 | Equivalent forces to take into account the initial imperfection of a column | 55 |
| 4.8 | Results obtained | 56 |
| 4.9 | Plastic zone | 56 |
| 4.10 | Lost column | 57 |
| 4.11 | Column replacement by support and application of support settlement | 58 |
| 4.12 | Bi-linear law | 58 |
| 4.13 | Element geometries to allow the loss of the central column | 59 |
| 4.14 | Load factor - vertical displacement relationship | 59 |
| 4.15 | Representation of the load factor | 59 |
| 4.16 | Plastic zones at the time of failure | 60 |
| 4.17 | Axial forces in the beams at the time of failure | 60 |
| 4.18 | Deformation of a non-braced structure losing a column | 61 |
| 4.19 | Deformation of a braced structure losing a column | 61 |
| 4.20 | Deformed at the time of ruin | 61 |
| 4.21 | Axial forces in beams when the column is completely lost ($\lambda = 1$) | 62 |
| 4.22 | Designed joints | 63 |
| 4.23 | Law of behavior of joints in traction | 63 |
| 4.24 | Element geometries | 65 |
| 4.25 | Load factor - vertical displacement at the top of the lost column relationship | 65 |
| 4.26 | Deformed at the time of failure | 65 |
| 4.27 | Plastic zones at the time of failure | 66 |
| 4.28 | Axial forces in beams at the time of failure | 66 |
| 4.29 | Balance of efforts | 66 |
| 4.30 | Example of a header plate connection | 67 |
| 4.31 | Designed joints | 68 |
| 4.32 | Longitudinal view of the joint | 68 |
| 4.33 | Top view of the joint | 68 |
| 4.34 | Front view of the joint | 68 |
| 4.35 | Law of behavior of the joint in traction | 69 |
| 4.36 | Model 1 | 70 |
| 4.37 | Model 2 | 70 |
| 4.38 | Behavior law of a horizontal extensional spring modeling the axial behavior of a single joint | 70 |
| 4.39 | Behavior law of a horizontal extensional spring modeling the axial behavior of two joints | 70 |
| 4.40 | Element geometries | 72 |
| 4.41 | Load factor - vertical displacement at the top of the lost column relationship | 73 |
| 4.42 | Axial force in beams at point 1 | 74 |
| 4.43 | Support reaction representing the lost column in point 1 | 74 |
| 4.44 | Axial force in beams at point 2 | 74 |
| 4.45 | Support reaction representing the lost column in point 2 | 74 |
| 4.46 | Axial force in beams at point 3 | 74 |
| 4.47 | Support reaction representing the lost column in point 3 | 74 |
| 4.48 | Longitudinal view of the joint | 76 |
| 4.49 | Top view of the joint | 76 |

LIST OF FIGURES

| | |
|--|-----|
| 4.50 Front view of the joint | 76 |
| 4.51 Law of behavior of the joint in traction | 76 |
| 4.52 Model 1 | 77 |
| 4.53 Model 2 | 77 |
| 4.54 Behavior law of a horizontal extensional spring modeling the axial behavior of a single joint | 77 |
| 4.55 Behavior law of a horizontal extensional spring modeling the axial behavior of two joints | 77 |
| 4.56 Element geometries | 78 |
| 4.57 Relation between the load factor and the displacement at the top of the lost column for $\Delta_u = 5.14\text{mm}$ | 79 |
| 4.58 Relation between the load factor and the displacement at the top of the lost column for $\Delta_u = 15\text{mm}$ | 79 |
| 4.59 Example of flush end-plate connection | 80 |
| 4.60 End plate | 81 |
| 4.61 Law of behavior in traction of the joint | 81 |
| 4.62 Model 1 | 82 |
| 4.63 Model 2 | 82 |
| 4.64 Behavior law of a horizontal extensional spring modeling the axial behavior of a single joint | 83 |
| 4.65 Behavior law of a horizontal extensional spring modeling the axial behavior of two joints | 83 |
| 4.66 Element geometries | 83 |
| 4.67 Relationship between the load factor and the vertical displacement at the top of the lost column | 84 |
| 4.68 Typical relationship between axial force in the lost column and vertical displacement at the top of the lost column | 84 |
| 4.69 Plastic mechanism | 85 |
| 4.70 Representation of the load factor | 85 |
| 4.71 Bending moments in the beams at the time of the formation of the plastic mechanism | 86 |
| 4.72 Normal forces in the beams at the time of the formation of the plastic mechanism | 86 |
| 4.73 New relationship between the load factor and the vertical displacement at the top of the lost column | 87 |
| 4.74 Axial force in beams for a load factor of 1 | 87 |
| 4.75 Law of behavior in traction of the joint | 88 |
| 4.76 Consequences of increasing the number of spans | 89 |
| 4.77 Consequences of increasing the number of storeys | 90 |
| 5.1 The strategies to be considered for exceptional design situations according to the Eurocode 1 Part 1-7 | 92 |
| 5.2 Development of approaches for exceptional design situations | 93 |
| 5.3 Procedure by opting for the prescriptive approach after having chosen the alternative load paths strategy | 95 |
| 5.4 Procedure by opting for the analytical approach after having chosen the alternative load paths strategy | 95 |
| 5.5 Procedure by opting for the numerical approach after having chosen the alternative load paths strategy | 96 |
| 5.6 Procedures for possible approaches by opting for the key element strategy | 96 |
| 5.7 Procedures for possible approaches to design the structure under impact loading | 97 |
| 5.8 Procedures for possible approaches to design the structure under blast loading | 98 |
| 5.9 Law of behavior in traction of a joint | 104 |
| 5.10 Law of behavior in traction of a joint | 109 |
| 5.11 End plate | 111 |
| 5.12 Initial geometries of a 4-storey, 4-span structure | 113 |

LIST OF FIGURES

| | | |
|------|---|-----|
| 5.13 | Geometries reinforced with a 4-storey, 4-span structure | 113 |
| 5.14 | Initial geometries of a 5-storey, 4-span structure | 114 |
| 5.15 | Geometries reinforced with a 5-storey, 4-span structure | 114 |
| 5.16 | Initial geometries of a 6-storey, 4-span structure | 114 |
| 5.17 | Geometries reinforced with a 6-storey, 4-span structure | 114 |
| 5.18 | Initial geometries of a 7-storey, 4-span structure | 114 |
| 5.19 | Geometries reinforced with a 7-storey, 4-span structure | 114 |
| 5.20 | Initial geometries of a 8-storey, 4-span structure | 115 |
| 5.21 | Geometries reinforced with a 8-storey, 4-span structure | 115 |
| 5.22 | Initial geometries of a 4-storey, 5-span structure | 115 |
| 5.23 | Geometries reinforced with a 4-storey, 5-span structure | 115 |
| 5.24 | Initial geometries of a 4-storey, 6-span structure | 115 |
| 5.25 | Geometries reinforced with a 4-storey, 6-span structure | 115 |
| 5.26 | Initial geometries of a 4-storey, 7-span structure | 115 |
| 5.27 | Geometries reinforced with a 4-storey, 7-span structure | 115 |
| 5.28 | Initial geometries of a 4-storey, 8-span structure | 116 |
| 5.29 | Geometries reinforced with a 4-storey, 8-span structure | 116 |

List of Tables

- 3.1 System of equations to solve if the plastic hinges are located in the beam 19
- 3.2 System of equations to solve if the plastic hinges are located in the joints 20

- 4.1 Horizontal elongations for a load factor of 1 66
- 4.2 Variation of the number of spans 89
- 4.3 Variation of the number of storeys 90